



**UNIVERSIDADE FEDERAL DO PARÁ
INSTITUTO DE GEOCIÊNCIAS
PROGRAMA DE PÓS-GRADUAÇÃO EM GEOLOGIA E GEOQUÍMICA**

TESE DE DOUTORADO Nº 155

**O NEÓGENO E PLEISTOCENO DA AMAZÔNIA CENTRAL:
PALINOESTRATIGRAFIA, PALEOAMBIENTE E RELAÇÃO COM
OS EVENTOS EVOLUTIVOS DO RIO AMAZONAS**

Tese apresentada por

WALMIR DE JESUS SOUSA LIMA JÚNIOR

Orientador: Prof. Dr. Afonso César Rodrigues Nogueira (UFPA)

Coorientador: Dr. Carlos Jaramillo

**BELÉM
2021**

Dados Internacionais de Catalogação na Publicação (CIP) de acordo com ISBD
Sistema de Bibliotecas da Universidade Federal do Pará

- L732n Lima Júnior, Walmir de Jesus Sousa.
O Neógeno e Pleistoceno da Amazônia Central: Palinoestratigrafia, Paleoambiente e relação com os eventos evolutivos do Rio Amazonas / Walmir de Jesus Sousa Lima Júnior.— 2021.
xvi, 147 f. : il. color.
Orientador(a): Prof. Dr. Afonso César Rodrigues Nogueira
Coorientador(a): Dr. Carlos Alberto Jaramillo
Tese (Doutorado) - Universidade Federal do Pará, Instituto de Geociências, Programa de Pós-Graduação em Geologia e Geoquímica, Belém, 2021.
1. Neogeno. 2. Rio Amazonas. 3. Lago Pebas-Solimões. 4. Formação Içá. 5. Palinomorfos. I. Título.

CDD 551.7009811



Universidade Federal do Pará
Instituto de Geociências
Programa de Pós-Graduação em Geologia e Geoquímica

**O NEÓGENO E PLEISTOCENO DA AMAZÔNIA CENTRAL:
PALINOESTRATIGRAFIA, PALEOAMBIENTE E RELAÇÃO
COM OS EVENTOS EVOLUTIVOS DO RIO AMAZONAS**

TESE APRESENTADA POR:

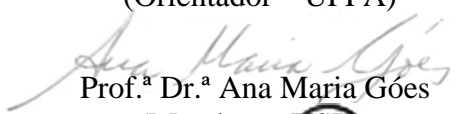
WALMIR DE JESUS SOUSA LIMA JÚNIOR

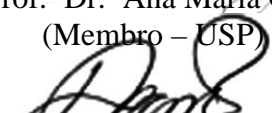
**Como requisito parcial à obtenção do Grau de Doutor em Ciências na Área de
GEOLOGIA**

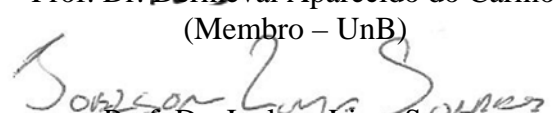
Data de Aprovação: 19 / 03 / 2021

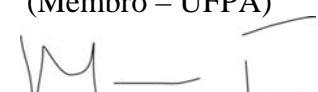
Banca Examinadora:


Prof. Dr. Afonso César Rodrigues Nogueira
(Orientador – UFPA)


Prof.^a Dr.^a Ana Maria Goes
(Membro – USP)


Prof. Dr. Dermeval Aparecido do Carmo
(Membro – UnB)


Prof. Dr. Joelson Lima Soares
(Membro – UFPA)


Prof. Dr. Marlon Carlos França
(Membro – IFPA)

AGRADECIMENTOS

Agradeço a Deus pelo dom da vida, a Ti Senhor toda honra e glória.

À minha família pelo incentivo, dedicação e infintos momentos de felicidade. Meus filhos Breno Lima, Nataly Lima, Blenda Lima, Pedro Dias e Stelle Lima.

Ao Conselho Nacional de Desenvolvimento Científico e Tecnológico (CNPq) pela concessão da bolsa de estudo.

O presente trabalho foi realizado com apoio da Coordenação de Aperfeiçoamento de Pessoal de Nível Superior – Brasil (CAPES) – Código de financiamento 001. Como também a concessão de bolsa pelo Programa de Doutorado-Sanduíche no Exterior (PDSE).

Ao Programa de Pós-Graduação em Geologia e Geoquímica (PPGG) da Universidade Federal do Pará, pela infraestrutura e apoio financeiro disponibilizados.

Ao Smithsonian Tropical Research Institute (STRI) por proporcionar um excelente ano de estágio, bem como disponibilizar toda a infraestrutura e meios possíveis para o desenvolvimento dessa tese. Aos pesquisadores Enrique Moreno e Carlos de Gracia pelo acolhimento e discussões. Aos demais amigos Alejandro Giraldo, Daniela Carvalho, Dayenari Caballero, Karén Cardenas, Natalia Ovalle e Sebastian Gomez ¡¡Muchas gracias por todo!!

Ao meu amigo e orientador Prof. Dr. Afonso Nogueira por todo o auxílio e ensinamentos, pela confiança e por não me permitir desmotivar nos momentos turbulentos dessa caminhada.

Ao meu coorientador Dr. Carlos Jaramillo pela receptividade, paciência e oportunidade de aprofundar meus conhecimentos palinológicos.

Ao Laboratório de Paleontologia e Palinologia da Universidade Federal de Mato Grosso (PALMA), em especial à Prof. Dr. Silane Silva-Caminha e Dr. Carlos D’Apolito pelas inúmeras discussões e sugestões.

Ao Prof.(s) Dr.(s) José Bandeira e Werner Truckenbrodt pela grande colaboração no desenvolvimento deste projeto.

À Biblioteca Geólogo Raimundo Montenegro Garcia de Montalvão, do Instituto de Geociências da UFPA, bem como a bibliotecária Lúcia de Fátima Imbiriba de Sousa, pela normalização dessa tese.

Aos amigos do Grupo de Bacias Sedimentares da Amazônia (GSED), em especial, Ivan

Romero, Lucas Noronha e Renan Fernandes. Meus amigos de longa data Dr.(s) Anna Nogueira, Cleber Rabelo, Flávio Semblano, Guilherme Raffaeli, Hudson Santos, Isaac Salém, Luis Saturnino, Sebastian Neita, Pedro Augusto e Renato Sol.

Aos amigos Paula Machado e Walnei Batista pela amizade e companheirismo.

À minha bela namorada e futura geóloga Vivian Prado, pelo incentivo e por todos os momentos de felicidade.

A todos mais que participaram deste projeto, minha eterna gratidão!

RESUMO

A análise de fácies baseada em afloramentos de uma sucessão neógena com 25 m de espessura foi realizada na porção oriental da Bacia do Solimões, Amazônia Central. A Formação Solimões, Mioceno, inclui depósitos de lago / depósito de inundação, canal fluvial sinuoso de carga em suspensão com rompimento de diques marginais em subdeltas e depósitos de planície de inundação / rompimento de dique marginal, confirmando o sistema de mega-pântanos Pebas-Solimões anteriormente interpretado. A Formação Içá, Pleistoceno Superior, recobre de forma erosiva a Formação Solimões e compreende fluxo de carga mista a carga de fundo para o sistema fluvial meandrante e depósitos de planície de inundação. A palinoestratigrafia da Formação Solimões foi realizada nesta sucessão exposta e em testemunho de sondagem (196-291 m), geralmente, de lamitos ricos em matéria orgânica. A ocorrência de fósseis exclusivamente continentais associados a fitoclastos e algas de água doce, como os *Ovoidites*, confirmam um ambiente de mega-pântanos restrito à Amazônia Ocidental. *Monoporopollenites annuulatus* e outras gramíneas indicam uma oscilação entre as fases arbustiva e arbórea associada a flutuações nos intervalos seco e úmido. As idades do Mioceno-Plioceno superior para a Formação Solimões obtidas a partir de zonas de amplitudes identificadas principalmente *Crassoretitriletes vanraadshovenii*, *Echiperiporites akanthos*, *Echiperiporites stelae*, *Fenestrites spinosus*, *Psilastephanoporites tesseroporus*, *Grimsdalea magnaclavata* e *Alnipollenites verus*. A primeira aparição de *Alnipollenites verus* foi modificada para o Mioceno. Palinomorfos retrabalhados encontrados nesta sucessão indicam processos autocíclicos relacionados à dinâmica ambiental, enquanto acritarcas indicam erosão de áreas de origem paleozoica. A tectônica andina afetou dramaticamente a Amazônia Central, causando o soergimento progressivo da Bacia do Solimões, que gerou um subsequente surgimento e obliteração da sucessão de mega-pântanos Pebas-Solimões. Este evento de progradação foi amplificado pela queda expressiva do nível do mar no Tortoniano médio (11-8 Ma), concomitando com o surgimento do Rio Amazonas Andino. A discordância gerada resultou num hiato deposicional com **bypass** de ~ 9,5 Ma. Apenas no Pleistoceno Superior, a Bacia do Solimões cedeu, ocasionando a implantação de um sistema de meandros de carga mista a carga fundo que representa o reinício da sedimentação do rio Amazonas na Amazônia Central.

Palavras-chave: Neogeno. Palinomorfos. Rio Amazonas. Lago Pebas-Solimões. Formação Içá.

ABSTRACT

Outcrop-based facies analysis of 25 m-thick Neogene succession was carried out in the Eastern Solimões Basin, Central Amazonia. The Miocene Solimões Formation includes lake/overbank, suspended-load meandering fluvial channel with subdelta crevasse, and flood plain/crevasse splay deposits, confirming the previously interpreted Pebas-Solimões mega-wetland system. The Upper Pleistocene Içá Formation unconformably overlies the Solimões Formation and comprises mixed load to bedload meandering fluvial channel and floodplain deposits. The Solimões Formation's palynostratigraphy was carried in this exposed succession and a drill core (196-291 m), generally in organic matter-rich mudrock. The occurrence of exclusively continental fossils associated with phytoclasts and freshwater algae such as *Ovoidites* confirm the wetland setting restricted to Western Amazonia. *Monoporopollenites annuulatus* and other grasses indicate an oscillation between shrub and tree phases linked to dry and humid interval fluctuations. The upper Miocene-Pliocene ages for the Solimões Formation obtained since amplitudes zones identified mainly *Crassoretitriletes vanraadshovenii*, *Echiperiporites akanthos*, *Echiperiporites stelae*, *Fenestrites spinosus*, *Psilastephanoporites tesseroporus*, *Grimsdalea magnaclavata*, and *Alnipollenites verus*. The first appearance of *Alnipollenites verus* is modified for the Miocene. Reworked palynomorphs found in this succession indicate autocyclic processes related to the environmental dynamic, while acritarchs indicate erosion of Paleozoic source areas. The Andean tectonics affected Central Amazonia dramatically, causing the progressive uplift of the Solimões Basin and the emergence and demise of the Pebas-Solimões mega-wetland succession. This progradation event was amplified by the expressive sea-level fall in the middle-Tortonian (11-8 Ma), resulting in the Andean Amazon River's onset. The generated unconformity resulted in a gap and bypass sediment of ~ 9,5 Ma. Only in the Late Pleistocene, the Solimões Basin subsided, causing the implantation of a mixed- to bedload meandering system that represents the sedimentation restart of the Amazon River in the Central Amazonia.

Keywords: Neogene. Palynomorphs. Amazon River. Pebas-Solimões Lake. Içá Formation.

LISTA DE ILUSTRAÇÕES

CAPÍTULO 1

- Figura 1- Seção esquemática W-E desde as bacias do Acre, Solimões, Amazonas e Marajó mostrando os arcos e altos estruturais (Modificado: Wanderley Filho & Travassos 2009). Observar que os depósitos Cretáceos afloram nas bacias do Acre e Amazonas. A área de Urucu-Coari, objeto desta pesquisa, está localizada próximo do Arco de Purus.5
- Figura 2- Porção leste da Bacia do Solimões. A) Bacias da Amazônia no norte da América do Sul. B) Arcabouço estratigráfico da região circundante do Arco Purus, limite entre as bacias dos Solimões e Amazonas (modificado de Abinader 2012). A Formação Solimões alcança até 5m de espessura na região de Coari, sendo recoberta por depósitos da Formação Içá. C) Região de Urucu-Coari com indicação dos pontos estudados.....6

CAPÍTULO 3

- Figure 1- Geotectonic units of the Central-Eastern Amazonia. A) Simplified geological map (Modified from Wanderley-Filho *et al.* (2007), Brazilian Geological Survey - CPRM, 2010 & Rossetti *et al.* 2005). B) The study area and location of measured sections.18
- Figure 2- Neogene lithostratigraphy of the eastern Solimões Basin, Central Amazônia. Biozones “a” and “b” are respectively from Jaramillo *et al.* (2011) and Nogueira *et al.* (2013). The “b” biozones were defined to the studied succession and refers to Fenestrites longispinosus and Fenestrites spinosus with Echitricolporites spinosus Bombacacidites ciriloensis that indicate upper Miocene to Pliocene age. The Alnipollenites verus is typical, but not exclusive, of Pleistocene strata. The initial mark in 10 Ma for the unconformity match with the Andean Amazon River's onset (cf. Gorini *et al.* 2013, Hoorn *et al.* 2019) and indicate a gap that includes the Pliocene and Lower to Middle Pleistocene. The minimum age for Içá Formation of ~400 Ka BP is provided for OSL age (Rozo 2005, Rossetti *et al.* 2015, Pupim *et al.* 2019). The average thickness for each formation is indicated in the composite section.22

- Figure 3- The unconformity between Solimões and Içá formations near Coari town. A) Greyish fine-grained sandstone alternated with mudrock composing large-scale inclined heterolithic stratification (IHS) overlaid by reddish-orangish sandstone. B) Undulated surface (white arrows) marks the erosive surface. C) Climbing-ripple cross lamination in IHS sandstone, D) root marks and E) *Taenidium* trace fossil with organic matter remains occur in F) mottled rhythmite forming coarsening upward cycles of the Içá Formation.....23
- Figure 4- Stratigraphic sections of Neogene succession exposed in the right margin of Solimões River, between Tefé and Coari towns, Eastern Solimões Basin, Central Amazonia. The base of sections represents the lowermost water level of the river. Locations of sections are given in Figure 1.24
- Figure 5- Faciological aspects of LOV association in Central Amazonia. A) Laterally continuous tabular beds of laminated and massive mudrock. (B) Detail of A highlighted the even parallel lamination in mudrock. C) Well preserved leaves. D) Plant debris like "coffee grounds". E) Heterolithic beds with wavy-linsen structures composing a coarsening upward cycle. F) Detail of E) linsen bedding.28
- Figure 6- Faciological aspects of CCS association. A) Panoramic view of measured section 9 with indications of illustrations B, C, D, E, and F. B) Large-scale complex cross-stratification (Scc facies) with low-angle to sigmoidal cross-stratified sandstone with migration to ESE. C) Amalgamated lobate sandstone with sigmoidal cross-bedding in longitudinal and D) transversal views. E) Pinch and swell pattern related to the superposition of the sigmoidal lobe. F) Isolated trough cross-bedding (black arrow) and normal syndimentary faults (orange arrows).30
- Figure 7- Small- to large-scale crevasse splay. A) Evolution of a crevasse splay in the Cumberland Marshes in east-central Saskatchewan, Canadá, a) and b) show an early small lobate splay prograding through the levee of the trunk channel and with further growth, a sympodial pattern appears, and the channel becomes extensive and anastomosed in the most mature phase (Smith *et al.* 1989). B) Proximal, medial and distal parts of a crevasse splay complex developing subdelta comprise, respectively by 1) channelized erosively based sandstone, 2) interbedded sharply based sandstone and single to multiple coarsening upward successions forming lobate bodies (cf. Fielding 1984). Note de differences in scale between the crevasse subdelta and small-scale crevasse splay.32

- Figure 8- Faciological e geometric aspects of SLMC association. A) Large-scale inclined heterolithic stratification (IHS) in sandstone and mudrock. B) IHS of Solimões deposits truncated by the unconformity with Içá Formation. C) Inclined heterolithic beds and fine-grained sandstone with even parallel lamination. D) Subcritically and E) supercritically climbing ripple-cross lamination. F) Conglomerate lamina with mudrock intraclast. G) ferruginized plant debris (seeds?).....34
- Figure 9- Deformed facies from the SLMC association from Solimões Formation. A) and B) Tilted blocks underlaid by horizontal mudrock beds. C) Fold in heterolithic beds. D) Contorted beds in contact with undeformed laminated mudrock. F) inverse fault forming drag fold.....35
- Figure 10- Faciological aspects of MBMC association. A) Massive conglomerate with rounded mudrock clasts and sandy matrix. B) Trough cross-bedding in fine- to medium-grained sandstone. The orangish curved lines crossing the facies are ionic of iron oxide-hydroxide due to the recent weathering..... **Erro! Indicador não definido.**
- Figure 11- Faciological e geometric aspects of MBMC association. A) Medium-scale inclined heterolithic stratification (IHS) in sandstone and mudrock alternate with the cross-bedded sandstone. B) Detail of A showing the master bedding of IHS truncate by cross-stratified sandstone. C) Heterolithic inclined beds exhibiting fresh grey color and orangish weathered tonalities. D) Trunk fragment in master bedding showed E and F, generally in the horizontal position to the bedding..41
- Figure 12- Faciological e geometric aspects of FDP association. A) Panoramic view of The Içá Formation exhibiting abundant sandstone beds. B) Tabular and C) lenticular mudstone layer (mud plug). D) and E) root traces in mottled mudstone, note wood fragment with white halo of iron leaching. F) dissection cracks. G) Mottled rythmite with rip-up clast and dissection cracks.....43
- Figure 13- Crevasse splay deposits of FPC association. A) Coarsening upward cycles formed by fine-grained sandstone and mudrock layers. B) Sigmoidal cross-bedding with sets separated by mudrock layers. C) gutter cast filled by laminated mudrock. Cross-bedding highlighted by mud drapes.44
- Figure 14- Depositional model for the Miocene and Pleistocene succession in central Amazonia. See text for more explanation. A) The mega-wetland system in western Amazonia implanted in the subsiding Solimões Basin. B) Implantation of the Andean Amazon River caused by Andean tectonics and expressive sea-level fall resulting in the erosion and sediment bypass. C) The implantation of a mixed-to-bedload meandering system (Içá Formation) represents the Amazon River's sedimentation restart in Central Amazonia.....46

CAPÍTULO 4

- Figure 1- A) North of South America, the eastern border of the Solimões Basin, a region bordering the Amazon Basin, separates by the Purus Arch. B) Stratigraphic framework of the Solimões Basin. C-D) Urucu-Coari region with an indication of the points studied.....76
- Figure 2- A Stratigraphic profiles of the Neogene succession outcropping on the banks of the Solimões River, near the Urucu-Coari region, Central Amazonia. The profiles were marked with the lowest water level in the river—the location of the profiles in figure 1.....82
- Figure 3- Integrated areas of abundance of *M. franciscoi*, *G. magnaclavata*, and *M. annulatus* for the Miocene of Amazonia according to the intensity of the energy flow of paleoenvironments, based on palynological and geophysical data (Jorge *et al.* 2019). b) Diagram with % *M. annulatos* x other angiosperms for Central Amazonia (this work). c) Diagram with % *M. annulatos* x other angiosperms for the Amazon fan (Hoorn *et al.* 2017) and Western Amazonia (Jaramillo *et al.* 2017) as described by Kirschner and Hoorn (2020). d) Temperature curve for the Neogene (Zachos *et al.* 2008) with emphasis on the climatic optimum that occurred in the Middle Miocene. The dotted line in red represents a trend of variation for *M. annulatus*, in green the percentage variation of that pollen for the Miocene90
- Figure 4- Degree of preservation of pollen grains versus the amount of sporopollenin, with emphasis on the *Alnus* area, considered as semi-stable because it contains a large amount of sporopollenin. (mod. Havinga 1964, 1967, Brooks & Shaw 1972, Tomescu 2000).92
- Figure 5- Difference between reworked pollen grains. a) in diastema and b) in regional unconformity.94
- Figure 6- Quantitative graphical representation (percentage) of the main groups of palynomorphs found in the transition between Solimões and Içá Formation in Coari region, Central Amazonia. Observe the frequency of reworked palynomorphs present mainly at the top of the Solimões Formation.....96

Figure 7- The Purus Arch may have acted as a barrier to the development of a transcontinental drainage, capturing the influx of the Amazon River. A) The exposed Paleozoic rocks contain a diversified palynoflora, whose age is no older than that of Lochkovian, the basis of the Devonian period (Steeman *et al.* 2008). During the Late Miocene and the Lower Pliocene, it seems to have played the role of geographical barrier between the Solimões and Amazon Basins. The disagreement at the top of the Solimões Formation, observed over hundreds of kilometers, implies that the central and eastern Solimões Basin and the Purus Arch were uplifted and eroded, an event that could have lasted from the Upper Miocene to the Pliocene. B) The Cenozoic barrier of Purus Arch was confirmed by genetic and paleogeographic data from the ancestral distribution of *Psophia*, a trumpeter bird, restricted to the eastern Amazon during the Pliocene (Ribas *et al.* 2011). C) During the Pleistocene, this arch subsidized and deposited sediments of the Içá Formation. Thus, this event may represent the first stage in the evolution of the transcontinental drainage of the Amazon River.....99

Figure 8- Stratigraphic range of guide species identified in this work according to the literature.
.....78

Figure 9- Neogene-Pleistocene evolution of Central Amazônia and their relation with the palynomorphs amplitudes zones from Solimões Formation. A) During late Burdigalian the progressive subsidence of the Solimões Basin (SB), Western Amazonia cause the installation of Pebas-Solimões lake system (PSLS) confined by the uplift Purus Arch and Amazon Basin (AB) with the onset of the Cratonic Amazon River (CAR) record in the Novo Remanso Formation. Detrital zircon ages confirm the uplift of Andean west cordillera supplying the PSLS and cratonic inflow to CAR (cf. Mappes 2005). B) The increase of subsidence of SB in the Langhian-Serravalian was concomitant with the maximum eastward progradation of CAR with the developing a delta in the Atlantic Ocean (cf. Nogueira *et al.* 2021). C) The conjunction between the Lower-Middle Tortonian sea-level fall and the uplift of East Cordillera promoted a significative uplift and erosion of SB by the onset of Andean Amazon River (AAR) in 9,5 Ma, generating a sediment by-pass zone and an unconformity. The uplift AB during the Pliocene-Pleistocene has reduced accommodation space and the sediments are preserved locally. Lateritic crust forms during this period. The transcontinental drainage sedimentation is transferred to the delta and submarine fan in the Atlantic Ocean. D) During Pleistocene (400 Ka BP) a secondary drainage accumulates the Içá deposits covering the unconformity in the top of Solimões Formation. The gap estimate for the unconformity is ~9,5 Ma. The palynomorph amplitude zones of the Solimões Formation were truncated by the unconformity and recorded only as maximum age the base of Upper Miocene (Tortonian). 104

Figure 10- Percentage diagram of plant families and subfamilies for which botanical affinity is known drill core STG-02 (profile 3)..... 175

Figure 11- Range charts with pollen counts from drill core STG-02 (Profile 3) 176

LISTA DE TABELAS**CAPÍTULO 4**

Table 1- Lithofacies and sedimentary processes Urucu-Coari Region, Amazon state, Brazil..	62
Table 2- Facies Associations of Cenozoic succession in the Urucu-Coari Region.....	66
Table 3- Pollen raw counts of samples from the Solimões Formation, Central Amazonia, Brazil. RW = reworked. Sample 5-01, 5-07 e 5-21 (profile 5), sample 1-02 (profile 1), samples 4-01, 4-02 e 4-07 (profile 4). (see figure 2. Cap. 3).....	111
Table 4- Pollen raw counts of samples from the Core STG-02 (profile 3), Central Amazonia, Brazil. RW = reworked.	116

SUMÁRIO

RESUMO.....	vi
LISTA DE TABELAS	xiv
SUMÁRIO	xv
CAPÍTULO 1 INTRODUÇÃO	1
1.1 APRESENTAÇÃO.....	1
1.2 ORGANIZAÇÃO DA TESE	2
1.3 OBJETIVOS.....	3
1.4 ÁREA DE ESTUDO	4
1.5 O REGISTRO GEOLÓGICO E PALENTOLÓGICO DO NEÓGENO DA AMAZÔNIA.	4
1.5.1 Aspectos gerais.....	4
1.5.2 Bacia do Solimões	5
1.5.2.1 Formação Solimões	6
1.5.2.2 Formação Içá	7
1.5.2.4. O Gênero <i>Alnus</i> (estado da arte).....	8
CAPÍTULO 2 MATERIAL E MÉTODOS.....	11
2.1 PALINOLOGIA	11
2.1.1 Processo de extração de pólen	11
2.1.2 Tratamento com Ácido Clorídrico (HCl)	11
2.1.3 Tratamento com Ácido Fluorídrico (HF) concentrado.....	12
2.1.4 Tratamento com Ácido Acético Glacial (C₂H₄O₂).....	12
2.1.5 Tratamento com Acetólise	12
2.1.6 Montagem de lâminas para microscopia.....	13
2.2 ANÁLISE DE FÁCIES E ESTRATIGRÁFICA	13
CAPÍTULO 3 THE MIOCENE AND PLEISTOCENE DEPOSITS OF THE CENTRAL AMAZONIA: A RECORD OF THE PEBAS-SOLIMÕES MEGA-WETLAND SYSTEM DEMISE BY THE IMPLANTATION OF AMAZON RIVER.....	14
3.1 INTRODUCTION	15

3.2 GEOLOGICAL SETTING.....	18
3.3 STRATIGRAPHIC AND FACIES ANALYSIS	21
3.3.1 General Aspects	21
3.3.2 Facies Association.....	27
3.3.2.1 <i>Lake/overbank (LOV)</i>	27
3.3.2.2 <i>Composite Crevasse-splay (CCS)</i>	29
3.3.2.3 <i>Suspended-load meandering channel (SLMC)</i>	32
3.3.2.4. <i>Mixed-load to bedload meandering channel (MBMC)</i>	36
3.3.2.5. <i>Flood plain/crevasse splay (FPC)</i>	39
3.4 DEPOSITIONAL MODEL	43
3.5 CONCLUSIONS	45
ACKNOWLEDGMENTS.....	46
CAPÍTULO 4 PALYNOSTRATIGRAPHY OF NEOGENE DEPOSITS IN THE EASTERN SOLIMÕES BASIN: EVIDENCE FOR 9,5 Ma OF BY-PASS IN THE RECORD OF THE GREAT UNCONFORMITY IN THE CENTRAL AMAZONIA	51
4.1 INTRODUCTION	52
4.2 GEOLOGICAL AND PALEONTOLOGICAL CONTEXT	55
4.3 MATERIAL AND METHODS.....	58
4.3.1 Facies analysis.....	59
4.4 FACIES AND PALEOENVIRONMENT	60
4.4.1.1 <i>Lake/overbank (LOV)</i>	64
4.4.1.2. <i>Suspended-load meandering channel (SLMC)</i>	64
4.4.1.3. <i>Mixed-load to bedload meandering channel (MBMC)</i>	64
4.4.1.4. <i>Flood plain/crevasse splay (FPC)</i>	65
4.5 PALYNOLOGY	68
4.6 INDIGENOUS AND REWORKED POLLEN GRAINS.....	70
4.7 A PALYNOLOGICAL ZONATION FOR THE URUCU-COARI REGION	75
4.8 NEOGENE-PLEISTOCENE EVOLUTION OF CENTRAL AMAZONIA	79
4.8.1 The sediment bypass zone and origin of unconformity	79
4.8.2 The Andean Amazon River evolution influencing the palynomorphs amplitude zones	81

4.9 SUGGESTION FOR NEW RANGE OF ALNIPOLLENITES VERUS	85
4.10 CONCLUSIONS	86
CAPÍTULO 5 CONSIDERAÇÕES FINAIS.....	88
REFERÊNCIAS	90
SUPPLEMENTARY MATERIAL	111
SYSTEMATIC DESCRIPTION	124

CAPÍTULO 1 INTRODUÇÃO

1.1 APRESENTAÇÃO

Na região norte da América do Sul, particularmente nas bacias intracratônicas da Amazônia brasileira, o efeito do soerguimento andino desencadeou importantes modificações paleogeográficas e paleoambientais na região amazônica (Hoorn *et al.* 1995, Roddaz *et al.* 2005). A consequência direta da dinâmica evolutiva dos eventos tectônicos se reflete na ocorrência de numerosas bacias e sub-bacias como a do Solimões e Amazonas, as quais são separadas por arcos estruturais com registros de histórias de subsidência desconhecidas em unidades litoestratigráficas do Cretáceo e Cenozoico (Milani & Zalán 1999). As mudanças paleoambientais e paleogeográficas, associadas às variações climáticas, moldaram esta parte da América do Sul com implicações importantes para a implantação da drenagem transcontinental, desenvolvimento da floresta amazônica e sua biodiversidade. A maioria dos dados cronológicos das unidades neógenas são calcados em dados bioestratigráficos, enquanto unidades quaternárias têm sido datadas por C14 e luminescência opticamente estimulada (OSL).

O número limitado de determinações de idade frente à vasta área da região amazônica, obtidas a partir de palinomorfos e rochas vulcânicas raras, ainda são insuficientes para organizar as sequências de eventos e consequentemente aumentar a resolução estratigráfica desta região (Silva-Caminha *et al.* 2010, Guimarães *et al.* 2013, 2015, Nogueira *et al.* 2013, Silveira & Souza 2015, 2016, Kachniasz & Silva-Caminha 2016, Leite *et al.* 2016, D'Apolito 2016, D'Apolito *et al.* 2018, Lima Jr. *et al.* 2018, Jorge *et al.* 2019, Leandro *et al.* 2019, Pupim *et al.* 2019, Gomes *et al.* 2020, Leite *et al.* 2020). Apesar do conhecimento razoável das unidades estratigráficas, ainda faltam estudos detalhados dos sistemas deposicionais e, principalmente, o reconhecimento das discordâncias para assim restringir e refinar a amplitude das idades relativas que os palinomorfos fornecem.

As datações palinológicas e de carbono 14 têm balizado a maioria dos modelos geológicos sobre a evolução da paisagem amazônica, embora ainda não exista um consenso sobre a sequência de eventos para o sistema de drenagem. Os principais modelos são baseados, em grande parte, na análise de testemunhos de sondagens próximos à foz do Rio Amazonas, os quais sugerem que a implantação da drenagem transcontinental foi responsável pela instalação do Leque do Amazonas no Neomioceno entre 9,5 -8,0 Ma (Hoorn 1994, Hoorn *et al.* 1995, Potter 1997, Gingras *et al.* 2002,

Roddaz *et al.* 2005, Gorini *et al.* 2014, Figueiredo *et al.* 2009, Hoorn *et al.* 2017, Cruz *et al.* 2019). Esta proposta reflete apenas uma parte da história e não contempla os depósitos da calha principal do Rio Amazonas.

A mudança deste cenário até a instalação da drenagem transcontinental foi direcionada pela tectônica Andina e não ocorreu de forma abrupta, mas em etapas desde o final do Oligoceno-Mioceno inicial até o Quaternário (Nogueira 2008, Nogueira *et al.* 2013, van Soelen *et al.* 2017, Reis *et al.* 2016, Nogueira *et al.* 2021). As idades mais antigas obtidas em amostras de furos e afloramentos da porção oeste da bacia do Solimões remontam ao Paleoceno e Mioceno Médio (Daemon & Contreiras 1971, Hoorn 1993, 1994, Latrubesse *et al.* 2007, 2010, Leite *et al.* 2016).

Durante o Mesomioceno (14-10 Ma) o oeste da Amazônia era dominado pelo Sistema Lago Pebas-Solimões, confinado a leste pelo Arco de Purus (Hoorn 1993, Hoorn *et al.* 2010, Shepard 2010, Nogueira *et al.* 2013). Concomitantemente, a leste deste arco, o Rio Amazonas Cratônico fluía para o Oceano Atlântico durante o Mioceno Médio (14-10 Ma) e precedeu o Rio Amazonas andino (Nogueira *et al.* 2013, Nogueira *et al.* 2018, Nogueira *et al.* 2021). Idades palinológicas mais jovens como Plioceno (Latrubesse *et al.* 2010) e Plioceno-Pleistoceno (Campbell *et al.* 2006, Nogueira *et al.* 2013, Horbe *et al.* 2013) coincidem com dados biológicos (Ribas *et al.* 2012). Estas idades vão de encontro também com aquelas obtidas por meio do uso de OSL e sugerem pulsos sedimentares mais recentes ligados ao Rio Amazonas Moderno (Campbell *et al.* 2006, Rossetti *et al.* 2015, Nogueira *et al.* 2013, Gonçalves Jr. 2016, Pupim *et al.* 2016, Cremon *et al.* 2016, Soares *et al.* 2017).

Embora tenha havido um relativo avanço, principalmente na última década, na identificação dos subambientes e interpretações paleoambientais, existe a carência de maior integração dos resultados de subsuperfície e superfície visando um melhor entendimento bioestratigráfico. A pesquisa teve o intuito de avaliar as variações paleovegetacionais, paleoambientais e paleoclimáticas desde os eventos relacionados à implantação do sistema lago Pebas/Solimões, sua relação com o proto-Amazonas, até os eventos de soerguimento e erosão, posteriormente sucedidos pela progradação de depósitos fluviais pleistocenos da Formação Içá ligados a evolução do Rio Amazonas Moderno.

1.2 ORGANIZAÇÃO DA TESE

A estrutura organizacional desta tese se deu na forma de 5 capítulos, onde o

primeiro corresponde a uma seção introdutória cujo propósito foi remeter ao leitor uma abordagem geral a respeito da temática principal, bem como expor os objetivos e justificativas que motivaram a presente pesquisa de doutorado. A geologia da Bacia do Solimões é apresentada apenas nesta parte introdutória para que não haja repetição nos capítulos que versam sobre artigos científicos desenvolvidos durante o programa de doutoramento. No segundo capítulo foi descrito as metodologias utilizadas para elaboração dos artigos que compõe os capítulos terceiro e quarto. Os capítulos terceiro e quarto contextualizam os resultados correlacionados como artigos científicos, onde o primeiro refere-se a “**The Miocene and Pleistocene deposits of the Central Amazonia: a record of the Pebas-Solimões mega-wetland system demise by the implantation of Amazon River**” e o seguinte aborda a “**Palynostratigraphy of Neogene deposits in the eastern solimões Basin: evidence for 9,5 ma of by-pass in the record of the great unconformity in the Central Amazonia**”. O último capítulo apresenta as considerações finais compreendidas a partir de uma análise global da tese.

1.3 OBJETIVOS

Este trabalho teve como objetivo geral compor um arcabouço estratigráfico completo para o Cenozoico da porção central da Amazônia, com base em dados palinológicos e sedimentológicos, para isso foram alcançados os seguintes objetivos específicos:

a) elaboração de um perfil colunar composto-de-unidade utilizando dados de subsuperfície do poço STG-02 e de afloramentos na região de Urucu-Coari, integrando sucessões do Mioceno e Pleistoceno,

b) reconstituição do paleoambiente, paleovegetação, e as implicações paleoecológicas e paleogeográficas das formações Solimões (Mioceno) e Içá (Pleistoceno) da Bacia do Solimões,

c) correlações e interpretações geológicas da região estudada com os eventos ligados a orogenia andina,

d) avaliação das mudanças paleoclimáticas e a influência da variação relativa do nível do mar nos depósitos estudados durante o Neógeno e Pleistoceno na Amazônia.

Respondendo, dessa forma, perguntas como:

- 1) Como se comportaram tectonicamente as bacias do Solimões e do Amazonas durante o Neógeno e sua influência no controle paleogeográfico e

paleobiogeográfico?

- 2) Qual a importância dos arcos estruturais para a dinâmica evolutiva dos paleoambientes durante o Neógeno e Pleistoceno?
- 3) Qual o papel das sucessões do Neógeno e Pleistoceno no estabelecimento do Rio Amazonas?

1.4 ÁREA DE ESTUDO

A área estudada situa-se no norte do Brasil, região de Urucu-Coari, Estado do Amazonas. O Município de Coari encontra-se à margem esquerda do rio Solimões, local onde foram observados, descritos e coletados os materiais provenientes de depósitos aflorantes ligados a dinâmica fluvial. Pertencente ao território de Coari, a Província Petrolífera de Urucu foi o outro ponto analisado, através do testemunho de sondagem, STG-02, cedido pela PETROBRAS que o obteve durante o “Projeto Carvão no Alto Solimões”.

1.5 O REGISTRO GEOLÓGICO E PALEONTOLÓGICO DO NEÓGENO DA AMAZÔNIA.

1.5.1 Aspectos gerais

Depósitos cenozoicos têm sido considerados pelas primeiras explorações geológicas da Amazônia Ocidental como os únicos aflorantes nas calhas principais das bacias amazônicas, bordejados por rochas sedimentares paleozoicas. Os primeiros levantamentos foram baseados principalmente em dados geofísicos e de testemunhos de sondagem pela Petrobras e na década de 70, pelo DNPM por meio do Projeto Carvão no Alto Solimões (Maia *et al.* 1977). A densa cobertura vegetal e escassez de afloramentos tem limitado o mapeamento dessas unidades, bem como a falta de material adequado para a datação, dominados por depósitos arenosos expostos nas bacias do Solimões e Amazonas, denominadas anteriormente como bacias do Alto e Baixo Amazonas.

A premissa de que todos os depósitos aflorantes seriam cenozoicos foi novamente corroborada por Caputo & Soares (2016) que indiscriminadamente estenderam essa idade cenozoica desde a Bacia do Acre a oeste até a foz do Rio Amazonas, a leste. Estes autores não consideraram estudos prévios que fornecem dados sobre a ocorrência de rochas do Cretáceo aflorantes na Bacia do Amazonas e em subsuperfície recobertos principalmente por depósitos do Neógeno. Destacam-se o estudo dos paleossolos

lateríticos bauxíticos de idade paleógena enraizadas nos depósitos cretáceos e as crostas ferruginosas marcando os depósitos do Mioceno (Kotschoubey & Truckenbrodt 1981, Truckenbrodt *et al.* 1982, Costa 1991, Rossetti 2001, Rozo *et al.* 2005).

Além disso, palinomorfos índices do Cretáceo têm sido relatados como componentes retrabalhados nos depósitos do Neógeno da Bacia do Amazonas, assim como folhas fósseis de espécies extintas típicas dessa idade (Bezerra *et al.* 2018). Desta forma, a comprovação do embasamento Cretáceo (Fig. 1) implica na utilização desta superfície-chave para balizar as investigações bioestratigráficas do Cenozoico nas bacias amazônicas.

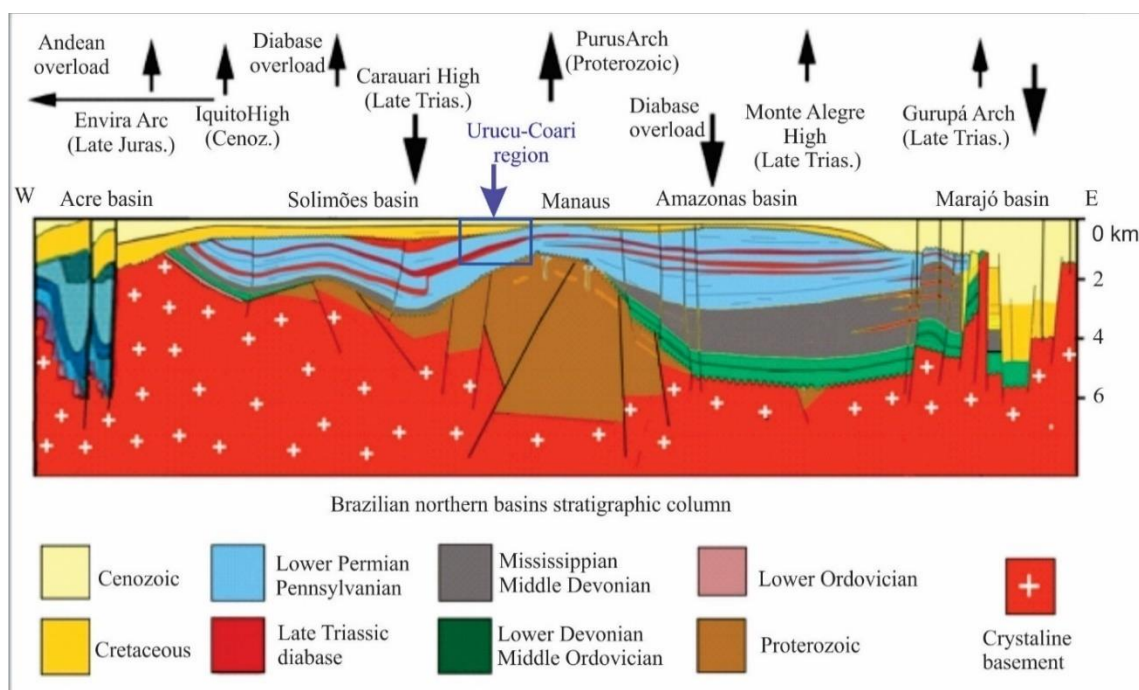


Figura 1- Seção esquemática W-E desde as bacias do Acre, Solimões, Amazonas e Marajó mostrando os arcos e altos estruturais (Modificado: Wanderley Filho & Travassos 2009). Observar que os depósitos Cretáceos afloram nas bacias do Acre e Amazonas. A área de Uruçu-Coari, objeto desta pesquisa, está localizada próximo do Arco de Purus.

1.5.2 Bacia do Solimões

A Bacia do Solimões é considerada uma sinéclise do tipo intracratônica de orientação leste-oeste, implantada em rochas cristalinas e sedimentares do Proterozoico da Província Amazônia Central (Fig. 2). A bacia é separada pelo Arco de Carauari que a divide nas sub-bacias de Jandiatuba e Juruá, ao leste, é limitada pelo Arco de Purus, que a separa da Bacia do Amazonas, e ao oeste pelo Arco de Iquitos, limite com as bacias subandinas e planície amazônica. Ao Sul, a Bacia do Solimões limita-se com o escudo Brasileiro Central e ao norte pelos escudos das Guianas (Fig. 2).

O registro sedimentar da Bacia do Solimões é marcado por múltiplos eventos de

regressão e transgressão marinha relacionados aos processos de subsidência e soerguimento, controlados pela atividade nos arcos estruturais ativos principalmente no Paleozoico (Caputo & Silva 1991). O Arco de Carauari teve controle decisivo na distribuição e espessura das sucessões sedimentares, principalmente no pré-Pensilvaniano, e provavelmente influenciou o acúmulo de sedimentos dos depósitos do Neocretáceo e Neógeno (Eiras *et al.* 1994). A última sequência deposicional da bacia do Solimões, correspondente ao Grupo Javari, individualiza-se em rochas do Cretáceo Superior da Formação Alter do Chão, que é separada por uma discordância erosiva da Formação Solimões, de idade Mioceno-Plioceno (Cruz 1984).

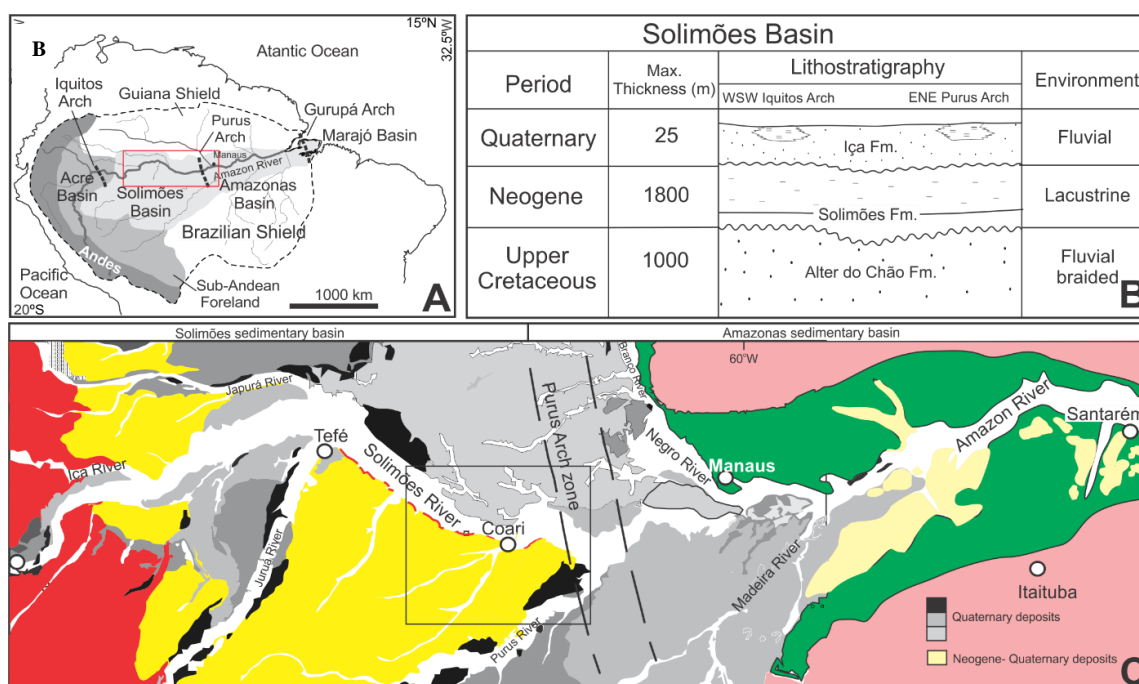


Figura 2- A) Norte da América do Sul, fronteira oriental da Bacia do Solimões, região limítrofe com a Bacia do Amazonas, separada pelo Arco do Purus. B) Arcabouço estratigráfico da Bacia do Solimões, onde em afloramento, a Formação Solimões alcança até 5m de espessura, sendo recoberta por depósitos da Formação Iça. C) Área de estudo situada na região de Urucu-Coari (modificado de Abinader 2012).

1.5.2.1 Formação Solimões

A Formação Solimões foi denominada por Rego (1930) para designar a seção cenozoica argilosa exposta ao longo do Rio Solimões. Esta unidade consiste de argilitos plásticos de cor cinza esverdeado com intercalações de linhitos fossilíferos (Maia *et al.* 1977). Esta unidade estende-se até as bacias do Acre e bacias subandinas com idade Mesomiocena (Hoorn 1994). Dados obtidos por meio de datação de U-Pb em zircões detríticos da Formação Solimões da região de Urucu-Coari indicaram população que inclui 190, 525, 1190 e 1400 Ma, com a máxima idade de 1515 ± 35 Ma (65 grãos), indicando que a proveniência é andina (Mapes *et al.* 2006). A unidade desta região foi

datada no Mioceno-Plioceno por palinomorfos (Silveira 2005, Nogueira *et al.* 2013, Guimarães *et al.* 2013, Silveira & Souza 2015, 2016).

O cenário paleogeográfico que precedeu a implantação da drenagem transcontinental do Rio Amazonas ocorrido provavelmente no Plio-Pleistoceno, era representado por um sistema lacustre extenso conectado a sistemas deltaicos rasos, bem expostos na região de Urucu-Coari, Estado do Amazonas (Nogueira *et al.* 2013). Este sistema deltaico-lacustre do Neomioceno-Plioceno não ultrapassava a região do Arco de Purus e provavelmente foi conectado a uma drenagem a leste desta estrutura desenvolvida na Bacia do Amazonas, o proto-Amazons (Mapes *et al.* 2006, Vega *et al.* 2007, Nogueira *et al.* 2013). Esta história ainda não foi completamente desvendada e representa um dos pontos motivadores do desenvolvimento desta pesquisa de doutorado.

1.5.2.2 Formação Içá

Maia *et al.* (1977) descreveram os arenitos da Formação Içá, na seção tipo, localizada ao longo do rio homônimo até sua foz no rio Solimões e, segundo estes autores, é discordante dos pelitos e arenitos da Formação Solimões. Essa discordância tem sido confirmada por Latrubesse *et al.* (1994), Rossetti *et al.* (2005), Silveira (2005), Vega (2006) e Nogueira *et al.* (2013) na região de Coari. Santos *et al.* (1974) e Lourenço *et al.* (1978) descrevem restos vegetais carbonificados na Formação Içá relacionados ao Pleistoceno. Segundo Melo & Villas Boas (1993), a Formação Içá foi depositada em ambiente fluvial de oeste para leste e é composta por arenitos silto-argilosos de coloração amarelo-avermelhado. Segundo Maia *et al.* (1977), a Formação Içá é uma sequência psamítica intercalados com pelitos e conglomerados, cujo contraste textural em imagem de radar permitiu delinear seu contato com a Formação Solimões.

A deposição desta unidade foi atrelada ao desenvolvimento de extensos canais meandantes, relacionada desenvolvimento do Rio Amazonas, com migração para NE-E em direção ao Atlântico (Rossetti *et al.* 2005, Nogueira *et al.* 2013). Estas planícies de inundação foram colonizadas por espécies de palmeiras, pteridófitas de água doce e florestas de várzea durante o Pleistoceno (Nogueira *et al.* 2015). Além disso, não foram observados algas e fungos, fato esse que pode estar relacionado às condições climáticas mais secas e / ou diferentes condições morfológicas da Formação Solimões (Guimarães *et al.* 2013).

A ocorrência do grão fóssil *Alnipollenites verus*, relacionado a Biozona *Alnipollenites verus* de Lorente (1986), encontrado na região de Coari confirma o

Pleistoceno para o topo da Formação Içá (Silveira 2005, Nogueira *et al.* 2013, Silveira 2015). No entanto esse importante marcador do Pleistoceno tem seus limites de primeiro aparecimento aqui revisados, afim de melhor compreender sua total zona de amplitude e assim baliza-lo aos principais eventos geológicos ocorridos na região.

1.5.2.4. O Gênero *Alnus* (estado da arte)

O Gênero *Alnus* inclui entre 29 e 35 espécies, ocorrendo principalmente no Hemisfério Norte, sendo sua morfologia única e diferenciada dentre à família Betulaceae (Murai 1964, Furlow 1979, Ashburner 1986, Faegri *et al.* 1989, Chen 1994, Govaerts & Frodin 1998, Blackmore *et al.* 2003, Chen & Li 2004, Sakalli *et al.* 2017). Heywood (1993), descreveu registros de *Alnus* ao longo das margens de riachos, rios e pântanos, em planícies úmidas ou nas encostas das montanhas, principalmente distribuídas nas zonas boreais e temperadas do Norte (Sakalli *et al.* 2017). Destas, pelo menos 18 espécies de *Alnus* ocorrem na Ásia (Hulten 1968, Murai 1968), onde apresentam um dos mais antigos registros de pólen de todas as dicotiledôneas, sendo posicionados no Cretáceo Superior (Srivastava 1967, Rouse 1971, Wolfe 1973, Miki 1977, Brown 1993).

Cerca de oito espécies de *Alnus* ocorrem na América do Norte, os mais antigos surgiram entre o Paleoceno e Eoceno (MacGinitie 1941, Johnson 1968, Leffingwell 1971, Wolfe 1977, Crane 1989, Lavrenko & Fot'janova 1993) bem como ao longo da orla do Pacífico (Leopold & Wright 1985, Leopold & Liu 1994, Liu & Leopold 1994, Reinink-Smith 2010). Duas espécies no México e somente uma se estende para a América do Sul tendo migrado em 1 milhão de anos (Hooghiemstra & Cleef 1995) ou mais recente (Pupim *et al.* 2019), já o restante das espécies de *Alnus* ocorrem na Europa (Chen & Li 2004).

Na América do Sul, os gradientes íngremes e a distribuição elevatória estreita dos tipos de vegetação tornam os Andes sensíveis a mudanças climáticas que induzem migrações verticais de espécies (van der Hammen & Gonzalez 1960, van der Hammen 1974, Hooghiemstra 1984, Bush *et al.* 1990, Colinvaux *et al.* 1996). Dados biogeográficos indicam que o *Alnus* se encontra em altitudes entre 2000 e 3000 m, zona de maior abundância em relação a chuva polínica (Bush 2000, Weng *et al.* 2004). O *Alnus* é comumente encontrado em assemblagens de pólen andinas modernas ou fósseis (Furlow 1979, Grabandt 1980, 1985, Hansen & Rodbell 1995, Weng *et al.* 2004), cujo único representante é o *Alnus acuminata*, (Furlow 1979, Gentry 1993). Nessas áreas as temperaturas médias anuais estão entre 8 e 18 ° C e mínimas de -10 ° C (Furlow &

Furrow 1979, Weng *et al.* 2004, Punyasena *et al.* 2011). Por não ser nativo do Brasil, os registros de *Alnus* apresentam baixos valores percentuais, sendo que sua disseminação pelo vento é mais significativa em até 100 km de sua árvore dispersora (Davis & Deevey 1964, Davis *et al.* 1973).

A alta acumulação de *Alnus* por liberação polínica é observada em depósitos localizados em altitudes abaixo de sua vegetação natural (Cleef & Hooghiemstra 1984). As diferentes espécies de *Alnus* são importantes no entendimento da história da sucessão vegetacional que corrobora a dinâmica climática do Quaternário (Connell & Slatyer 1977, Bormann & Sidle 1990, Chapin *et al.* 1994, Hu *et al.* 2001, Titus 2009, Lacourse 2009, May & Lacourse *et al.* 2012, Lima Jr. *et al.* 2018). Sakalli *et al.* (2017) cita que a distribuição potencial do *Alnus* não apenas depende exclusivamente de variáveis climáticas e composição de solo, mas sim da combinação de todas as variáveis que influenciam o desenvolvimento de uma árvore, por exemplo, diferenciação genética, competição e estresse biótico (Nowosad 2016).

O grão fóssil correspondente do *Alnus* é o *Alnipollenites* cuja variada diversidade de gêneros é representada por *Alnipollenites verus*, *Alnipollenites trina*, *Alnipollenites scoticus*, *Alnipollenites eminens*, *Alnipollenites speciipites*, e *Paraalnipollenites*. Registros para diferentes períodos ao redor do mundo foram publicados, como Cretáceo Superior -Japão (Takahashi 1970), Paleoceno - Ilhas Faroé - Atlântico Norte (Lund 1988), Mar do Norte - Europa (Schroder 1992, Kender *et al.* 2011), Wyoming - EUA (Wing *et al.* 2003), Groelândia (Jolley & Whitham 2004), Dakota do Norte - EUA (Zetter *et al.* 2011), Eoceno Superior - Malásia (Fong and Said 2002), Canadá (McDonald 1992), Eoceno Médio - Mar da Filipina, nordeste da China (Quan *et al.* 2011), Eoceno inferior - norte da Alemanha (Lenz *et al.* 2020), Oligoceno Superior-Mioceno Médio na Tailândia, (Watanasak 1990), República Tcheca (Dašková 2008), Mioceno Superior na Índia, (Mandaokar 2003), Polônia (Worobiec & Worobiec 2016), Mioceno Médio - Polônia (Słodkowska 2009), Plioceno-Pleistoceno no Alaska (Haeussler *et al.* 2017).

A tendência de retração das florestas tropicais durante o Mioceno, devido a diminuição de temperatura (Jaramillo *et al.* 2010), pode ter impulsionado o processo migratório das vegetações adaptadas ao clima frio, em direção a regiões mais tropicais. Assim, para a América do Sul, Germeraad *et al.* (1968) consideraram que a migração do pólen fóssil *Alnipollenites verus* ocorreu no Pleistoceno, essa dispersão foi facilitada por baixas temperaturas registradas para o período, já Lorente (1986), considerou o grão

fóssil como marcador do Plio-Pleistoceno (1,8 Ma -11 ka), tendo sido confirmado por outros autores (Muller *et al.* 1987, Hooghiemstra 1989, Nogueira *et al.* 2013, Soares *et al.* 2017) mas sendo raro nas terras baixas amazônicas (Nogueira *et al.* 2013, Silveira & Souza 2015).

A possibilidade da migração de vegetação do *Alnipollenites verus* até as terras baixas amazônicas antes do Pleistoceno é levantada no Capítulo 4, considerando o caráter pioneiro e adaptativo que responde favoravelmente às perturbações da floresta, de seu representante atual *Alnus* (Furlow 1979), além de pesquisas que registram a presença desse grão fóssil para o Mioceno superior (9.6 Ma) na Formação Gatun situada no Panamá (Jaramillo *et al.* 2014), Formação Chiquimil Mioceno superior (11.6-5.3 Ma), Argentina (Mautino & Anzótegui 2002) dados radiométricos corroboram essa idade (Kleinert & Strecker 2001). Dessa forma, se comprovada a natureza indígena deste pólen na região central da Amazônia será um forte indício que o *Alnipollenites verus* fazia parte da vegetação do Mioceno.

O resfriamento climático que se seguiu no Neopleistoceno, reduziu em cerca de 30% as concentrações atmosféricas de CO², quando comparado aos níveis do Holoceno, além de reduzir em 20% a precipitação, impulsionou táxons atualmente restritos aos Andes, como o *Alnus*, que apresenta alta capacidade de fixação de nitrogênio e tolerância à luz (Furlow 1979, Mayle *et al.* 2004), a migrar em direção às terras baixas da Amazônia e coexistisse com taxas equatoriais (Absy 1979, Colinvaux *et al.* 2000, Mayle *et al.* 2004, Feitosa *et al.* 2015, Sá *et al.* 2016), sendo presença comum em registros sedimentares da região (Soares *et al.* 2017).

Durante a deglaciação ocorrida a cerca de 11.000 anos o *Alnus* restringiu-se nas faixas atuais modernas onde se encontram desde aproximadamente 9000 anos. Buso Jr *et al.* (2013), analisaram que durante Holoceno Médio grãos de pólen de *Alnus* foram, provavelmente, transportados por massas de ar do sul da América do Sul geradas com o aumento da insolação de verão no Hemisfério Sul. Grãos desse pólen transportados dos Andes em direção às terras baixas da Amazônia raramente apresentam percentuais altos, sendo registrado menos de 1% em suspensão nas águas do Rio Solimões, próximo a Manaus (2100 km dos Andes) diminuindo com o aumento da distância da área fonte (Haberle 1997). Geralmente, entre 2 e 20% em pântanos e lagos, valores mais altos estão relacionados à presença indígena na vegetação local (Hooghiemstra 1984, Bush *et al.* 1990, Clapperton 1993, Colinvaux *et al.* 1997).

CAPÍTULO 2 MATERIAL E MÉTODOS

Para a elaboração deste projeto foram analisados afloramentos às margens do Rio Solimões com máxima espessura de 20 m, como também um testemunho de sondagem cedidos pela PETROBRAS (STG 02) com mais de 300 m de profundidade. As amostras fazem parte do acervo do Laboratório de Sedimentologia e do Grupo de Análises de Bacias Sedimentares da Amazônia (GSED) na Universidade Federal do Pará.

2.1 PALINOLOGIA

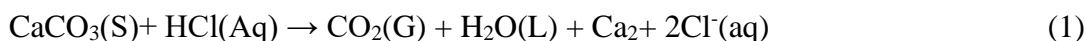
2.1.1 Processo de extração de pólen

De um modo geral, as amostras de sedimento coletadas exibiram grande concentração de matéria orgânica, cuja granulometria variou de areia até argila, fatos que a priori impossibilitam a identificação dos palinomorfos que estejam presentes. Em virtude disso, foram necessários procedimentos laboratoriais, como reações químicas, que enfatizaram a seleção dos grãos de pólen e a eliminação das demais partículas orgânicas e inorgânicas.

Para tal, utilizou-se um padrão de amostragem calibrado em 1 cm^3 , que é feita com precisão, para posterior cálculo de concentração polínica, sendo que o equipamento utilizado consisti num cilindro produzido a partir de aço inoxidável, onde o sedimento é inserido dentro de sua cavidade, sendo em seguida expelidos por um embolo, cujo produto adquirido são pastilhas que posteriormente serão introduzidas em tubos de centrífuga graduados em 15 ml e com fundo cônico, os quais são constituídos de polipropileno, tendo em vista sua utilização como meio receptor do ácido fluorídrico.

2.1.2 Tratamento com Ácido Clorídrico (HCl)

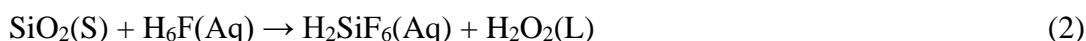
Nesta etapa os tubos previamente preparados com o material sedimentar e marcador exótico, foram submetidos a uma solução contendo 5 ml de HCl a 10%, cujo intuito foi a eliminação do carbonato de cálcio (CaCO_3). A reação ocorrida é expressa por (Equação 1):



Após, o material foi homogeneizado utilizando-se o Agitador Vórtex, modelo QI-901, que gera até 2800 rpm. O passo seguinte consistiu na separação da solução do material residual, por meio de centrifugação num período de 10 minutos com velocidade de 5000 rpm. Um ponto importante neste processo é o de lavagem do material com água destilada, seguindo os mesmos procedimentos acima citados, até que o sobrenadante encontre-se incolor ou transparente, que significará uma correta separação, assim não havendo perda do conteúdo decantado.

2.1.3 Tratamento com Ácido Fluorídrico (HF) concentrado

O segundo passo é o tratamento com HF, tendo em vista que as grandes quantidades de material silicático observado nas amostras poderiam impossibilitar a identificação dos grãos de pólen. Para tal, utilizou-se 3 ml desse ácido, que foi homogeneizado e deixado em repouso por 24 horas para dissolver a maior quantidade possível de sílica, cuja reação é expressa por (Equação 2):



Finalizado esse tempo, o material é levado à Centrífuga para separação e posterior retirada do líquido residual, sendo submetido a uma nova lavagem, para que assim possamos iniciar a terceira etapa.

2.1.4 Tratamento com Ácido Acético Glacial (C₂H₄O₂)

Nesta etapa foi visada a desidratação da amostra, sendo considerado um passo delicado do processo, preparando-as para inserção da acetólise, tendo em vista a reação entre água e ácido sulfúrico ser altamente exotérmica, podendo o material ser expelido do tubo de forma perigosa.

Para isso, adicionou-se 8 ml de C₂H₄O₂ aos tubos por um período de 20 minutos, cujos procedimentos seguintes foram a homogeneização e centrifugação com posterior descarte do líquido residual.

2.1.5 Tratamento com Acetólise

O último tratamento ácido a ser realizado foi a acetólise, cuja técnica desenvolvida por Erdtman (1952) e modificada em Melhem *et al.* (2003) consiste na remoção de celulose e polissacarídeos por meio de uma mistura contendo a proporção de

nove partes de anidrido acético (CH_3COCH_3) para uma parte de ácido sulfúrico concentrado (H_2SO_4).

Nesta etapa foi adicionado 3 ml da mistura para cada tubo, os quais foram acondicionados em banho-maria por 30 minutos a temperatura média de 70°C para catalisar a reação, sendo os mesmos homogeneizados em intervalos de 10 minutos. Após esse período o material foi centrifugado e realizada a lavagem com água destilada.

Por fim, o produto obtido desses tratamentos ácidos foi transferido para tubos de Eppendorf e preenchidos com água destilada e álcool.

2.1.6 Montagem de lâminas para microscopia

O material armazenado nos Eppendorfs foi retirado através do uso de pipetas de Pasteur e posteriormente adicionado sobre as lâminas Bioslide cujas dimensões são de 25,4 x 76,2 mm, sendo inserida também uma pequena quantidade de glicerina, cujo propósito foi estabelecer uma melhor fixação do conjunto (Moore *et al.* 1991). Feito isso, assentou-se as lamínulas 22 x 22 mm. Finalmente, a selagem foi realizada utilizando-se balsamo do Canada e Araldite, evitando assim exposição à umidade do ar.

2.2 ANÁLISE DE FÁCIES E ESTRATIGRÁFICA

As técnicas de modelamento de fácies proposto por Walker & James (1992) incluem *i*) a individualização e descrição das fácies (composição, geometria, texturas, estruturas sedimentares e conteúdo fossilífero), *ii*) a compreensão dos processos sedimentares, e *iii*) a associação de fácies, refletindo os diferentes ambientes e sistemas deposicionais representados na forma de blocos diagramas. A descrição de fácies será auxiliada por perfis verticais e seções panorâmicas obtidas a partir de fotomosaicos dos afloramentos seguindo o procedimento de Wizevic (1991) e Arnot *et al.* (1997). As superfícies-chaves identificadas serão usadas na correlação das seções e ciclos deposicionais.

CAPÍTULO 3 THE MIOCENE AND PLEISTOCENE DEPOSITS OF THE CENTRAL AMAZONIA: A RECORD OF THE PEBAS-SOLIMÕES MEGA-WETLAND SYSTEM DEMISE BY THE IMPLANTATION OF AMAZON RIVER

Walmir J.S. LIMA JR^a, Angela M. L. VEGA, Afonso C. R. NOGUEIRA^{a,b}, José BANDEIRA^{a,b}

^aPrograma de Pós-Graduação em Geologia e Geoquímica, Faculdade de Geologia, Instituto de Geociências, Universidade Federal do Pará, Rua Augusto Corrêa s/no, 66075-110, Belém, PA, Brazil, (anogueira@ufpa.br, jbandeira@ufpa.br, walmir.junior@ig.ufpa.com).

^bResearch Productivity of CNPq

ABSTRACT

Outcrop-based facies analysis of 25m-thick Miocene and Pleistocene deposits exposed along the Solimões River, Eastern Solimões Basin, Central Amazonia, revealed eleven sedimentary facies grouped in five associations: 1) lake/overbank (LOV), constituted by tabular beds of organic matter-rich laminated mudrock and subordinate sandstone, laterally continuous for dozens of kilometers, 2) composite crevasse splay (CCS) represent a 5 m-thick coarsening upward succession, laterally continuous for dozens of kilometers, of complex cross-stratified sandstone that include sigmoidal cross stratification, even parallel bedding, climbing ripple cross lamination and deformed beds and frequently shows eastward inclined foresets related to proximal crevasse subdelta lobes and tabular distal crevasse deposits interbedded with LOV association, 3) suspended-load meandering channel (SLMC), represented by point bar deposits consisting of large-scale inclined heterolithic stratified sandstone and mudrock with vegetal debris, oriented to ESE, interbedded with thin layers of intraclastic (mudrock) conglomerate, and deformed beds (disharmonic folds, convolute bedding and tilted mudrock block), 4) Mixed- to bedload meandering channel (MBMC), related to the point bar deposits consisting of medium-scale inclined heterolithic stratified sandstone and mudrock with trunks and vegetal debris, fine- to medium-grained pebbly sandstone and conglomerate (quartz and mudrock clasts) with trough and planar cross-bedding dipping predominantly to ENE, and 5) flood plain/crevasse splay (FPC), comprising bioturbated and vegetal debris-rich mudrock and fine-grained sandstone organized in meter-scale coarsening upward succession. During the upper Miocene, the extensive

lacustrine system, feeder by suspended-load meandering channels, dominated the subsiding Solimões Basin in the Central Amazônia. These large overbank areas were constantly flooded and filled by crevasse subdelta deposits. This extensive mega-wetland system was limited to the E with the Purus Arch. The Andean tectonics affected Central Amazonia dramatically, causing the progressive uplift of the Solimões Basin and the emergence and erosion of the mega-wetland succession. This event was amplified by the expressive sea-level fall in middle-Tortonian (11-8 Ma), resulting in the Andean Amazon River's onset. Only in the Late Pleistocene, the Solimões Basin subsided, causing the implantation of a mixed- to bedload meandering system that represents the sedimentation restart of the Amazon River in the Central Amazonia.

Keywords: Neogene, Amazon River, Solimões Formation, Içá Formation, Pebas-Solimões Lake.

3.1 INTRODUCTION

Significant changes in the landscape marked the Late Paleogene-Neogene of the western Amazonia, where paleoenvironmental conditions influenced the formation of the modern Amazon rainforest and the onset of the Amazon fluvial system (e.g., Hoorn, 1993, Latrubesse *et al.* 2010, Hoorn *et al.* 2010, Hoorn & Wesselingh 2010, Wesselingh & Salo 2006, Hoorn *et al.* 2010). Remarkably, the early-middle Miocene depositional system in the western Amazonia was characterized by a mega-wetland system with short marine inundations (Hoorn 1993, Boonstra *et al.* 2015, Jaramillo *et al.* 2017, Linhares *et al.* 2017). This depositional system comprising continental, predominating fluvial-lacustrine system (Westaway *et al.* 2006, Latrubesse *et al.* 2010) and mixed-tide coastal settings (Räsänen *et al.* 1995, Hovikoski *et al.* 2005, Rebata-H *et al.* 2006) extending almost 2000 km to the east, along the Solimões-Amazonas River (Nogueira 2008, Nogueira *et al.* 2013). Therefore, this conception is dependent on the authors and location, that include these deposits in different lithostratigraphic units such as Pebas, Ipururo, Iñapari, Curaray, Madre de Dios, Nauta, La Tagua layers, Amazonian Tertiary, and Solimões (Maia *et al.* 1977, Hoorn 1994, Hoorn *et al.* 2010, Campbell *et al.* 2001, Roddaz *et al.* 2005, 2006, Nogueira 2008, Nogueira *et al.* 2013). These deposits consist mainly of black to gray organic matter-rich mudrock, rhythmites, siltstone, sandstone, conglomerate, levels of carbonate rocks, and lignite beds (e.g., Hoorn *et al.* 1995,

Wesselingh & Salo, 2006, Cozzuol 2006, Latrubesse *et al.* 2010, Hoorn *et al.* 2010, Silva-Caminha *et al.* 2010, Nogueira *et al.* 2013, Leite *et al.* 2017, 2020).

The history of Pebas-Solimões mega-wetland system is intimately connected with the evolution of the Amazonian landscape and the Amazon River, despite there is still no consensus on the sequence of geological events. The main models are based mainly on the analysis of drill cores near the mouth of the Amazon River and assume that the implementation of the Andean transcontinental drainage was responsible for the installation of the Amazon fan in the Upper Miocene between 9.5 and 8.0 Ma (Hoorn 1994, Hoorn *et al.* 1995, Potter 1997, Gingras *et al.* 2002, Roddaz *et al.* 2005, Gorini *et al.* 2014, Figueiredo *et al.* 2009, Hoorn *et al.* 2017, Cruz *et al.* 2019). This proposal reflects only part of the history, not including the record of the Amazon River's main channel in Central Amazonia, distant for thousands of kilometers of the coastal region. The change from this scenario since the implantation of mega-wetland until the installation of transcontinental drainage driven by the Andean tectonics did not occur abruptly but took place in steps from the late Oligocene-early Miocene until the Quaternary (Nogueira 2008, Nogueira *et al.* 2013, van Soelen *et al.* 2017, Reis *et al.* 2016, Nogueira *et al.* 2021).

The older ages obtained in the borehole and outcrop samples of the western portion of the Solimões Basin go back to the Miocene until Pliocene (Daemon and Contreiras 1971, Hoorn 1993, 1994, Latrubesse *et al.* 2007, 2010, Leite *et al.* 2016, 2020). During the Middle Miocene (14-10 Ma), the western Amazon was dominated by Pebas-Solimões lacustrine environments, confined to the east by the Arch of Purus (Hoorn 1993, Hoorn *et al.* 2010, Shepard 2010, Nogueira *et al.* 2013). Concomitantly, east of this arc, the cratonic Amazon River flowed into the Atlantic Ocean during the Middle Miocene (14-10 Ma) and preceded the Andean Amazon River (Nogueira *et al.* 2018, Nogueira *et al.* 2013, Nogueira *et al.* 2021). Younger palynological ages such as Pliocene (Latrubesse *et al.* 2010) and Pliocene-Pleistocene (Campbell *et al.* 2006, Nogueira *et al.* 2013, Horbe *et al.* 2013) coincide with biological data (Ribas *et al.* 2012). These recent ages by pollen match with Quaternary ages obtained by optically stimulating luminescence (OSL), suggesting deposition since 400 Ka BP linked to the Modern Amazon River (Campbell *et al.* 2006, Rossetti *et al.* 2015, Nogueira *et al.* 2013, Rossetti *et al.* 2015, Gonçalves Jr. 2016, Pupim *et al.* 2016, Cremon *et al.* 2016, Soares *et al.* 2017). The stratigraphic proposals for Neogene deposits formulated in the

western Solimões and sub-Andean basins not including the Central Amazonia, which comprises the eastern Solimões and the Amazonas basins, where the studies with this focus are still incipient (Rossetti *et al.* 2005, Dino *et al.* 2012, Nogueira *et al.* 2013).

For decades, the Neogene deposits in the Central Amazonian lowlands have been stacked in two lithostratigraphic units, the Miocene-Pliocene Solimões Formation and Upper Pleistocene Içá Formation overlaid by Upper Pleistocene-Quaternary deposits (Fig. 1). These units are separated by an angular unconformity observed by hundreds of kilometers in the right margin of Solimões River (Maia *et al.* 1977, Nogueira 2008, Nogueira *et al.* 2013, Horbe *et al.* 2013, Rossetti *et al.* 2015). Recently, Pupim *et al.* (2019) disregarded this stratigraphic framework and the age by pollen for the Solimões Formation, based mainly on OSL ages of 95 to 35 ka BP, suggesting that the Solimões and Içá formations represent a single unit of the upper Pleistocene. This age-restricted range has led the authors to state that these units represent the current Terra Firme forest substrates of the Central Amazonia. According to Pupim *et al.* (2019), these deposits cannot be named and mapped using lithostratigraphy, which implies a rock unit and not recent fluvial terraces. Therefore, the OSL ages of Pupim *et al.* (2019) could not be certified due to the lack of specific and statistical details of the palynological content of only two samples of the studied succession. Following these authors' proposal, pollen grains provided Miocene-Pliocene ages like *Grinsdalea magnaclavata* were considered reworked, and the Pleistocene pollen as *Alnus* was overestimated to reinforce the OSL ages. These authors also interpreted the Solimões-Içá succession as multiple fluvial bar aggradation episodes composed of continuous fining-upward cycles without performing a detailed facies analysis. Pupim *et al.* (2019) reduces the geologic history to only 200 Ka BP, ignoring the previous older pollen ages used to the evolution of the Miocene cratonic and Andean Amazon River (cf., Hoorn *et al.* 1995, 2010, 2017, Wesselingh & Salo 2006, Cozzuol 2006, Nogueira 2008, Figueiredo *et al.* 2009, Silva-Caminha *et al.* 2010, Hoorn *et al.* 2010, 2017, Nogueira *et al.* 2013, Horbe *et al.* 2013, Leite *et al.* 2017, 2020, Nogueira *et al.* 2021).

The most evident problems that hinder to unravel of this Neogene evolution are 1) the misinterpretation that the deposition occurred continuously in a unique basin with the same tectonic behavior, 2) absence of faciological study in the central Amazon to demonstrate the depositional scenario changes before, during and after the establishment of the transcontinental Amazon drainage, 3) the modification of the

drainage system never was showed with paleocurrents data, 4) the difficulty in identifying regional unconformities in deposits with similar lithologies, 5) the use of relative ages to the Neogene succession as if there was no break in the geological record, 6) do not consider the activity of the arches and the different tectonic behavior of the basins. This last key point raises significant questions about when and how these arcs (i.e., Purus Arc) or the basin tectonics influenced the connection between Solimões and Amazonas basins during the onset of the Amazon River. The outcrop-based facies and stratigraphic analysis of this Neogene succession exposed near Coari and Tefé towns are strategic to solve these questions. We rescue the previous lithostratigraphy of the Central Amazonia, considering the Solimões and Içá formations units of the Solimões Basin. New paleoenvironmental data are presented with paleogeographic information for the Central Amazonia during the Miocene (Fig. 1).

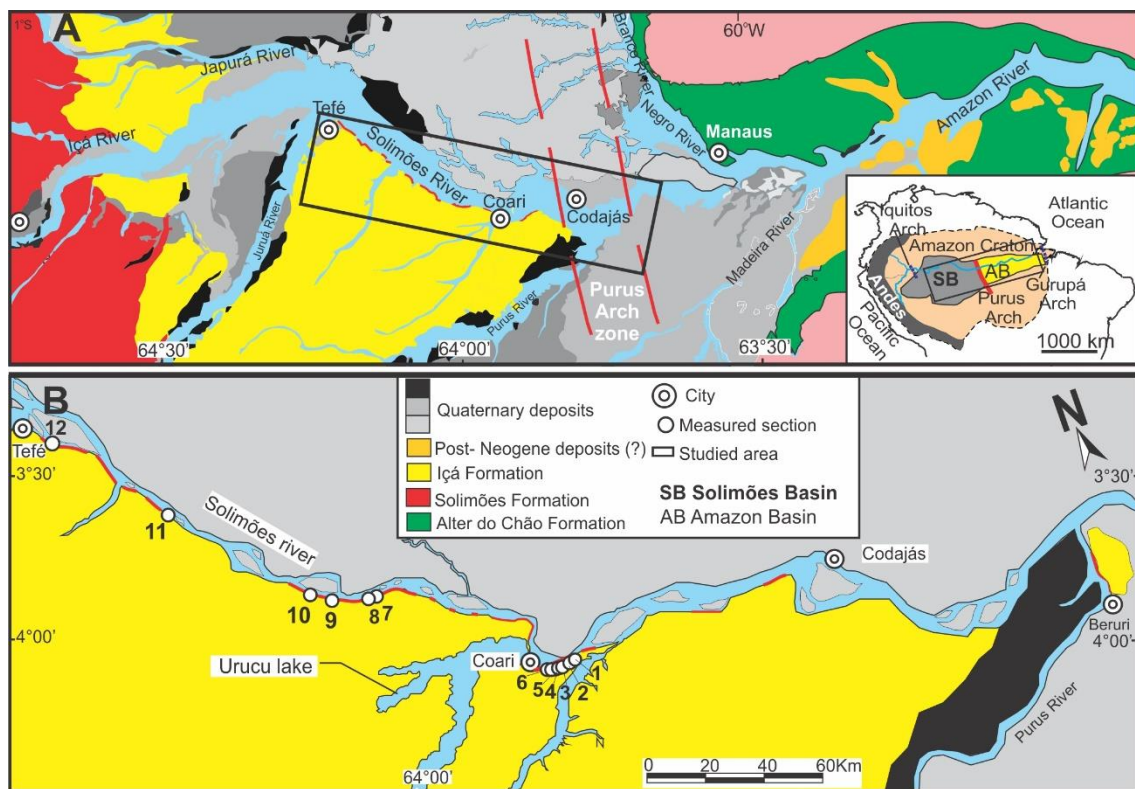


Figure 1- Geotectonic units of the Central-Eastern Amazonia. A) Simplified geological map (Modified from Wanderley Filho *et al.* (2007), Brazilian Geological Survey -CPRM, 2010 and Rossetti *et al.* 2005). B) The study area and location of measured sections.

3.2 GEOLOGICAL SETTING

The Meso-Cenozoic Amazonian retro arc foreland basin is installed in western South America, including currently Amazonas-Putumayo, Oriente, Pastaza-Marañón, Huallaga, Madre de Dios, Beni-Mamore, Solimões and Acre basins, respectively in

Colombia, Ecuador, Peru, Bolívia and Brazil (Caputo *et al.* 1990, Roddaz *et al.* 2006, Hoorn *et al.* 2010, Louterbach *et al.* 2018, Hurtado *et al.* 2018). The Miocene depositional environment of the Amazonian retro arc foreland basin is characterized by the Pebas-Solimões mega-wetland system composed of lakes and swamps, with fluvial and marginal marine influence (Wesselingh & Salo 2006, Cozzuol 2006, Latrubesse *et al.* 2010, Hoorn *et al.* 2010, Silva-Caminha *et al.* 2010, Nogueira *et al.* 2013, Leite *et al.* 2017). The use of the term Pebas-Solimões in this work is because the Pebas unit defined in Peru extends as Solimões Formation almost 2000 km to the east in Brazilian Amazon, along the Solimões-Amazonas River until the Purus Arch zone (Hoorn *et al.* 1995, Wesseling *et al.* 2002, Latrubesse *et al.* 2007, 2010, Nogueira *et al.* 2013) (Fig. 1). Hoorn (1993) concluded that the Pebas Formation included at least three pollen zones, spanning an age between late Early Miocene and early Late Miocene (c. 17-10 Ma) coincident with the biozones found in Solimões Formation (cf., Leite *et al.* 2017, 2020). Following the stratigraphic code and recent facies analysis, the Solimões Formation is restricted to the Solimões Basin (Nogueira *et al.* 2013). It is correlated to units of the same age in sedimentary basins of Acre, Bolivia, Peru, and Colombia, so contesting Caputo *et al.* (1971)' proposal.

The Fitzcarrald, Iquitos, and Purus arches can be formed significant interfluvial reliefs that influenced the Neogene Amazonian drainage and the sediment distribution in the Amazonian retro arc foreland basin (Roddaz *et al.* 2005, Espurt *et al.* 2007, Nogueira 2008, Hoorn *et al.* 2010, Nogueira *et al.* 2013, 2021). The westward cratonic drainage in lowland Amazonia, before the Miocene (c. 23 Ma), was captured by Andean rivers that flowed to the lake and coastal regions connected to the Maracaibo Lake and forming a seaway to the Caribbean Sea (Hoorn *et al.* 1995, Lundberg *et al.* 1998, Wesselingh & Salo 2006, Roddaz *et al.* 2010, Nogueira *et al.* 2013, Hurtado *et al.* 2018).

The Solimões Basin has an east-west orientation, located in the West to Central Amazonia, between the Guianas and Brazilian shields (Wanderley-Filho *et al.* 2010). It is separate from Acre and Pastaza/Marañon basins to the west by Iquitos Arc and the Amazonas basin to the east by Purus Arc (Fig. 1A). The sedimentary record of the Solimões Basin is marked by multiple climatic changes, marine regression, and transgression during the Paleozoic and tectonic activity that promotes subsidence and uplift of structural arcs (Caputo & Silva 1991). The Paleozoic sequence in the Solimões

basin is divided into two sub-basins by the Carauari Arch, which controlled the distribution and thickness of the sedimentary successions, mainly before Pennsylvanian time. However, the Carauari arch seems to have influenced the Cretaceous and Neogene deposition, represented respectively by the Alter do Chão and Solimões formations, both units separated by a regional unconformity (Eiras *et al.* 1994). The Cretaceous Alter do Chão Formation corresponds to a westward migration high-energy fluvial system developed under humid climate extended from the Amazonas Basin until sub-Andean basins (Caputo 1984, Mendes *et al.* 2012).

The Neogene tectonic history of the Solimões Basin and other basins of northern South America were marked by the uplift of the northern-eastern Andes with the development of the sub-Andean fold belt, the product of readjustments of the plate tectonics (Hoorn *et al.* 1995). The eastern propagation of orogenesis produced by the Andean activity caused a loading stage in the foreland Amazon system (Roddaz *et al.* 2005), resulting in tectonic reactivation of structural arcs. Iquitos Arch's influence in these regions has been proved by sedimentological, pollen, and provenance analyses (Hoorn *et al.* 2010, Roddaz *et al.* 2005, Espurt *et al.* 2007, Horbe *et al.* 2013, 2019).

The tectonic significance of Purus Arc, east limit of the Solimões Basin (Fig. 1A), has been well addressed for the Paleozoic times when it was a significant barrier (Eiras 2000, Wanderley-Filho 2010). However, the influence of Purus Arc in the Neogene sedimentation is still uncertain. In the Neoproterozoic, the Purus Arch region was a graben filled by siliciclastic and carbonate deposits, afterward inverted (Wanderley Filho *et al.* 2010, Barbosa & Nogueira 2011). During the Paleozoic and Mesozoic, the Purus Arch controlled the migration of depositional systems of the Solimões and Amazonas basins and the extension of the mega-wetland (Mapes *et al.* 2006, Wanderley-Filho *et al.* 2010, Shephard *et al.* 2010, Nogueira *et al.* 2013, 2021).

The Solimões Formation unconformably overlies the Cretaceous deposits of Alter do Chão Formation. It is composed of whitish to greenish-grey mudrock with massive to laminated bedding, interbedded with lignite, forming layers from 2 to 10 m thick, and fine- to coarse-grained sandstone with subangular to subrounded grains, deposited in a continental system related to a fluvial-lacustrine setting (Maia *et al.* 1977, Caputo 1984, Milk 1988, Gross *et al.* 2011, Silva-Caminha *et al.* 2010, Latrubesse *et al.* 2010, Nogueira *et al.* 2013). This unit is unconformably covered by the Içá Formation that consists of fine to medium-grained sandstones, siltstones, and locally by reddish-

yellow conglomerates (Maia 1977, Nogueira *et al.* 2013). The Upper Miocene-Pliocene age for the Solimões Formation in Central Amazonia is provided by the high concentrations of *Fenestrites longispinosus*, *Fenestrites spinosus*, associated with *Echitricolporites spinosus* and *Bombacacidites ciriloensis* (Nogueira *et al.* 2013). Additionally, the presence of *Bombacacidites bellus*, *Echiperiporites akanthos* Van Der Hammen & Wijmstra, 1964, *Echiperiporites estelae*, *Psilatricolporites crassoexinatus* Hoorn 1993 and *Cyathidites annulatus* reinforce this age interpretation (Hoorn 1993, Torres & Méon 1993, Nogueira *et al.* 2013, Leite *et al.* 2017, 2020). This age agrees with the previous dating of the upper Solimões based on mammalian biostratigraphy (Latrubesse *et al.* 1997, 2007 and 2010).

The Pliocene-Pleistocene Içá Formation is defined by the high concentration of *Bombacacidites bellus*, *Clavamonocolpites lorentei*, *Echiperiporites lophatus*, *Perisyncolporites pokornyi*, *Cingulatisporites laevigatus*, *Leiotriletes adriennis* and *Psilatriteles peruanus*, which last appearance datum (LAD) restricted to the Pliocene (Lima & Amador 1985, Lorente 1986, Muller *et al.* 1987, Lima & Melo 1994, Hoorn 1994b, Stuchlik *et al.* 2001, Silva-Caminha *et al.* 2010, Nogueira *et al.* 2013). The top of Içá Formation is marked by the first appearance datum (FAD) of *Alnipollenites verus* of Pleistocene age coincident with the T-18 Biozone of Jaramillo *et al.* (2011).

3.3 STRATIGRAPHIC AND FACIES ANALYSIS

3.3.1 General Aspects

The terminology used in this work follows the proposal of Maia *et al.* (1977) and Nogueira *et al.* (2013). The age of studied deposits exposed in the eastern Solimões Basin, between Tefé and Coari towns was based on the palynologic study of Nogueira *et al.* (2013) compared with the biozones of Jaramillo *et al.* (2011) T-16 to T-18 that include the middle to upper Miocene and Pleistocene (Fig. 2). The Solimões Formation reaches a thickness of 4m and up to 14 m in the Tefé region and comprises grey mudrock, and fine-grained sandstone rich in organic matter and plant remains. This unit is unconformably overlaid by the Içá Formation constituted by fine to coarse-grained sandstone, mudrock and, conglomerates with mudrock pebbles (Fig. 2 and 3).

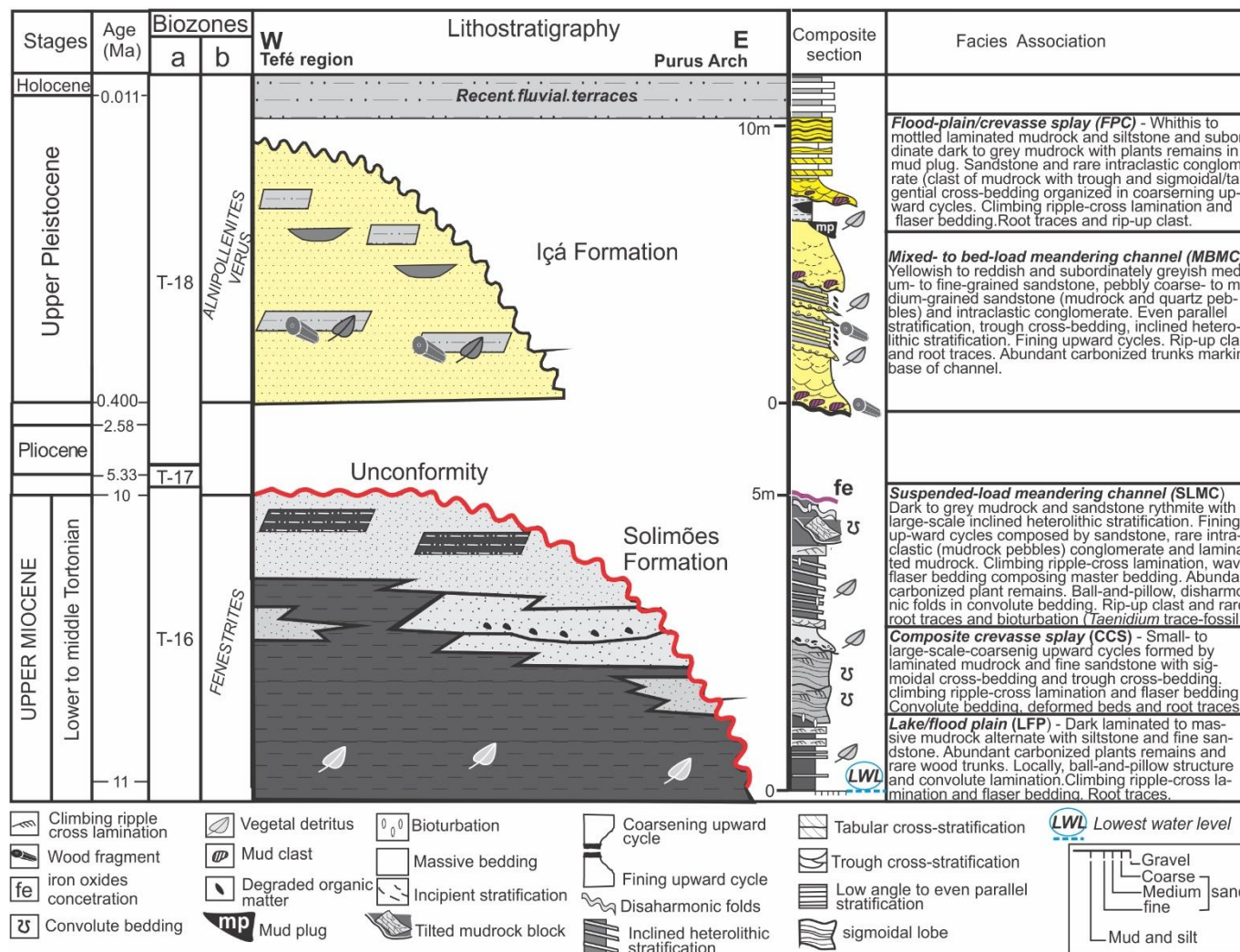


Figure 2- Neogene lithostratigraphy of the eastern Solimões Basin, Central Amazônia. Biozones “a” and “b” are respectively from Jaramillo *et al.* (2011) and Nogueira *et al.* (2013). The “b” biozones were defined to the studied succession and refers to Fenestrites longispinosus and Fenestrites spinosus with Echitricolporites spinosus Bombacacidites ciriloensis that indicate upper Miocene to Pliocene age. The Alnipollenites verus is typical, but not exclusive, of Pleistocene strata. The initial mark in 10 Ma for the unconformity match with the Andean Amazon River's onset (cf. Gorini *et al.* 2013, Hoorn *et al.* 2019) and indicate a gap that includes the Pliocene and Lower to Middle Pleistocene. The minimum age for Içá Formation of ~400 Ka BP is provided for OSL age (Rozo 2005, Rossetti *et al.* 2015, Pupim *et al.* 2019). The average thickness for each formation is indicated in the composite section.

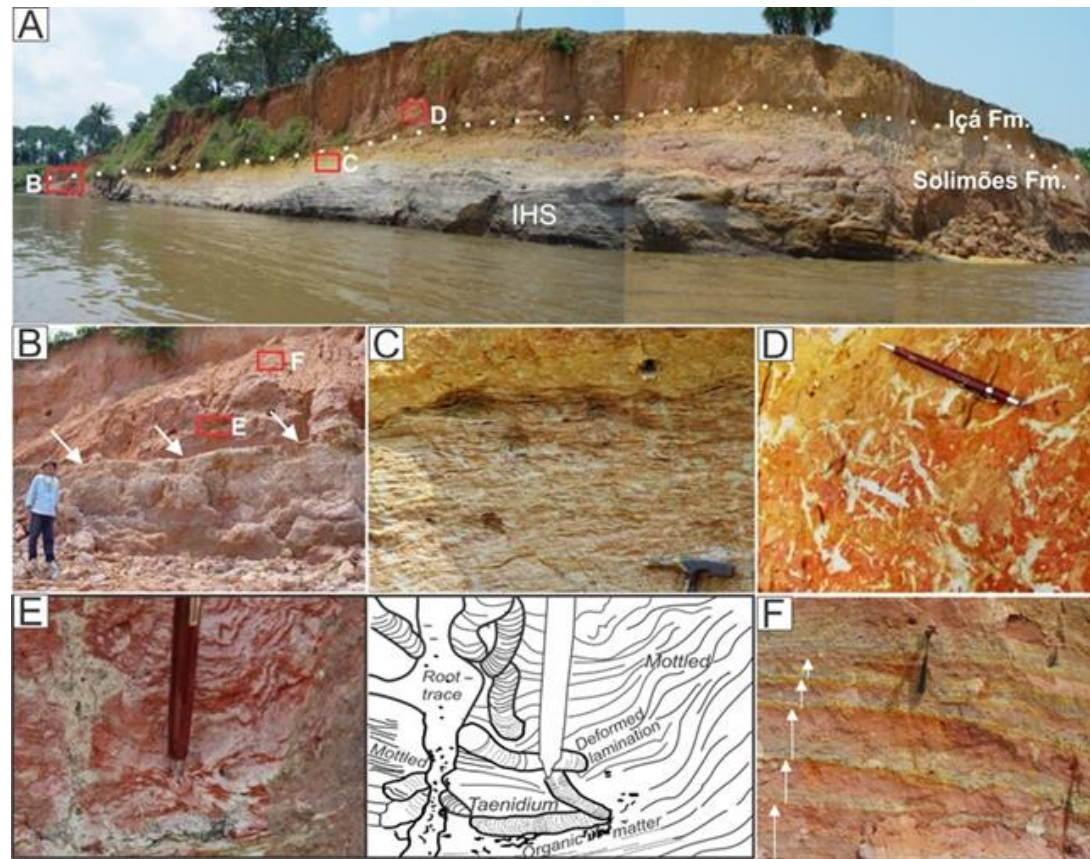


Figure 3- The unconformity between Solimões and Içá formations near Coari town. A) Greyish fine-grained sandstone alternated with mudrock composing large-scale inclined heterolithic stratification (IHS) overlaid by reddish-orangish sandstone. B) Undulated surface (white arrows) marks the erosive surface. C) Climbing-ripple cross lamination in IHS sandstone, D) root marks and E) Taenidium trace fossil with organic matter remains occur in F) mottled rhythmite forming coarsening upward cycles of the Içá Formation.

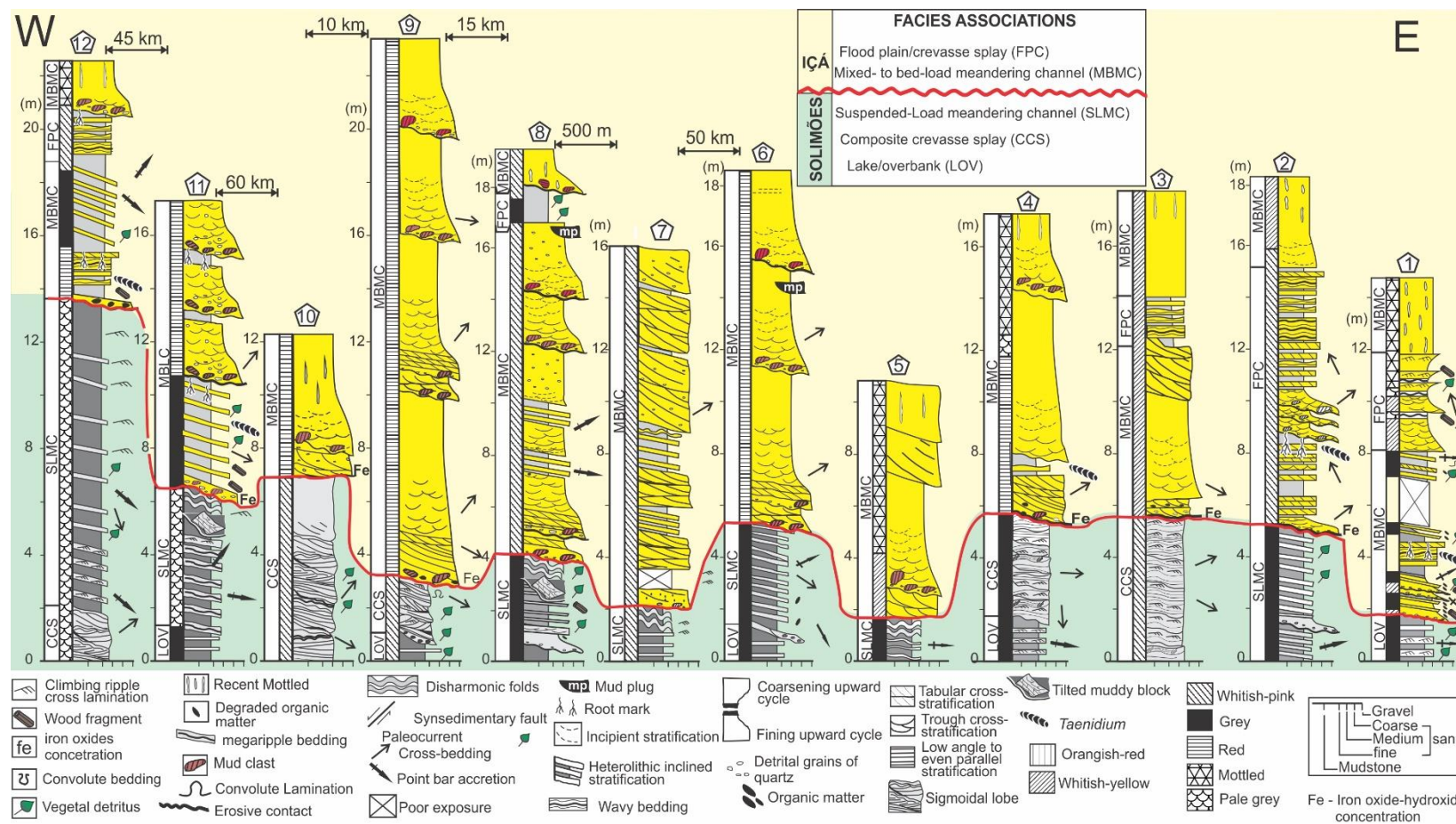


Figure 4- Stratigraphic sections of Neogene succession exposed in the right margin of Solimões River, between Tefé and Coari towns, Eastern Solimões Basin, Central Amazonia. The base of sections represents the lowermost water level of the river. Locations of sections are given in Figure 1.

The unconformity is observed for hundreds of kilometers along the outcrops in the Central Amazonia, marked by iron oxide-hydroxide concentration, a sharp change in lithology, structure, color, and depositional system (Figs 2, 3, and 4). The Içá overbank deposits are frequently found covering this contact characterized by coarsening upward cycles, generally mottled with root marks and trace fossils (Figs 2, 3, and 4). The regional unconformity coincident with the Andean Amazon River's onset in 10 to 8,5 Ma linked to the Tortonian global sea-level lowstand observed in the Amazon fan deposits (Pasley *et al.* 2005, Figueiredo *et al.* 2009, Gorini *et al.* 2013, Hoorn *et al.* 2019, Nogueira *et al.* 2013, 2021). It is associated with a (Figueiredo *et al.* 2009, Gorini *et al.* 2013). The difference of ages between both units indicates a gap of approximately 9,5 Ma without a lithologic record.

Twelve measured sections were described, and eleven sedimentary facies were identified and codified following Miall (1985). The bedding in the studied succession is horizontal or inclined, and deformed beds occur on the erosive top of the Solimões Formation. The Içá Formation comprises thick beds of fine- to medium-grained sandstone and conglomerate with trough cross-bedding (Figs 2, 3, and 4). Eleven facies were grouped into five associations: lake/overbank, meandering channel, floodplain, and crevasse splay settings (Fig. 2 and 3, Table 1).

The paleocurrent measures from cross-bedding and inclined heterolithic beds indicate the migration of bedforms and point bar accretion (Fig. 4). In the Solimões Formation, the dip angle of inclined heterolithic beds ranges from 5° to 25°, the direction of these beds ranges from 30° to 158°, forming a large unimodal shape towards SE-E (Fig. 4). The paleoflow indication is not associated with inclined beds ranges from 186° to 240°, presenting a tight unimodal pattern with SW direction. The mean vectors of accretion of inclined beds and paleocurrents of directional structures produced an angle of around 30°. The Içá Formation shows bedforms with a strong tendency towards NE and SE in layers with tabular and trough cross-stratification and inclined heterolithic beds with an E orientation (Fig. 4). The small-scale inclined heterolithic layers present a dip of up to 35° SE. In general, the dip angle of these inclined layers varied from 6° to 175° and the average vector between 22° to 104°. The cross-bedding indicates a relative dispersion between NE to SE but inserted yet in a unimodal pattern.

Table 1- Facies and sedimentary processes of Neogene succession in Central Amazonia.

Facies	Structures	Process
Mudrock with even parallel lamination <i>Mp</i>	Dark laminated to massive, very fine sandstone occurs subordinately.	Deposition by suspension with the sporadic influx of terrigenous and debrites of plants.
Massive mudrock/sandstone <i>MSm</i>	Abundant plant remains, and carbonized trunks can also be observed.	Deposition from traction and suspension.
Rithmyte sandstone/mudrock with wavy-linsen structure <i>Rwl</i>	Locally can be observed ball and pillow structures and convolute lamination.	Migration of ripple marks under suspension and traction currents. Plastic adjustments by overload and liquefaction.
Deformed sandstone/mudrock <i>SMd</i>	Convolute bedding showing disharmonic folds, medium-scale load cast structures, convolute lamination, flame structures, synsedimentary fault, and tilted mudrock filling channel geometry.	Plastic deformation is associated with slumping and sliding processes. Plastic adjustment by liquefaction.
Sandstone with climbing-cross lamination <i>Scl</i>	Subcritical and supercritical bedforms. Locally, convolute lamination can be observed.	Deposition from suspension and traction currents, abundant sandy inflow. Secondary liquefaction process.
Bioturbated sandstone/mudrock <i>Smb</i>	Vertical to curved tubes, some presenting spreiten similar to <i>Taenidium</i> trace fossils. Radial tube structures with white halos in mottled horizons.	Reworking by the activity of roots and benthic fauna. Concentration and leaching of iron oxides and hydroxides.
Sandstone with cross-stratification <i>Ses</i>	Trough and tabular cross-stratifications in individual beds or composing inclined heterolithic stratification. Convolute lamination.	Migration of 3D and 2D bedforms under unidirectional flow. Gravitational instability and liquefaction process.
Inclined heterolithic stratified sandstone/mudrock <i>SMI</i>	Low-angle stratification forming master bedding in heterolithic beds. Trough, tangential and tabular cross-stratifications developing complex bedding. Climbing-ripple cross lamination. Root marks, mottled horizons, and bioturbation.	Deposition by lateral migration of point bars. Bar emergence and colonization by vegetation. Biological activity of benthic fauna.
Sandstone with complex cross-stratification <i>Scc</i>	Sandstone with planar, undulating, cross-, trough, and sigmoidal stratification. Reactivation surfaces, synsedimentary faults, and convolute lamination. Mud drapes and mudrock beds separating lobate forms.	Deposition by traction currents under upper flow regime with a fast deceleration of water energy. Gravitational instability and adjustments by liquefaction process.
Massive sandstone <i>Sm</i>	It is generally associated with sandier facies.	Liquefaction, high inflow of sediment and gravitational instability, fast deposition. Recent weathering obliterating primary structures.
Massive and stratified Conglomerate <i>Cms</i>	It has around 40 cm thick, rounded pebbles of mudrock and quartz. Trunk fragments marking the channelized surface. Incipient cross-bedding	Deposition for bedload discharge. Reworking of mudrock beds by channelized flows.

3.3.2 FACIES ASSOCIATION

3.3.2.1 *Lake/overbank (LOV)*

The LOV association is observed in the lower portion of the studied outcrops, varying from 50 cm to 3 m thick (Figs 2 and 4). It mainly comprises the Mp, MSm, Rwl, and Scl facies constituted of mudrock, siltstone, and subordinately laminated to massive, very fine sandstone (Figs 2 and 4, Table 1). The geometry of beds is tabular and occasionally with low-angle inclinations ($\leq 5^\circ$). It also contains several leaves, rare trunks, coal, and other organic debris but without bioturbation. The lamination is evident when the layers are separated by fine sandstone and siltstone laminae (Fig. 5). The facies Mp can be lenticular and, sometimes, form layers laterally continuous, reaching thicknesses of few centimeters up to 6 m (Fig. 5). Fine-grained sandstone and siltstone with subcritically and supercritically climbing ripple-cross lamination, occurring in 5 cm-thick sets in tabular beds of up to 3.5 m thick (Fig. 5). Heterolithic layers consist of up to 30 cm-thick of mudrock, siltstone, and very fine-grained sandstone with wavy-linsen structure interbedded with facies Mp and Scl. (Table 1, Fig. 5). Ball and pillow structure, convolute lamination, and load cast structures occur mainly in the facies Rwl. are locally observed. This association e facies Mp contains abundant organic matter with plant remains like coffee grounds and leaves between lamination (Fig. 5).

The suspension process is well-related with sporadic fine-grained terrigenous inflow and plant debris. Also, the LOV facies association's lateral continuity for hundreds of kilometers suggests an extensive, flat, and low-energy environment. The dark color and frequently plant debrites in all outcrops indicate stagnant and anoxic shallow-water bodies setting with an exceptional preservation potential for the organic matter. The migration of ripples currents occurred during high aggradation rates and rapid deposition (e.g., Collinson 1996). The alternation of traction flow and suspension processes was concomitant with ripple marks' migration, indicative of continuous sand and mud inflows. Plastic deformation in the sand-mud interface is produced by the load and sinking of a sand layer on a muddy substrate by liquefaction processes.

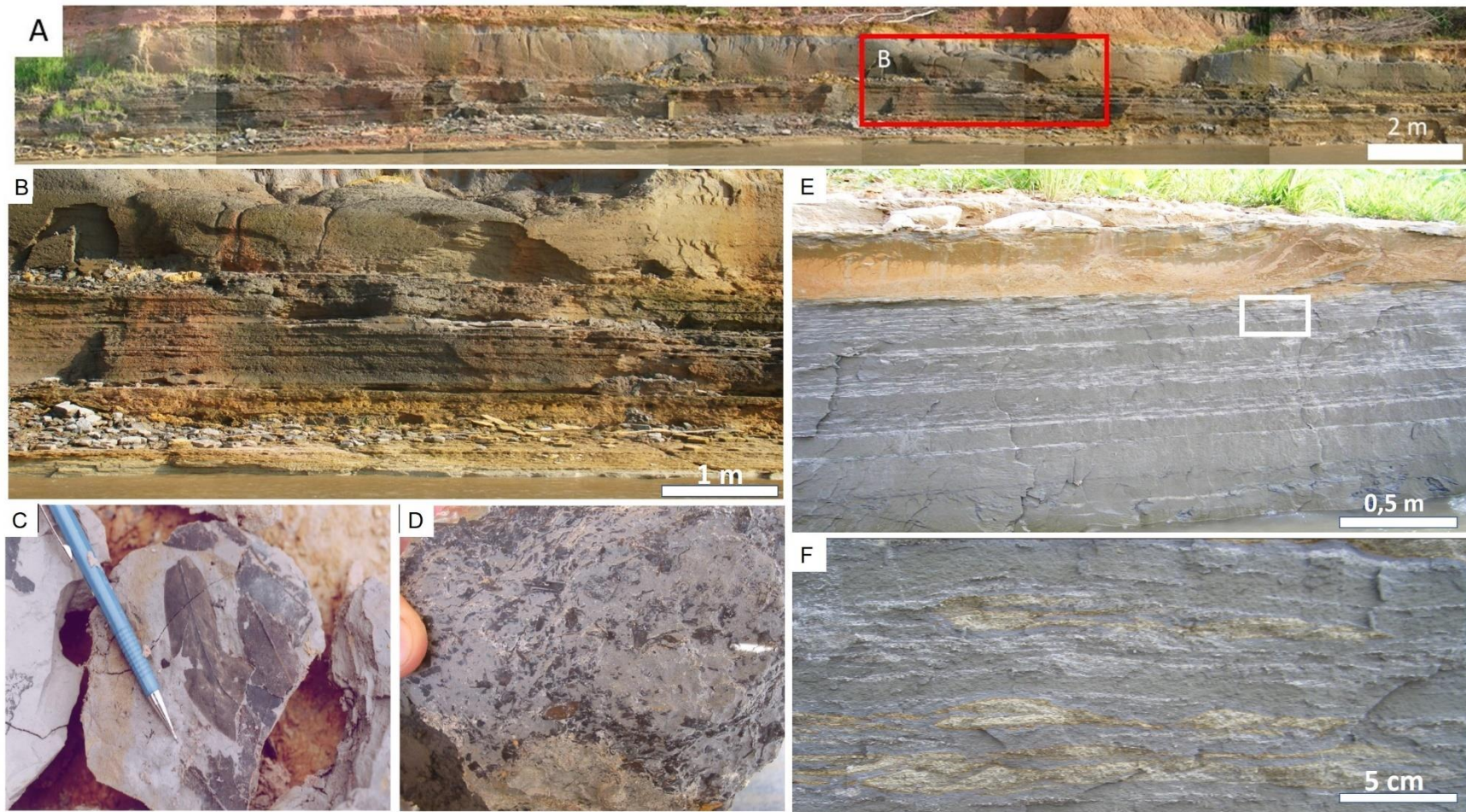


Figure 5- Faciological aspects of LOV association in Central Amazonia. A) Laterally continuous tabular beds of laminated and massive mudrock. (B) Detail of A highlighted the even parallel lamination in mudrock. C) Well preserved leaves. D) Plant debris like "coffee grounds". E) Heterolithic beds with wavy-linsen structures composing a coarsening upward cycle. F) Detail of E) linsen bedding.

The LOV association corresponds to a low energy environment with periodic sand inflows, such as observed in other modern and ancient lacustrine deposits of terminal river systems (e.g., Hyne *et al.* 1979, Talbot & Allen 1996, Buchheim *et al.* 2000). This association's lateral continuity for several kilometers without bioturbation, dark mudrocks with well-developed laminations, and leaves following bedding planes suggest deposition from suspension under anoxic conditions. Deformation structures such as convolute bedding may be related to slumping produced by crevasse splay deposits. (Coleman 1981, Coleman *et al.* 1983). It is a challenge to separate distinct overbank deposits in this association due to reduced exposition of up to 4 m-thick. Therefore, the lake setting was associated with floodplains and levees linked to the perennial meandering channels with vegetated margins. Root marks and mottled horizons indicate the development of organic paleosoil in abandoned overbank areas. Furthermore, high sediment loads or fast drop in the lake level likely induced large-scale composite crevasse splay progradation that explains meter-scale coarsening upward cycles in LOV association.

3.3.2.2 Composite Crevasse-splay (CCS)

The CCS association is observed in the lower portion of the studied succession, generally overlying the LOV association, varying from 2 m up to 7 m 3 m thick and can be laterally continuous for tens of meters and reach 20 km correlating the measured sections 9 and 10 (Fig. 4). It mainly comprises the facies Sc, Scl, and Rwl facies constituted of fine-grained sandstone forming horizontal and inclined beds with paleocurrent towards NW and ESE (Fig. 2 and 4, Table 1). The facies are organized in beds around 50 cm-thick and internally show even parallel and cross-bedding with slight erosive (scoured) based sandstone (Fig. 2 and 4). The lobate beds form single to multiple coarsening upward successions forming lobate bodies. Discontinuous laminae of mudrock eventually cover layers of undulated top exhibiting pinch and swell patterns (Fig. 6). Horizontal to lenticular beds exhibit internally sigmoidal cross-stratification and even parallel to undulating stratification (Fig. 6). This facies is generally intercalated with Scl facies. Sigmoidal cross-stratification develops lenticular beds with convexities toward the top, and it can be observed in longitudinal and cross-section as lobed forms (Fig. 6). The asymptotic form in the top of this structure is rare due to the

eroded topset, while the basal low-angle or tangential cross-strata is frequently identified (Fig. 6). Facies St occurs isolated, marking the top of the beds. Even parallel cross-stratification laterally exhibits slight undulations cut by reactivation surfaces producing low-angle truncations (Fig. 6). Massive bedding or incipient lamination occurs in some beds, and normal faults with centimetric displacement are restricted to cross-stratification sets (Fig. 6). The faulted blocks show well-preserved acute features confirming the syndimentary nature. Convolute lamination is associated with these deformed beds.

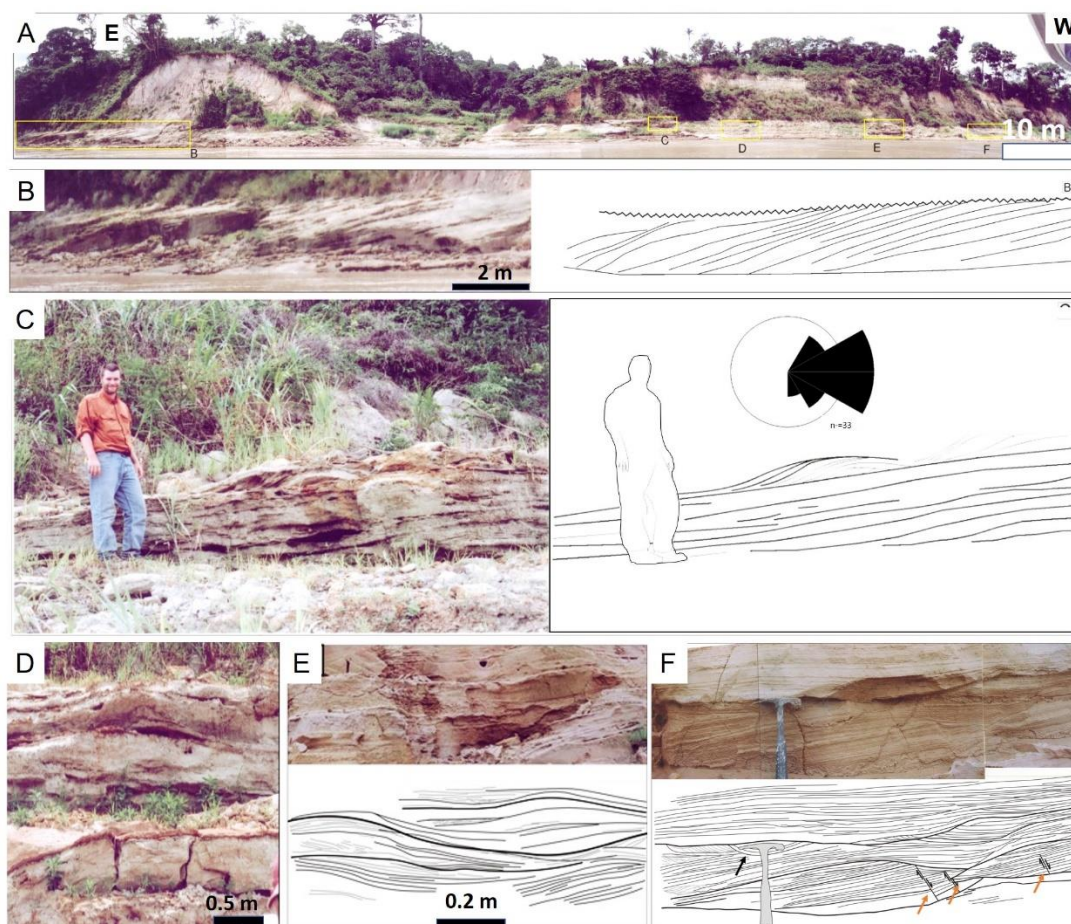


Figure 6- Faciological aspects of CCS association. A) Panoramic view of measured section 9 with indications of illustrations B, C, D, E, and F. B) Large-scale complex cross-stratification (Scc facies) with low-angle to sigmoidal cross-stratified sandstone with migration to ESE. C) Amalgamated lobate sandstone with sigmoidal cross-bedding in longitudinal and D) transversal views. E) Pinch and swell pattern related to the superposition of the sigmoidal lobe. F) Isolated trough cross-bedding (black arrow) and normal syndimentary faults (orange arrows).

The CCS association was previously interpreted as delta front deposits (Vega 2016, Nogueira *et al.* 2013). Other settings such as delta plain, distributary, and prodelta

were interpreted for Solimões Formation but not adequately demonstrated (Vega 2016, Nogueira *et al.* 2013). Deltas range in scale, from continental-scale systems, such as the modern Mississippi Delta in the Gulf of Mexico, with almost 30000 km² (Bhattacharya 2006, 2010). Despite the facies similarity and reasonable scale of lobate bedforms, the lateral continuity for hundreds of meters or even kilometers contrasts with the few meters-thick Solimões deposits (Fig. 4) not compatible with a delta front or the identification of a complete delta system (e.g., Wright & Coleman 1974, Smith & Jol 1997, Bhattacharya 2006, 2010). Many continental-scale deltas may contain smaller-scale crevasse deltas within larger-scale delta lobes, resulting in a complex, hierarchical facies architecture similar to delta front facies (e.g., Wright & Coleman 1974, Smith & Jol 1997, Bhattacharya 2006, 2010). Thus, the single to multiple coarsening upward cycles of CCS composed of scoured-based lobate sandstone are interpreted as crevasse splay deposits. The great extent (up to 20 km in length) and few CCS thicknesses are compatible with large-scale composite crevasse splay sandstone (Fig. 7). Similar examples occur in the recent Mississippi delta (Smith *et al.* 1989), the Jurassic Ravenscar Group in Yorkshire, UK, and the Perm-Triassic Beaufort Group, South Africa (MjØs *et al.* 1993, Gulliford *et al.* 2017).

The CCC association overlies the LOV association and comprises two distinct deposits laterally and vertically related to the distal and proximal crevasse lobe. The Scc facies intercalated with Scl facies prograding as concentrated flows feeder by a suspended-load meandering channel over the lake and overbank areas (LOV association). Facies MSm and Mp can also be observed sporadically, forming lenses of around 10 cm- thick. Three main types of bed geometry, such as 1) amalgamated, sigmoidal lobes separated by mud drapes, 2) inclined foresets (clinoforms), and 3) sheet geometry, corroborate with a complex bedform (lobe). The amalgamated lobes are accumulated by episodic overlay and decreased flow competence as it approaches a low-energy basin (LOV association). Cross-stratified beds indicate that fluvial flow generates secondary bedforms. Penecontemporaneous deformation structures suggest a disturbance of unconsolidated or semiconsolidated sediments (Lowe 1975, Elliot 1986, Glover & O'Beirne 1994, Bhattacharya 2006, 2010). The facies array in coarsening upward cycles is consistent with gravitational/plastic adjustments in the progradational lobe in subdeltaic front. Massive beds may be related to bioturbation, compaction,

cementation, rapid deposition and weathering (e.g. Reineck & Singh 1980, Collinson 1996).

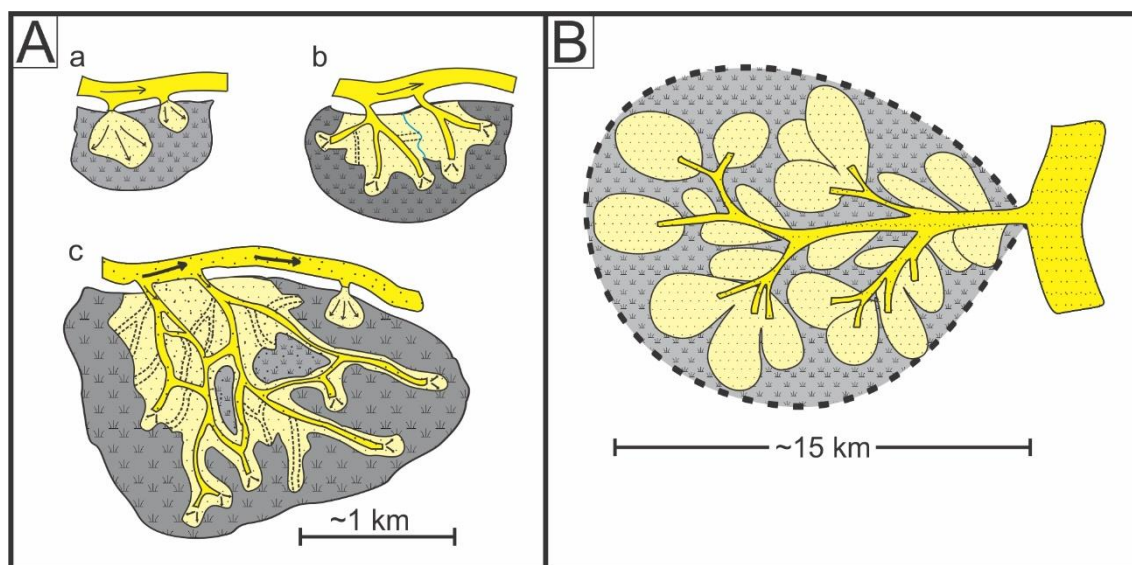


Figure 7- Small- to large-scale crevasse splay. A) Evolution of a crevasse splay in the Cumberland Marshes in east-central Saskatchewan, Canada, a) and b) show an early small lobate splay prograding through the levee of the trunk channel and with further growth, a symposial pattern appears, and the channel becomes extensive and anastomosed in the most mature phase (Smith *et al.* 1989). B) Proximal, medial and distal parts of a crevasse splay complex developing subdelta comprise, respectively by 1) channelized erosively based sandstone, 2) interbedded sharply based sandstone and single to multiple coarsening upward successions forming lobate bodies (cf. Fielding 1984). Note the differences in scale between the crevasse subdelta and small-scale crevasse splay.

The distal portion of the crevasse lobes deposits is organized in incipient coarsening upward cycles characterized by intercalation of Hw1, Scl, Ml, and MSm facies (Table 1, Fig. 5E, F). These deposits frequently have a high content of vegetable debris and without bioturbation. The assemblage of sandy/heterolithic facies with pelitic facies registers episodic inflow of sand into low energy environment associated with distal crevasse bars prograding over lacustrine prodelta. The absence of bioturbation and high organic content are indicative of anoxic conditions of a restricted basin. The small-scale deformation structures indicate sands overloading mud layers plastically.

3.3.2.3 Suspended-load meandering channel (SLMC)

The SLMC association consists mainly of mudrocks, fine sandstones, and subordinately conglomerates relative to the facies Cm, SMi, Mp, MSm, and Rwl organized in meter-scale fining upward cycles (Figs 2, 3, 4 and 8, Table 1). Similarly,

the cosets of inclined heterolithic stratification (cf. Thomas *et al.* 1987) also form meter-scale fining upward cycles marked by Cm facies until mudrock beds in the top. The coarse-grained deposits consist mainly of conglomerate (Cm facies) with mudrock intraclasts interbedded with massive pebbly sandstone (pebbles with ~ 3 cm diameter) rich organic debris, forming a lag (Fig. 8). These inclined beds show dips of up to 30°, laterally decreasing to 10° oriented to ESSE (Fig. 4). The IHS sandstone is frequently interbedded with 1m-thick of Scl facies, and centimetric beds of facies St. Paleocurrent data from facies St indicates SE direction, with a mean vector of 118°. In contrast, IHS beds suggest accretion to SSE, with a mean vector of 146°. The SMd facies occurs in the upper portion of this association, generally truncated by the unconformity (Fig. 4). The SMd facies reach up to 2 m thick and consist of heterolithic beds with contorted bedding, disharmonic folds, and medium-scale ball-and-pillow structures (Table 1). The open sinform and antiform have 1.2 m length and up to 0.5 m height, displaying a vertical axial plane without preferential orientation (Fig. 9). The axial zone of antiform is acuter than sinform that is generally broader. Normal faults displace and rotate the layers as drag folds and meter-scale blocks (Fig. 9). The tilted blocks are indicated by internal stratification discordant with the horizontal bedding (Fig. 9). Convolute lamination and flame structures occur associated with these structures.

The SMi facies are the product of lateral accretion of point-bars of meandering channels (Thomas *et al.* 1987). The coarse-grained deposits represent high-energy flow into the fluvial channel and reworking of mudrock blocks from cut banks. Thus, lateral alternations in the cosets thickness represent the seasonal cyclicity of fluvial waters. Also, sub-areal exposure favored the establishment of vegetation and benthic fauna during low-water levels. Fining upward cycles are produced by the decrease of flow velocity and water levels (Thomas *et al.* 1987, Miall 2010), as well as cosets limited by erosional surfaces are related to unidirectional growing phases of seasonal floods.



Figure 8- Faciological e geometric aspects of SLMC association. A) Large-scale inclined heterolithic stratification (IHS) in sandstone and mudrock. B) IHS of Solimões deposits truncated by the unconformity with Içá Formation. C) Inclined heterolithic beds and fine-grained sandstone with even parallel lamination. D) Subcritically and E) supercritically climbing ripple-cross lamination. F) Conglomerate lamina with mudrock intraclast. G) ferruginized plant debris (seeds?).

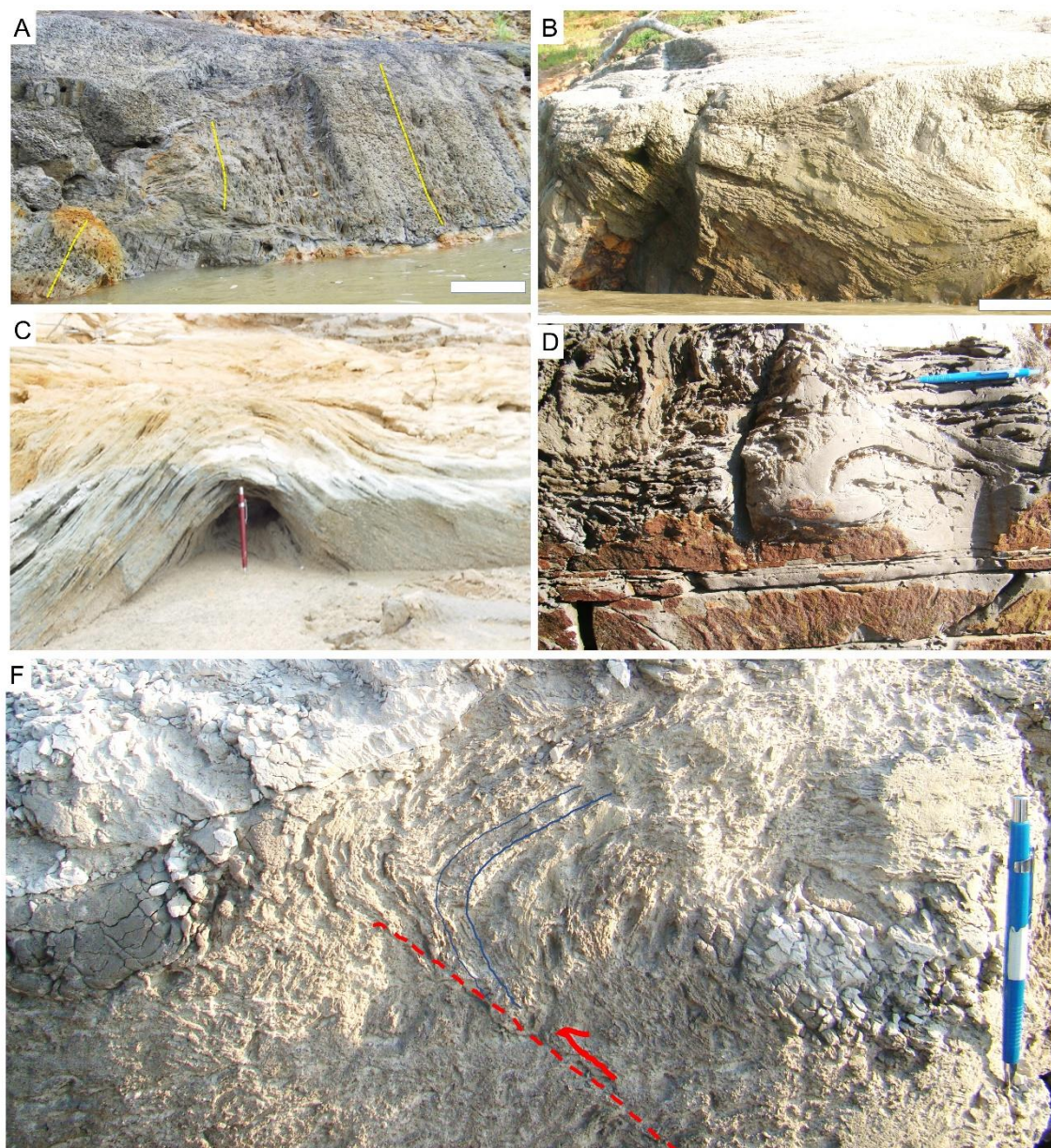


Figure 9- Deformed facies from the SLMC association from Solimões Formation. A) and B) Tilted blocks underlain by horizontal mudrock beds. C) Fold in heterolithic beds. D) Contorted beds in contact with undeformed laminated mudrock. F) inverse fault forming drag fold.

Alternations of facies Scc and Scl correspond to the predominance of suspension compared with the traction process. Local erosion in the cross-bedding bottom set suggests sand inflow with higher energy that rapidly decreases and is molded in an undulated lamina. The recurrence of beds with up to 50 cm indicates a sufficient amount of accommodation space to accumulate sand deposits with lenticular geometry in successions of up to 5 m. This deposition may have formed intermittent shoals locally reworked by small bedforms with sinuous crests. The supercritical and subcritical climbing ripples indicate suspension in levees or scrolled flood plain (Miall 2010). The restart of deposition was marked by partial erosion of the foresets producing reactivation

surfaces in IHS. Also, fast sedimentation creates gravitational instability in macroforms, which is compensated by the development of normal and inverse faults preserved during rapid burial.

Facies Cm is formed during the deposition restart of point bar and linked to riverbank landslips (terras caídas process). The erosion of the cut bank generates instabilities that affected the weaknesses of semi compacted muddy margin. The listric fault causes the collapse of the cut bank forming blocks that slide into the channel. The reworking of pre-consolidated mud blocks favoring the development of intraclastic gravel. The rapid deposition in the channel flank laterally to the master bedding of IHS contributes to the high preservation of tilted blocks.

The recurrence of deformed layers among others without deformation indicates that the deformation was penecontemporaneous to the deposition. The deformed structures and the plastic behavior of deposits indicate their unconsolidated or partially consolidated status during deformation. These deformation processes involved sliding and slumping processes generating gravitational flows and rotation of layers. Convolute beds in these facies suggest liquefaction inducing plastic adjustments.

In the SLMC association, the overlap of crossbed and accretion-surface orientations regionally and locally cross-bedded are oriented nearly perpendicular to each other (Fig. 4). The mean vectors for E-SE and the dispersion ranging from 30° to 158° indicate the development of IHS facies was oblique and orthogonal to flow direction, such as described by Puidefabregas and Van Vliet (1973) and Edwards *et al.* (1973), characterizing a high-sinuosity point bar in suspended-load channels (e.g., Schumm 1963, Allen 1984, Miall 2010,). The lateral relation of SLMC association with lake and overbank deposits (LOV association) indicates that fluvial channels drained the wetland areas. The dark color observed in these deposits indicates much organic matter in the water from the degradation of vegetated margins. The acid black waters can be similar to those found today in Amazon Rivers. They developed anoxia conditions that partially prevented benthic activity, explaining the absence of bioturbation in these deposits.

3.3.2.4. *Mixed-load to bedload meandering channel (MBMC)*

This association has many faciological similarities with the SLMC deposits and is organized in fining upward cycles, but the sandstone frequency is high compared with mudrock beds (Fig. 2 and 4). The MBMC reach up to 20 m-thick and comprise fine- to

medium-grained sandstone with IHS (SMi facies), trough and tabular cross-bedding (Scs and Cm facies), even-parallel bedded sandstone, and conglomerate (facies Cm) marking the contact with the Solimões deposits (Fig. 2, 3, 4, 8B, 10 and 11, Table 1). The fine- to medium-grained sandstone interbedded with thin mudrock beds forming IHS (SMi facies) and intraformational conglomerates with mudrock pebbles (facies Cm) are the most frequent facies (Fig. 10). The massive intraformational conglomerate with an open and closed framework, a matrix composed of well-sorted, fine sandstone, and rounded to well-rounded mudrock pebbles with 5 cm diameter, but larger blocks of around 35 cm diameter may also be locally found. The inclined beds of SMi facies have a predominant northeastern orientation (50°). The cross-stratification comprises sets up to 40 cm-thick and cosets of around two m-thick with paleocurrent to NW. Coarse grains can be found segregated in the foresets. Many vegetable detritus such as trunks and leaves in sandstone marked channelized geometry and sometimes are found in horizontal positions in the base of heterolithic beds (Fig. 11). Sandstone with climbing ripple-cross lamination is associated with the SMi facies (Fig. 4).

The Facies St grading to facies Sc point to periods with current activity and deposition of 2D and 3D bedforms were followed by periods with high sediment influx. Basal successions with trough-cross bedding overlaid by climbing-cross stratification are typical of bedload point-bar deposits (e.g., Schumm 1963, Allen 1984, Miall 2010). The genesis of these facies is related to the migration of 3D bars into channelized flows. The concentration of coarse grains in the foresets corresponds to the migration of small-scale bedforms and segregation by reverse flows (Smith 1976).

The dominance of well-sorted, fine- to very fine-grained sandstones, related to several types of cross- and even parallel beddings and arranged in extensive macroforms with master bedding dips of around 20° suggest progradation with high sediment load in low energy distal environment. Like the SLMC association, the sandy point bar deposits in MBMC contain mud clasts from the floodplain deposits, probably derived by slumping from nearby cutbank. The abundant sandstone facies and the bimodal flow observed in this association confirm a mixed-load interpretation to bedload meandering fluvial channel with straight segments and low sinuosity for the MBMC association.



Figure 10- Faciological aspects of MBMC association. A) Massive conglomerate with rounded mudrock clasts and sandy matrix. B) Trough cross-bedding in fine- to medium-grained sandstone. The orangish curved lines crossing the facies are ionic of iron oxide-hydroxide due to the recent weathering.

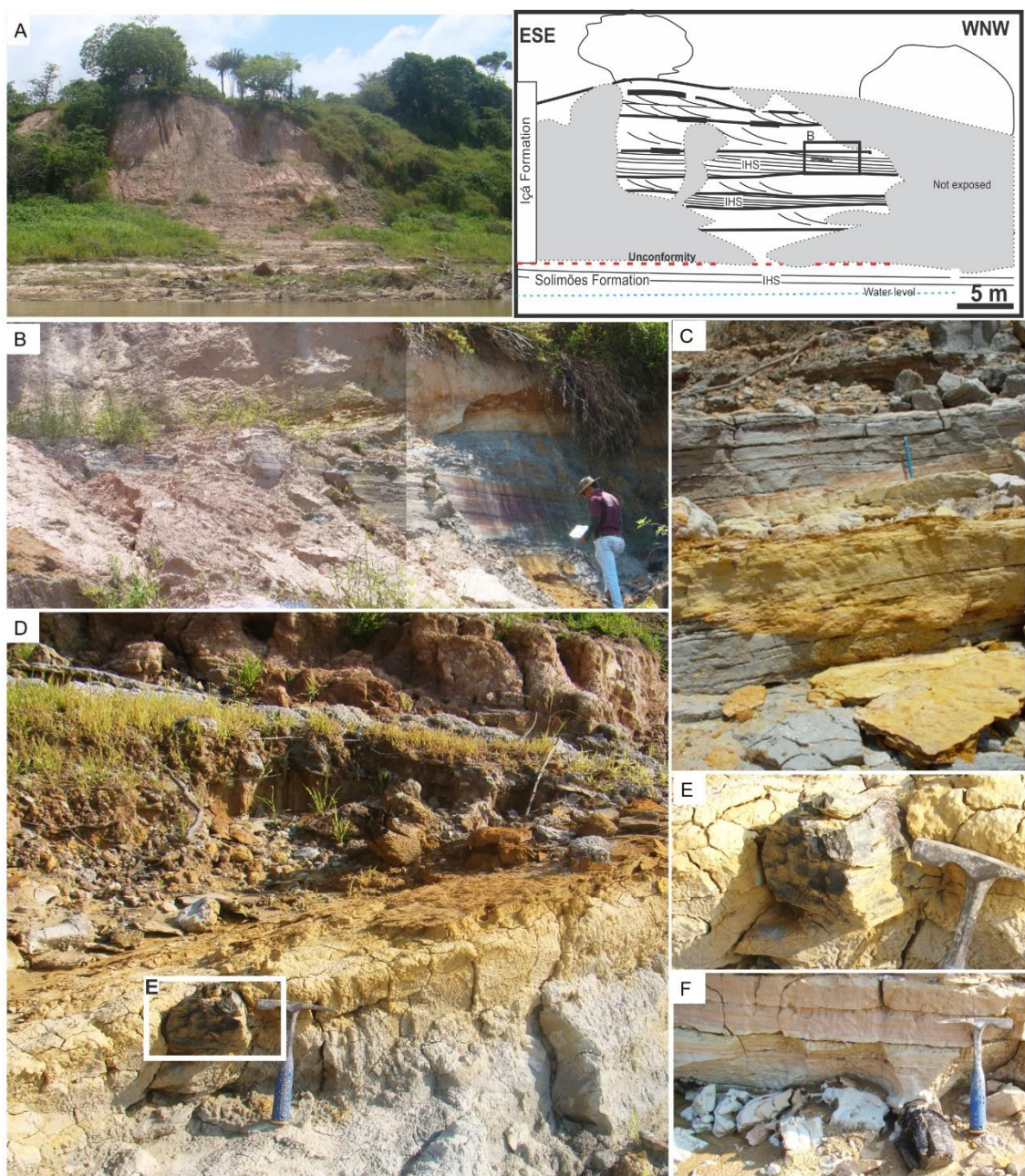


Figure 11- Faciological e geometric aspects of MBMC association. A) Medium-scale inclined heterolithic stratification (IHS) in sandstone and mudrock alternate with the cross-bedded sandstone. B) Detail of A showing the master bedding of IHS truncate by cross-stratified sandstone. C) Heterolithic inclined beds exhibiting fresh grey color and orangish weathered tonalities. D) Trunk fragment in master bedding showed E and F, generally in the horizontal position to the bedding.

3.3.2.5. Flood plain/crevasse splay (FPC)

The FPC consists of facies Mp, Rwl, MSm and Msl forming tabular to lenticular beds with up to 4 m-thick (Fig. 12). The intercalations with facies Slc and Rwl are frequent in the upper part of the association overlaying the Point bar deposits MBMC (association). This fine- to very fine-grained sandstone and reaches up to 60 cm thick, exhibits a mottled appearance, and is locally associated with massive sandstone (Fig. 3

and 4). Rip-up clasts, curled mud flakes, and dissection cracks occur associated to mottled beds (Fig. 12). Vegetable fragments are found mainly in grey beds, and bioturbation occurs locally. Endichnia, vertical and horizontal branching tubes, generally show reduction whiteness halo and sometimes with rare organic matter content, interpreted as root traces (Fig. 4, 12). Other bioturbation types include epichnia and endichnia, meniscated, tubular traces attributed to ichnogenera *Taenidium* (Fig. 3). Meter-scale coarsening upward consisting of mudrock and fine- to medium-sandstone with trough cross-stratification, sigmoidal cross-bedding forming lobate geometry, and locally, occurs convolute lamination (Fig. 3, 4, and 13). The cross-bedding is highlighted by mud layers/mud drapes and generally associated with Scl. The FPC can reach up to 8 m-thick overlying the unconformity directly. Sometimes, the association starts with channelized pebbly sandstone (mudrock clasts) in packages with up to 2 m-thick (Fig. 3, 4, and 13). Dissection cracks, gutter cast, and root marks occur in mottled horizons (Fig. 13).

These fine deposits of FPC are interpreted as floodplain deposits (e.g. abandoned channel) that were formed by cut-off of and subsequent abandonment of a river channel (Miall 2010). Sand intercalations in the upper part of the succession suggest episodic siliciclastic inflow into the overbank areas. Periods of subaerial exposition and colonization by plants are indicated by dissection cracks and root marks. The FPC has a great contribution of the palm pollen from lowland forests of *Mauritiides franciscoi* and *Alnipollenites verus* (Silveira 2005, Nogueira *et al.* 2013) is also marked by a high frequency, and it is related to temperate montane forests. *Echiperiporites estelae* and *M. annulatus* also occur with common frequency at this level (Nogueira *et al.* 2013).

The lobed sandstone, occasionally amalgamated or separated by thin beds of mudrock, with Scs and Slc facies are interpreted as crevasse splay deposits. Crevasse channels develop by breaching of a levee during high-runoff events, and may result in a permanent diversion of the main flow or avulsion (Miall 2010). Sections through of these deposits show width/thickness ratios less than 1500 and length/thickness ratios less than 2000 (MjØs *et al.* 1993, Gulliford *et al.* 2017). In the FDP association they are up to 2.5 m and widths and lengths are of similar magnitude with up to about 1000 m (Fig. 4). Some lenticular mudrock are interpreted as mud plugs associated to the filling of large-scale bedform trough. Rill marks (gutter cast feature) form by the escape of ground water when the water level falls below the water table indicate emergence of crevasse and stagnant water in ponds. Liquefaction cause plastic adjustments in rhytmite.

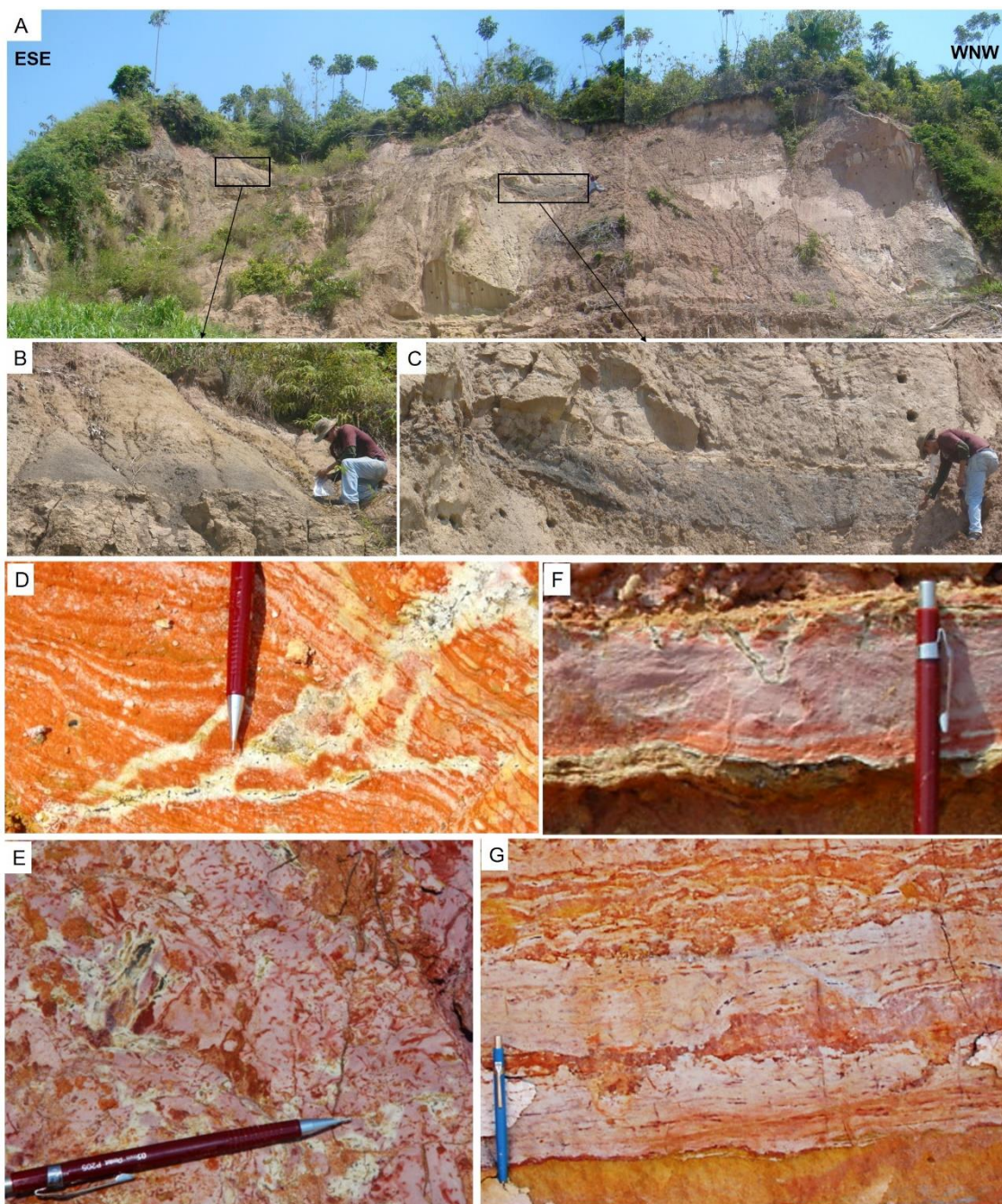


Figure 12- Faciological e geometric aspects of FDP association. A) Panoramic view of The Iça Formation exhibiting abundant sandstone beds. B) Tabular and C) lenticular mudstone layer (mud plug). D) and E) root traces in mottled mudstone, note wood fragment with white halo of iron leaching. F) dissection cracks. G) Mottled rythmite with rip-up clast and dissection cracks.

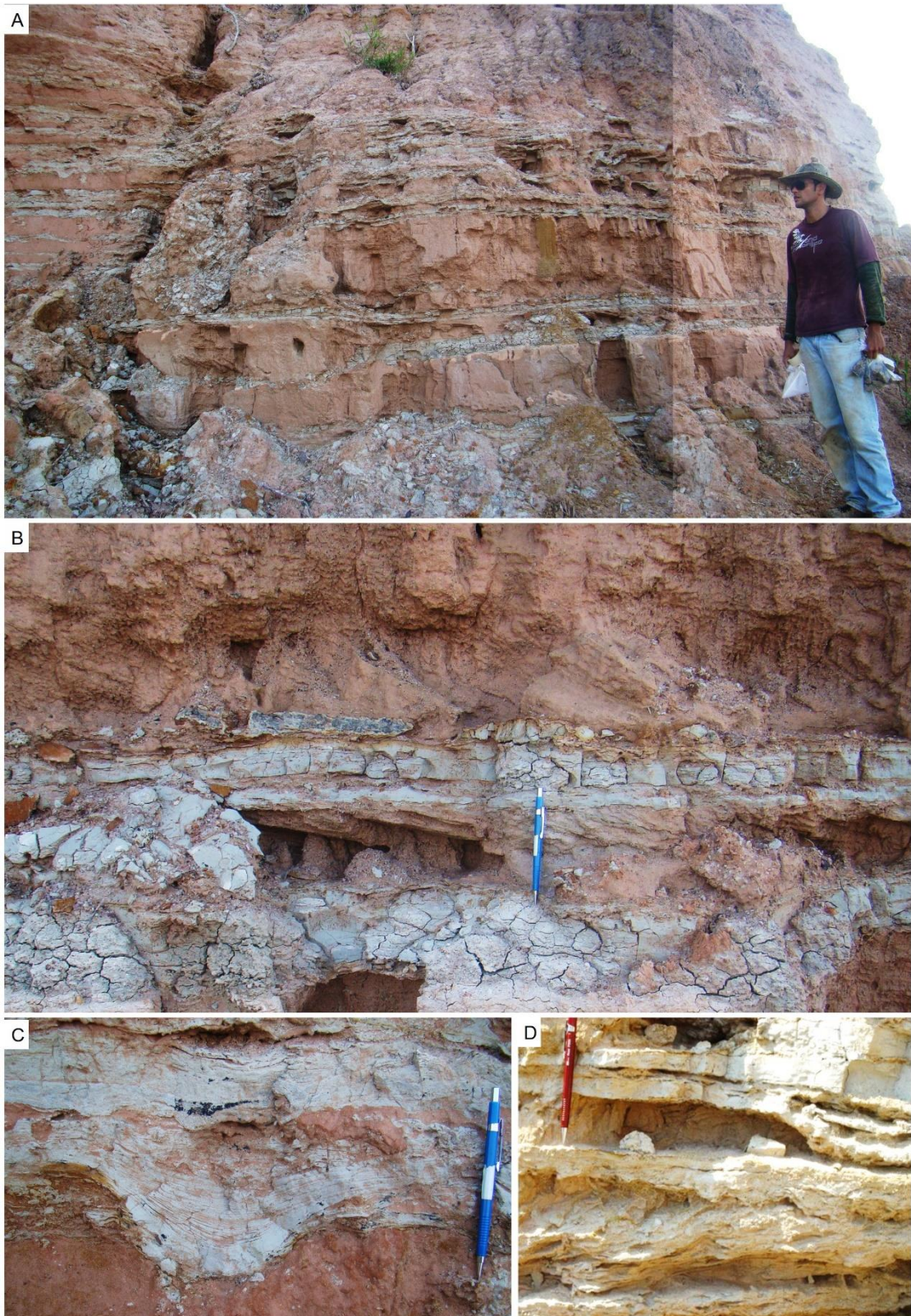


Figure 13- Crevasse splay deposits of FPC association. A) Coarsening upward cycles formed by fine-grained sandstone and mudrock layers. B) Sigmoidal cross-bedding with sets separated by mudrock layers. C) gutter cast filled by laminated mudrock. Cross-bedding highlighted by mud drapes.

3.4 DEPOSITIONAL MODEL

The Miocene Solimões Formation in the Central Amazônia includes several overbank areas that include lake, swamp, and flood plains with organic mud deposition drained by meandering channels (LOV association). These data confirm the previous interpretation of the Pebas-mega-wetland restricted to the Western Amazonia during Miocene (cf., Hoorn 1993, 1994, Hoorn *et al.* 2010, Shephard *et al.* 2010, Boonstra *et al.* 2015, Nogueira 2008, Nogueira *et al.* 2013, 2021). This setting seems not trespassing the Purus Arch zone, the limit with the Amazonas Basin (Fig. 14A). The Amazonas Basin's tectonic behavior more uplifted than Solimões Basin was also a natural geographic barrier to retain the wetland expansion during Miocene (Nogueira *et al.* 2013). The presence of point bar deposits with SE migration confirms a high sinuous meandering fluvial system with predominant suspension-load discharge (Fig. 14A). The large low energy setting allowed the progradation of crevasse splay complex developing subdeltas similar to those found in the continental deltaic system and large rivers (MjØs *et al.* 1993, Mertes 1996, Rozo *et al.* 2012, Gulliford *et al.* 2017). The episodic deposition of coarse-grained sediments during submergence by major floods is similar to those found in ancient and modern settings. The fluvial system acted as a feeder of the mega-wetland system with migration to E-SE and was connected to net drainage derived from the Andes or Iquitos Arch. However, this system has been contemporaneous with the Cratonic Amazon River (Nogueira 2008, Nogueira *et al.* 2013, 2021). A similar scenario like the Lake Victoria and the Nile River in North Africa (Faccena *et al.* 2019) cannot be ruled out, but further studies are needed.

The Andes' progressive uplift during the Miocene affected the Solimões Basin causing the emergence of the mega-wetland. The record of reworked Lower Paleozoic palynomorphs in the top of Solimões Formation strongly indicates the continuous erosion of Paleozoic basins (Silveira *et al.* 2005, Nogueira *et al.* 2013). This event was amplified by the expressive sea-level fall in middle-Tortonian (11-8 Ma), resulting in the Andean Amazon River's onset (Fig. 14B).

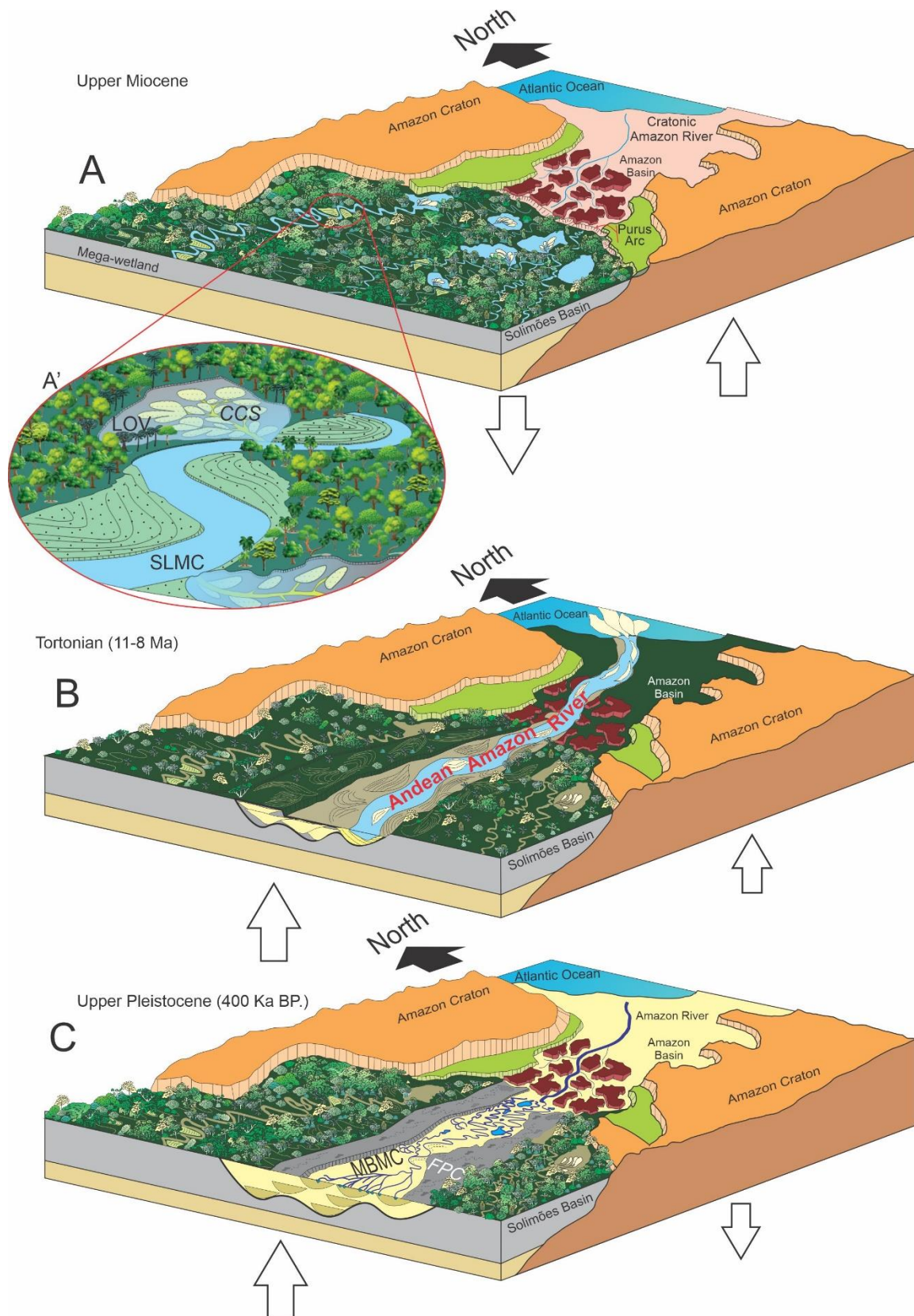


Figure 14- Depositional model for the Miocene and Pleistocene succession in central Amazonia. See text for more explanation. A) The mega-wetland system in western Amazonia implanted in the subsiding Solimões Basin. B) Implantation of the Andean Amazon River caused by Andean tectonics and expressive sea-level fall resulting in the erosion and sediment bypass. C) The implantation of a mixed-to-bedload meandering system (Içá Formation) represents the Amazon River's sedimentation restart in Central Amazonia.

Deposits related to the Andean Amazon implantation were not found, while in the Foz do Amazonas Basin, they are widely recorded (Figueiredo *et al.* 2009, Gorini *et al.* 2013). The erosion time that generated the unconformity during the Andean Amazon River implantation can be estimated considering the difference between the Tortonian (~ 10 Ma) and the estimated age for the Iça Formation of 400 Ka. Thus, the unconformity or sediment bypass lasted at least 9.5 Ma. The Pliocene and the lower and middle portion of the Pleistocene were not recorded in Central Amazonia. Only in the Late Pleistocene, the Solimões Basin subsided, causing the implantation of a mixed-to-bedload meandering system (Iça Formation) that represents the sedimentation restart of the Amazon River in the Central Amazonia (Fig. 14C).

3.5 CONCLUSIONS

The 25m-thick Miocene and Pleistocene succession exposed in the Eastern Solimões Basin, Central Amazonia, revealed eleven sedimentary facies grouped in five associations: 1) lake/overbank (LOV), constituted by tabular beds of organic matter-rich laminated mudrock and subordinate sandstone, laterally continuous for dozens of kilometers, 2) composite crevasse splay (CCS) represent a 5 m-thick coarsening upward succession, laterally continuous for dozens of kilometers, of complex cross-stratified sandstone that include sigmoidal cross stratification, even parallel bedding, climbing ripple cross lamination and deformed beds and frequently shows eastward inclined foresets related to proximal crevasse subdelta lobes and tabular distal crevasse deposits interbedded with LOV association, 3) suspended-load meandering channel (SLMC), represented by point bar deposits consisting of large-scale inclined heterolithic stratified sandstone and mudrock with vegetal debris, oriented to ESE, interbedded with thin layers of intraclastic (mudrock) conglomerate, and deformed beds (disharmonic folds, convolute bedding and tilted mudrock block), 4) Mixed- to bedload meandering channel (MBMC), related to the point bar deposits consisting of medium-scale inclined heterolithic stratified sandstone and mudrock with trunks and vegetal debris, fine- to medium-grained pebbly sandstone and conglomerate (quartz and mudrock clasts) with trough and planar cross-bedding dipping predominantly to ENE, and 5) flood plain/crevasse splay (FPC), comprising bioturbated and vegetal debris-rich mudrock and fine-grained sandstone organized in meter-scale coarsening upward succession of crevasse splay deposits.

Paleocurrent analysis of facies associations indicated a flow predominantly

towards east-southeast of the study area. The drainage migrates to the East in Central Amazonia before implanting the transcontinental drainage.

The unconformity or sediment bypass lasted at least 9.5 Ma. The Pliocene and the lower and middle portion of the Pleistocene were not recorded in Central Amazonia. Only in the Late Pleistocene, occurred the implantation of a mixed-to-bedload meandering system (Içá Formation) that represents the sedimentation restart of the Amazon River.

ACKNOWLEDGMENTS

This work is part of the Ph.D. dissertation of the first author with technical support from the Programa de Pós-Graduação em Geologia e Geoquímica (PPGG) of the University Federal of Pará (UFPA). This research program was supported by the Fundação de Amparo a Pesquisa do Estado do Pará (FAPESPA ICAAF 007/2014, Grant to A.C.R.N) and the Fundação de Amparo a Pesquisa do Estado de São Paulo (FAPESP, Grant 2012/50260-6 to Lucia Lohmann and NSF/NASA Grant 1241066 to Joel Cracraft). We thank to CNPq (The Brazilian Scientific and Technology Developing Council) for financial support (proc. 141791/2018-7) during the Ph.D. program of W.J.S.L.J. and to the Coordination for the Improvement of Higher Education Personnel for the research grant received during this study's development (CAPES/PDSE, Proc. nº 88881.190548/2018-01, financial code 001). Thanks, are also extended to Petrobras, which provided well log data from the Urucu region, indispensable for this study. The paper greatly benefited from critical reviews of two Journal anonymous referees, and we thank them for their helpful suggestions and comments.

CAPÍTULO 4 PALYNOSTRATIGRAPHY OF NEOGENE DEPOSITS IN THE EASTERN SOLIMÕES BASIN: EVIDENCE FOR 9,5 MA OF BY-PASS IN THE RECORD OF THE GREAT UNCONFORMITY IN THE CENTRAL AMAZONIA

Walmir J.S. LIMA JR^a, Afonso C. R. NOGUEIRA^{a,b}, Carlos A. JARAMILLO^c, Jorge Enrique MORENO^c, Silane A. SILVA-CAMINHA^d, Carlos D'APOLITO^d

^aPrograma de Pós-Graduação em Geologia e Geoquímica, Faculdade de Geologia, Instituto de Geociências, Universidade Federal do Pará, Rua Augusto Corrêa s/no, 66075-110, Belém, PA, Brazil, (anogueira@ufpa.br, walmir.junior@ig.ufpa.com).

^bResearch Productivity of CNPq

^cSmithsonian Tropical Research Institute, Panamá, (jaramilloc@si.edu, morenoe@si.edu)

^dUniversidade Federal de Mato Grosso (UFMT), Faculdade de Geociências, Av. Fernando Corrêa da Costa, 2367, Boa Esperança, Cuiabá, CEP:78060-900, Brazil, (silane.silva@gmail.com, carlosdapolito@gmail.com)

ABSTRACT

Palynostratigraphic study of the eastern Solimões Basin, Central Amazonia, revealed a 20- m-thick Neogene succession composed of two units, namely the Miocene-Pliocene Solimões Formation and Pleistocene Içá Formation. The Solimões Formation comprises grey fine-grained sandstone and mudrock rich in plant remains with complex cross bedding formed by sigmoidal lobes, climbing ripple-cross lamination, even parallel and deformed beds besides inclined heterolithic bedding, interpreted as lake, megacrevasse splay, and meandering fluvial deposits. The eastward continental inflow is also indicated by an abundance of phytoclasts and freshwater algae such as *Ovoidites*. The Içá Formation consists of white to pinkish siltstone, fine- to medium-grained sandstone, and intraformational conglomerate (clay pebbles). Trough cross-bedding, inclined heterolithic stratification, even parallel stratification, and laminated pelites with rare vegetal remains are present in this formation and were interpreted as bedload to mixed load meandering deposits. This previous hypothesis considers the Solimões and Içá deposits as terra firme forest and varzea forest of the Central Amazonia. The palynological reassessment of the Solimões Formation with *Grimsdalea magnaclavata*, *Cichoreacidites longispinosus*,

Psilastephanoporites tesseroporus, and *Ladakhipollenites? caribbiensis*, therefore, the persistence of this composition provided consistent data for an age group of the Middle-Pliocene Miocene, also previously corroborated by the occurrence of *Crassoretitriletes vanraadshoovenii*, and unequivocally this unit is the substrate for the deposits of the Upper-Holocene Pleistocene. The registration of a Miocene fluvial-lake system confirms the extensive Pebas-Solimões lake (wetland) system, confined in the Western Amazon, which precedes the Andean Amazon River's beginning by 9.5 Ma.

Key-words: Middle Miocene-Pliocene, Solimões Basin, Solimões Formation, Pebas/Solimões lake system

4.1 INTRODUCTION

In the South American continent, particularly in Brazilian Amazonia's intracratonic basins, the Andes uplift triggered important paleogeographical and paleoenvironmental modifications Amazonia region (Hoorn *et al.* 1995, Roddaz *et al.* 2005). The direct consequence of Andean tectonics is reflected in the occurrence of numerous basins and sub-basins like a Solimões and Amazon, separated by structural arches with unknown subsidence histories record in Cretaceous and Cenozoic lithostratigraphic units (Milani & Zalán 1999). The paleoenvironmental and paleogeographic changes associated with climatic variations molded this part of South America with important implications for the implantation of transcontinental drainage and the development of the Amazon rainforest and its biodiversity.

Most of the chronological data of the Neogene units are based on biostratigraphic data, while quaternary units have been dated by C14 and optically stimulated luminescence (OSL). Despite the reasonable knowledge of the stratigraphic units, detailed studies of depositional systems and, mainly, the recognition of disagreements to restrict the range of relative palynological ages are still lacking. The limited number of age determinations, obtained from palynomorphs and rare volcanic rocks, are insufficient to organize the sequences of events and consequently to increase the stratigraphic resolution of this region (Silva-Caminha *et al.* 2010, Guimarães *et al.* 2013, 2015, Nogueira *et al.* 2013, Silveira & Souza, 2015, 2016, Kachniasz & Silva-Caminha, 2016, Leite *et al.* 2016, D'Apolito 2016, D'Apolito *et al.* 2018, Lima Jr. *et al.* 2018, Jorge *et al.* 2019, Leandro *et al.* 2019, Pupim *et al.* 2019, Leite *et al.* 2020).

Palynological and carbon 14 dating has marked out most geological models on the evolution of the Amazonian landscape, although there is still no consensus on the sequence of events for the drainage system. The main models are based mainly on the analysis of test drill cores near the mouth of the Amazon River and assume that the implementation of the Andean transcontinental drainage was responsible for the installation of the Amazon fan in the Upper Miocene between 9.5 and 8.0 Ma (Hoorn 1994, Hoorn *et al.* 1995, Potter 1997, Gingras *et al.* 2002, Roddaz *et al.* 2005, Gorini *et al.* 2014, Figueiredo *et al.* 2009, Hoorn *et al.* 2017, Cruz *et al.* 2019). This proposal reflects only part of history and does not include deposits on the Amazon River's main channel. The change in this scenario until the installation of transcontinental drainage was driven by the Andean tectonics and did not occur abruptly, but took place in steps from the late Oligocene-Lower Miocene until the Quaternary (Nogueira 2008, Nogueira *et al.* 2013, van Soelen *et al.* 2017, Reis *et al.* 2016, Nogueira *et al.* 2021). The older ages obtained in a borehole and outcrop samples of the western portion of the Solimões Basin go back to the Paleocene and Middle Miocene (Daemon & Contreiras 1971, Hoorn 1993, 1994, Latrubesse *et al.* 2007, 2010, Leite *et al.* 2016).

During the Middle Miocene (14-10 Ma), the Western Amazonia was dominated by Lake Pebas-Solimões confined to the east by the Purus Arch (Hoorn 1993, Hoorn *et al.* 2010, Shepard 2010, Nogueira *et al.* 2013). Concomitantly, east of this arch, the Cratonic Amazon River flowed into the Atlantic Ocean and preceded the Andean Amazon River (Nogueira *et al.* 2018, Nogueira *et al.* 2013, Nogueira *et al.* 2021). Younger palynological ages such as Pliocene (Latrubesse *et al.* 2010) and Pliocene-Pleistocene (Campbell *et al.* 2006, Nogueira *et al.* 2013, Horbe *et al.* 2013) coincide with biological data (Ribas *et al.* 2012). These ages also match those obtained through the use of OSL and suggest more recent sedimentary pulses linked to the modern Amazon River (Campbell *et al.* 2006, Rossetti *et al.* 2015, Nogueira *et al.* 2013, Gonçalves Jr. 2016, Pupim *et al.* 2016, Cremon *et al.* 2016, Soares *et al.* 2017). For decades, the sedimentary cover in Solimões Basin, in the Central Amazonia lowlands has been stacked in two lithostratigraphic units, the Miocene-Pliocene Solimões Formation and Upper Pleistocene Içá Formation overlaid by Upper Pleistocene-Quaternary deposits. These units are separated by an unconformity observed by hundreds of kilometers in the right margin of Solimões River (Maia *et al.* 1977, Nogueira 2008, Nogueira *et al.* 2013, Horbe *et al.* 2013, Rossetti *et al.* 2015).

Recently, Pupim *et al.* (2019) disregarded this stratigraphic framework and the palynological ages for the Solimões Formation, based mainly on ages from 95 to 35 ka BP obtained by OSL, suggesting that the Solimões and Içá formations represent a single unit of the Upper Pleistocene. This age-restricted range has led the authors to state that these units represent the current Terra Firme forest substrates of the Central Amazonia and cannot be named and mapped using lithostratigraphy which implies a rock unit. OSL ages could not be certified due to the lack of specific and statistical details of the palynological content of only two samples of the studied succession. Also, pollen grains that provided Miocene-Pliocene ages, like *Grinsdalea magnaclavata*, were considered reworked. Palynomorphs of the Pleistocene and Modern age, like *Alnus*, were overestimated to reinforce the idea of a single Pleistocene succession without unconformity. Without performing a detailed facies analysis, these authors interpreted that the succession represents multiple cycles of fluvial bar aggradation composed of continuous fining-upward cycles. This geological proposal reduces the sedimentary history of the Central Amazonia by just 200 Ka BP and ignores other older records related to the evolution of the Cratonic and Andean Amazon River (cf. Nogueira 2008, Figueiredo *et al.* 2009, Hoorn *et al.* 2010, 2017, Nogueira *et al.* 2013, Horbe *et al.* 2013, Nogueira *et al.* 2021).

In this work, we rescue the original lithostratigraphy of the Central Amazonia, considering the Solimões and Içá formation as lithostratigraphic units of the Solimões Basin, corresponding to the top of Javari Group, that discordantly overlies in subsurface the siliciclastic rocks of the Upper Cretaceous Alter do Chão Formation (Cruz 1984). The contact between the Solimões and Içá formations is an erosive surface that is laterally continuous for hundreds of kilometers (Maia *et al.* 1977, Rossetti *et al.* 2012, 2015, Nogueira *et al.* 2018, Nogueira *et al.* 2013, Horbe *et al.* 2013). Upper Pleistocene to Holocene fluvial terraces locally cover these Neogene units.

This work addresses the Neogene palynostratigraphy of the Solimões Formation, exposed near the Urucu-Coari region, Central Amazonia (Fig. 1). The palynomorphs assisted paleoenvironmental interpretations and were used for regional correlation based on the zones established for the north of South America region (cf. Lorente 1986, Hoorn 1993, Silva-Caminha *et al.* 2010, Jaramillo *et al.* 2011, Nogueira *et al.* 2013, Silveira & Souza. 2015 Leite *et al.* 2017, 2020) and confirm the occurrence of expressive unconformity linked to the onset of the Andean

Amazon River.

4.2 GEOLOGICAL AND PALEONTOLOGICAL CONTEXT

The Solimões Basin is one of the most important intracratonic basins in the Brazilian geological scenery due to gas and hydrocarbons, mainly in the Urucu fields (Maia *et al.* 1977, Prinzhofer *et al.* 2014). It was implanted in Proterozoic crystalline and sedimentary rocks of the Amazonia Central Province and extending over 440.000 km² (Wanderley-Filho *et al.* 2007, 2010, Caputo *et al.* 2012, Caputo 2014). Internally, this basin is divided by the Carauari Arch in the Jandiatuba and Juruá sub-basins (Eiras *et al.* 1994, Caputo 1995, Wanderley-Filho *et al.* 2007). The eastern limit is the Purus Arch that separates it from the Amazon Basin (Caputo 1995), and the west, the Iquitos Arch, represents the limit with the sub-Andean basins and Amazon plain (Roddaz *et al.* 2002, 2005) (Fig. 1).

The sedimentary record of the Solimões Basin is marked by multiple events of marine regression and transgression associated with different subsidence and uplift histories that controlled the behavior of structural arches active mainly in the Paleozoic (Caputo & Silva 1991, Wanderley-Filho 2010). During the Miocene, mega-wetlands developed due to the regional subsidence related to the Andean elevation were generated (Hoorn *et al.* 2010). Several authors suggest discrete marine incursions in Amazonia to the Lower to Middle Miocene in Colombia, Peru, and Brazil (Hoorn 1993, 1994, Monsch 1998, Gingras 2002, Leite 2006, Homikoski 2007, Hoorn *et al.* 2010, Rodaz *et al.* 2010, Gross *et al.* 2014, Jaramillo *et al.* 2017, Linhares *et al.* 2017, 2019).

The “Pebas/Solimões Lake” include the Madre de Dios Formation, -Peru (Campbell *et al.* 2006), and Ucayali or Pebas Formation, that are correlated to Solimões Formation, -Brazil (Gross *et al.* 2011, Nogueira *et al.* 2013). The Solimões Formation reaches ~2000 meters thicknesses (Maia *et al.* 1977, Latrubesse *et al.* 2007, Maia & Marmos 2010), dated in the Lower to Upper Miocene to Pliocene by paleontological and stratigraphic investigations (Hoorn 1993, 1994, 2006, 2010, Wesselingh *et al.* 2002, 2006, Vonhof *et al.* 2003, Antoine *et al.* 2006, Latrubesse *et al.* 2010, Shephard *et al.* 2010, Gross *et al.* 2011, Nogueira *et al.* 2013, Salas-Gismondi 2015, Leite *et al.* 2016, Salas-Gismondi 2016, Jaramillo *et al.* 2017, Linhares *et al.* 2017, 2019).

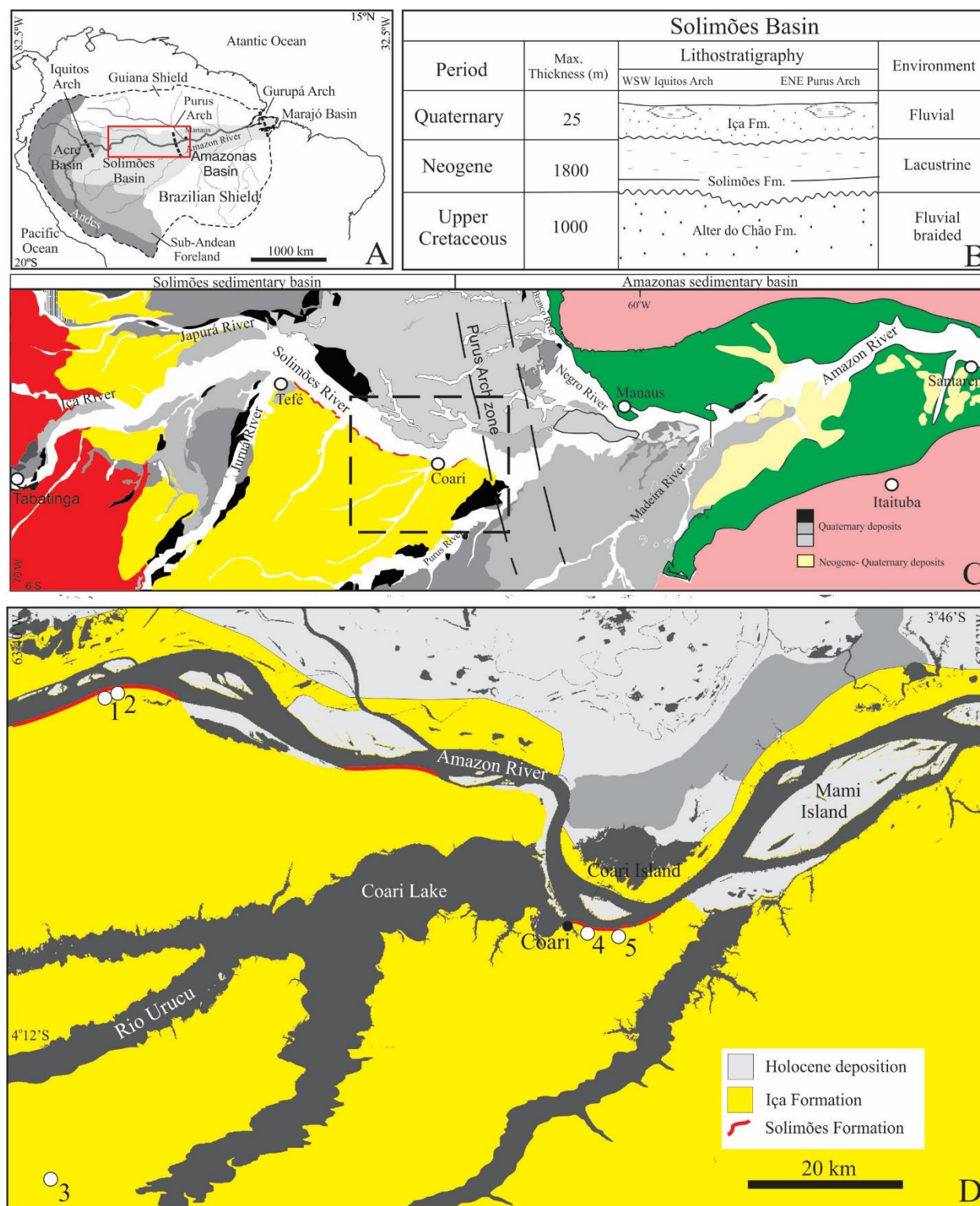


Figure 1- A) North of South America, the eastern border of the Solimões Basin, a region bordering the Amazon Basin, separates by the Purus Arch. B) Stratigraphic framework of the Solimões Basin. C-D) Urucu-Coari region with an indication of the points studied.

In Ramon Formation, this lake was described as the Lower Tertiary. The upper part

corresponds to the youngest strata of the Ipururo Formation in Peru has a mammal fauna and flora of Huayquerian (Sánchez & Herrera 1998), similar to that found in the Solimões Formation, Brazil (Maia *et al.* 1977, Schobbenhaus *et al.* 1984, Flynn & Swisher 1995, Woodburne *et al.* 2006, Goillot *et al.* 2011). The similarities in reported descriptions and ages suggest that the Solimões Formation also extends into Venezuela (Scheyer & Delfino 2016), south to southeastern Colombia (Jaramillo *et al.* 2017), confined to the Caquetá-Putumayo Basin, north and eastern Ecuador (Antoine *et al.* 2016).

The mega wetlands period related to Pebas and Solimões depositional system has extended for more than 15 Ma (Albert *et al.* 2018). The different Andean orogenic pulses likely caused continuous expansion and contraction of this system, thus generating substantial control over paleovegetation and paleoenvironment. (Leite *et al.* 2017, Goddard & Carrapa 2018, Carrapa *et al.* 2019). This temporary connection may have existed around 18.3 Ma (van Soelen *et al.* 2017), suggesting that the transcontinentalization of the Amazon River should not have been a continuous process, occurring between 2.6-0.01 Ma (Rossetti *et al.* 2015, Cremon *et al.* 2016). The tectonic dynamic resulted in strong subsidence, mainly in the Solimões Basin, and developed large accommodation space where packages of up to 1000m of sediment were deposited (Wesselingh *et al.* 2006, Latrubesse *et al.* 2007, 2010, Hoorn *et al.* 2010). The Upper Miocene is related to the final phase of this lake, a period when a connection between the Andes and the Amazonia lowlands enabled a new dispersion of species (Antonelli *et al.* 2009).

The rich megafauna fossil and palynomorphs assemblage recognized in the strata of the Solimões Formation, for example, the first record into Upper Miocene of *Amahuacatherium* (Frailey *et al.* 1996), *Purussaurus brasiliensis* from the Middle Miocene (Aguilera *et al.* 2006) and others crocodylian morphotypes of Lower Eocene-Pliocene (Souza *et al.* 2016). Palynomorphs analyses, infer Miocene age for Solimões Formation in regions such as Coari (Guimarães *et al.* 2013, Nogueira *et al.* 2013, Silveira & Souza 2015, 2016) and Miocene to Pliocene in other Amazonia areas (Hoorn 1994, Hoorn *et al.* 2010, Silva-Caminha *et al.* 2010, Leite *et al.* 2016, Kachniasz & Silva-Caminha, 2016, Sá & Carvalho 2017 Silveira & Souza 2017, Leandro *et al.* 2018, D'Apolito *et al.* 2019, Jorge *et al.* 2019, Linhares *et al.* 2017, 2019, Leite *et al.* 2020).

Besides, relevant geological barriers are stand out, such as the Iquitos and Purus arches

that possibly controlled the drainage and sedimentation during the Neogene, confining the Amazon River to the east. This last arch was only broken in the Pleistocene, registered in the deposits of the Içá Formation. (Espurt *et al.* 2007, Roddaz *et al.* 2005, Hoorn *et al.* 2010, Silva-Caminha *et al.* 2010, Horbe *et al.* 2013, Nogueira *et al.* 2013, Rossetti *et al.* 2015, Caputo & Soares 2016). Overlapping the Solimões, the Içá formation covered a vast area of the western Amazon plain (Caputo & Soares 2016, Hoorn *et al.* 2017, Jaramillo *et al.* 2017) and was defined as Pleistocene age estimated from OSL studies (Rossetti *et al.* 2015, Pupim *et al.* 2019).

Albert *et al.* (2018) consider that younger ages than Pleistocene obtained by OSL for Amazonia are difficult to predict or even enigmatic because the sediments are continuously recycled, adding to the heterogeneity of age of the sedimentary formations, as well as the lack of high-resolution stratigraphic surfaces that enable their chronological organization. Arguments supported by the specificity of its sedimentary cycle, which consists of burial, exposure, redeposition downstream and new burial, changing periods of exposure to sunlight registered in the crystalline reticulum of the quartz, thus raising several limitations regarding the use of this technique and its ages resulting. This large age discrepancy is probably due to the lack of detailed stratigraphic studies, poor palynomorphs age constraints, and OSL age application that have complicated the Neogene deposits' correlation along the Western, Central, and Eastern Amazonia.

4.3 MATERIAL AND METHODS

For the grain's location, the England Finder (EF) coordinate system was used. The slides are stored in the Laboratory of the Amazonia Sedimentary Basin Group (GSED), belonging to the Federal University of Pará, Brazil. In the identification, we followed the database made available by Jaramillo and collaborators and the pollen collection by Alan Graham, which can be found at the Smithsonian Tropical Research Institute (STRI, Panama). Was used Jaramillo *et al.* (2011) as a basis for the correlation of the taxon's biostratigraphic zones and amplitudes zones.

According to the current Brazilian stratigraphic code, an amplitude zone is constituted in the body of strata that represents the total amplitude of distribution of a determined taxon, whose limits are subject to continuous changes as new data emerge, being essential to emphasize that these limits do not represent the original true extension of the taxon. The amplitude zone's real

limits, of regional scope, should be established only after all the region's local geologic sections have been examined. The only case in which it could be said, with relative certainty, that the entire vertical amplitude of a taxon is represented in a particular area occurs when sections show complete gradation, from predecessor forms below, up to immediate descendants above

The adopted systematic classification (see supplementary material) of pollen grains and fossil spores of the Solimões Formation was based in the works (Potonié 1956, 1958, 1960, 1966, 1975, van der Hammen 1956a–b, van der Hammen & Wijmstra 1964, Germeraad *et al.* 1968, Dueñas-Jiménez 1980, Lorente 1986, Muller *et al.* 1987, Hoorn 1993, 1994a–b, Jaramillo & Dilcher 2001, Traverse 2007, Hesse *et al.* 2008, Jaramillo *et al.* 2010, 2014, Silva-Caminha *et al.* 2010, Jaramillo & Rueda 2013, 2017, Salamanca *et al.* 2016, Hoorn *et al.* 2017, D’Apolito *et al.* 2018, Leite *et al.* 2020) well as the revisions related to sporites classification (Traverse 2007). The basis for these cited groups' classification is identifying diagnostic features like apertures, wall ornamentation, thickness, and/or extension of exine, spore, and pollen sculptures. Thus, it was possible to identify 59 taxa (outcrop), 23 pollen grains of angiosperms and gymnosperms, 12 ferns spores. In the drill core was recorded 36 taxa, 32 pollen grains of angiosperms and gymnosperms, 4 species of ferns spores, as well as other palynomorphs (see supplementary material, table 3).

4.3.1 Facies analysis

The description and modeling of facies followed what was proposed by Walker (1992), which characterizes the term "facies" as a body of rock with specificities that differentiate it from bodies of adjacent rocks, such as predominant lithology, sedimentary structures, and biological effects generated by variations in sedimentary processes. In this model, genetically related facies are grouped into facies associations. The analysis of the vertical succession of facies and architectural elements is indispensable for the paleoenvironmental reconstruction of the depositional system (Reading 1980, Allen 1983, Miall 1992, Cross & Homewood 1997).

Lithostratigraphic profiles illustrate the vertical stacking of facies according to the model proposed by Wizevic (1991). The vertical stacking, aided by the construction of panoramic sections, contributes to identifying architectural elements in outcrops with great lateral continuity (Allen 1983, Miall 1985). Also, stratigraphic surfaces are identified and ordered according to the

magnitude of sedimentary processes (Allen 1983).

4.4 FACIES AND PALEOENVIRONMENT

Based on outcrops and drill core, the facies analysis was performed in the Barro Alto and Urucu-Coari regions were carried out on the margins of the Solimões River, in four outcrops with a thickness of up to 20m and one drill core STG-02 thickness 250m (Fig. 2). The limit between Solimões and Içá formations is an irregular unconformity, generally marked by iron oxides-hydroxides, separates the heterolithic deposits of Solimões Formation of sandy lithotypes of the Içá Formation. The Solimões Formation facies exhibit grey color and generally low angle beds, contrasting with pinkish to yellowish Içá deposits disposed of in subhorizontal beds. Four facies associations representing lacustrine, megacrevasse splay, and meandering fluvial deposits were recognized for the Solimões and Içá Formation, reinterpreting Vega's previous proposal. (2007) (Tab. 1-2).

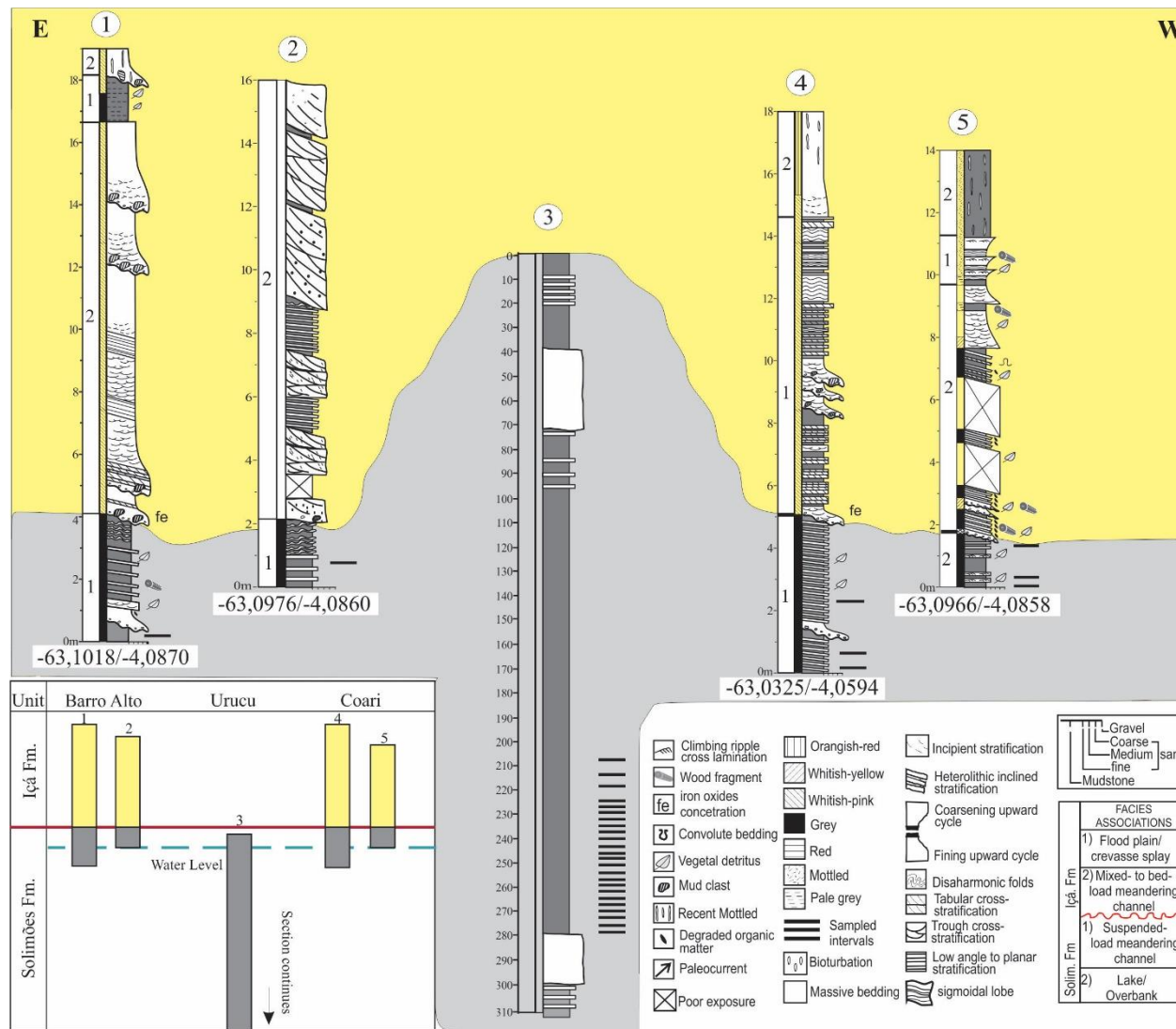


Figure 2- Stratigraphic profiles of the Neogene succession outcropping on the banks of the Solimões River, near the Urucu-Coari region, Central Amazonia. The profiles were marked with the lowest water level in the river—the location of the profiles in figure 1.

Table 1- Lithofacies and sedimentary processes Urucu-Coari Region, Amazon state, Brazil.

Lithofacies	Structures	Depositional processes
Mudrock with even parallel lamination <i>Mp</i>	Dark laminated to massive, very fine sandstone occurs subordinately.	Deposition by suspension with the sporadic influx of terrigenous and debrites of plants.
Massive mudrock/sandstone <i>MSm</i>	Abundant plant remains, and carbonized trunks can also be observed.	Deposition from traction and suspension.
Rhythmic sandstone/mudrock with wavy-linsen structure <i>Rwl</i>	Locally can be observed ball and pillow structures and convolute lamination.	Migration of ripple marks under suspension and traction currents. Plastic adjustments by overload and liquefaction.
Deformed sandstone/mudrock <i>SMd</i>	Convolute bedding showing disharmonic folds, medium-scale load cast structures, convolute lamination, flame structures, synsedimentary fault, and tilted mudrock filling channel geometry.	Plastic deformation is associated with slumping and sliding processes. Plastic adjustment by liquefaction.
Sandstone with climbing-cross lamination <i>ScI</i>	Subcritical and supercritical bedforms. Locally, convolute lamination can be observed.	Deposition from suspension and traction currents, abundant sandy inflow. Secondary liquefaction process.
Bioturbated sandstone/ mudrock <i>SMb</i>	Vertical to curved tubes, some presenting spreiten similar to <i>Taenidium</i> trace fossils. Radial tube structures with white halos in mottled horizons.	Reworking by the activity of roots and benthic fauna. Concentration and leaching of iron oxides and hydroxides.
Sandstone with cross-stratification <i>Scs</i>	Trough and tabular cross-stratifications in individual beds or composing inclined heterolithic stratification. Convolute lamination.	Migration of 3D and 2D bedforms under unidirectional flow. Gravitational instability and liquefaction process.
Inclined heterolithic stratified sandstone/mudrock <i>SMI</i>	Low-angle stratification forming master bedding in heterolithic beds. Trough, tangential and tabular cross-stratifications developing complex bedding. Climbing-ripple cross lamination. Root marks, mottled horizons, and bioturbation.	Deposition by lateral migration of point bars. Bar emergence and colonization by vegetation. Biological activity of benthic fauna.
Sandstone with complex cross-stratification <i>ScC</i>	Sandstone with planar, undulating, cross-, trough, and sigmoidal stratification. Reactivation surfaces, synsedimentary faults, and convolute lamination. Mud drapes and mudrock beds separating lobate forms.	Deposition by traction currents under upper flow regime with a fast deceleration of water energy. Gravitational instability and adjustments by liquefaction process.
Massive sandstone <i>Sm</i>	It is generally associated with sandier facies.	Liquefaction, high inflow of sediment and gravitational instability, fast deposition. Recent weathering obliterating primary structures.
Massive and stratified Conglomerate <i>Cms</i>	It has around 40 cm thick, rounded pebbles of mudrock and quartz. Trunk fragments marking the channelized surface. Incipient cross-bedding	Deposition for bedload discharge. Reworking of mudrock beds by channelized flows.

4.4.1.1 Lake/overbank (LOV)

Corresponds to a low energy environment with periodic sand inflows, such as observed in other modern and ancient lacustrine deposits of terminal river systems (e.g., Hyne *et al.* 1979, Talbot & Allen 1996, Buchheim *et al.* 2000). This association's lateral continuity for several kilometers without bioturbation, dark mudrocks with well-developed laminations, and leaves following bedding planes suggest deposition from suspension under anoxic conditions (Table 1). Deformation structures such as convolute bedding may be related to slumping produced by crevasse splay deposits. (Coleman 1981, Coleman *et al.* 1983). Therefore, the lake setting was associated with floodplains and levees linked to the perennial meandering channels with vegetated margins (Table 2).

4.4.1.2. Suspended-load meandering channel (SLMC)

The lateral relation of SLMC association with lake and overbank deposits (LOV association) indicates that fluvial channels drained the wetland areas. The dark color observed in these deposits indicates much organic matter in the water from the degradation of vegetated margins (Table 1). The acid black waters can be similar to those found today in Amazon Rivers. They developed anoxia conditions that partially prevented benthic activity, explaining the absence of bioturbation in these deposits (Table 2).

4.4.1.3. Mixed-load to bedload meandering channel (MBMC)

The dominance of well-sorted, fine- to very fine-grained sandstones, related to several types of cross- and even parallel beddings suggest progradation with high sediment load in low energy distal environment. Like the SLMC association, the sandy point bar deposits in MBMC contain mud clasts from the floodplain deposits, probably derived by slumping from nearby cutbank. The abundant sandstone facies and the bimodal flow observed in this association confirm a mixed-load interpretation to bedload meandering fluvial channel with straight segments and low sinuosity for the MBMC association (Table 2).

4.4.1.4. Flood plain/crevasse splay (FPC)

The FPC has a great contribution of the palm pollen from lowland forests of *Mauritiides franciscoi* and *Alnipollenites verus* (Silveira 2005, Nogueira *et al.* 2013) is also marked by a high frequency, and it is related to temperate montane forests. *Echiperiporites estelae* and *Monoporopollenites annulatus* also occur with common frequency at this level (Nogueira *et al.* 2013). The lobed sandstone, occasionally amalgamated or separated by thin beds of mudrock, with Scs and Slc facies are interpreted as crevasse splay deposits (Table 1). Crevasse channels develop by breaching of a levee during high-runoff events, and may result in a permanent diversion of the main flow or avulsion (Miall 2010).

Table 2- Facies Associations of Cenozoic succession in the Urucu-Coari Region.

Fm	Facies association (FA)		Interpretation
I Ç Á	1	The FPC consists of facies Mp, Rwl, MSm and Msl forming tabular to lenticular beds with up to 4 m-thick. The intercalations with facies Slc and Rwl are frequent in the upper part of the association overlaying the Point bar deposits MBMC (association). The cross-bedding is highlighted by mud layers/mud drapes and generally associated with Scl. The FPC can reach up to 8 m-thick overlying the unconformity directly. Sometimes, the association starts with channelized pebbly sandstone (mudrock clasts) in packages with up to 2 m-thick. These fine deposits of FPC are interpreted as floodplain deposits (e.g. abandoned channel) that were formed by cut-off of and subsequent abandonment of a river channel (Miall 2010).	Flood plain/crevasse splay
	2	This association has many faciological similarities with the SLMC deposits and is organized in fining upward cycles, but the sandstone frequency is high compared with mudrock beds. The MBMC reach up to 20 m-thick and comprise fine- to medium-grained sandstone with IHS (SMi facies), trough and tabular cross-bedding (Scs and Cm facies), even-parallel bedded sandstone, and conglomerate (facies Cm) marking the contact with the Solimões deposits (Table 1). The fine- to medium-grained sandstone interbedded with thin mudrock beds forming IHS (SMi facies) and intraformational conglomerates with mudrock pebbles (facies Cm) are the most frequent facies. Coarse grains can be found segregated in the foresets.	Mixed-load to bedload meandering channel
S O L I M Õ E S	1	The SLMC association consists mainly of mudrocks, fine sandstones, and subordinately conglomerates relative to the facies Cm, SMi, Mp, MSm, and Rwl organized in meter-scale fining upward cycles. The IHS sandstone is frequently interbedded with 1m-thick of Scl facies, and centimetric beds of facies St. The SMi facies are the product of lateral accretion of point-bars of meandering channels (Thomas <i>et al.</i> 1987). The coarse-grained deposits represent high-energy flow into the fluvial channel and reworking of mudrock blocks from cut banks. Thus, lateral alternations in the cosets thickness represent the seasonal cyclicity of fluvial waters. Alternations of facies Scc and Scl correspond to the predominance of suspension compared with the traction process.	Suspended-load meandering channel
	2	The LOV association is mainly comprises the Mp, MSm, Rwl, and Scl facies constituted of mudrock, siltstone, and subordinately laminated to massive, very fine sandstone (Table 1). The suspension process is well-related with sporadic fine-grained terrigenous inflow and plant debris. Also, the LOV facies association's lateral continuity for hundreds of kilometers suggests an extensive, flat, and low-energy environment. The dark color and frequently plant debrites in all outcrops indicate stagnant and anoxic shallow-water bodies setting with an exceptional preservation potential for the organic matter.	Lake/overbank

4.5 PALYNOLOGY

The paleoenvironmental analysis of the Solimões was based by microfloristic associations. The studied assembly is rich in specimens, however, diversity is low in almost all sampled levels. These results are compatible with alluvial plains (see Lorente 1986), corroborating our paleoenvironmental interpretation. In general, we found angiosperms pollen, highlighting the *Alnipollenites verus*, *Grimsdalea magnaclavata*, and *Monoporopollenites annulatus*, pteridophytes such as *Magnastriatites grandiosus*, *Crassoretitriletes vanraadshooveni*, and freshwater algae of genera *Ovoidites* and *Botryococcus* sp., as well as acritarchs (Fig. 10).

In the SLMC association, the pollen and spore grains exhibit better preservation and are more abundant when compared with those found in the LOV deposits. In the FPC deposits, the palynologic content is three times less than in the SLMC, suggesting shallow to emergence conditions. Some elements increase in frequency in some levels, for example, *Bombacacidites* and *Mauritiidites franciscoi* are abundant, and their frequency is inversely proportional to the occurrence of *Monoporopollenites annulatus* and other types of grasses, indicating oscillation between arbustive and arboreal phases during sedimentation, probably as a consequence of alternating dry and humid periods.

Our palynological data are similar to that proposed by Jorge *et al.* (2019), which, from the integration of geophysical and palynological data from the Solimões Formation, proposed 3 three temporal phases linked to the energy flow of the paleoenvironments, starting in the Lower Miocene in the zone *Mauritiidites franciscoi*, fossil palm, was associated with low energy environments, swamps. For the Middle Miocene, the zone *Grimsdalea magnaclavata*, a fossil palm, was related to a similar environment to *M. franciscoi*, but with alternations between high and low. The *Monoporopollenites annulatus* zone linked to the Upper Miocene and associated with high-energy environments with greater activity in the river dynamics, which coincides with global climate change events, as well as the influence of the orogenic pulses from the Andes in 12 Ma (Hoorn *et al.* 2010). The relationship between the increased abundance of *Monoporopollenites annulatus* from the Upper Miocene was also confirmed by Kirschner & Hoorn (2020). Wherefrom the optimum climate that occurred in the Middle Miocene, it is possible to

observe a sharp and continuous increase in the abundance of this pollen, which may be related to climatic factors (fig. 3)

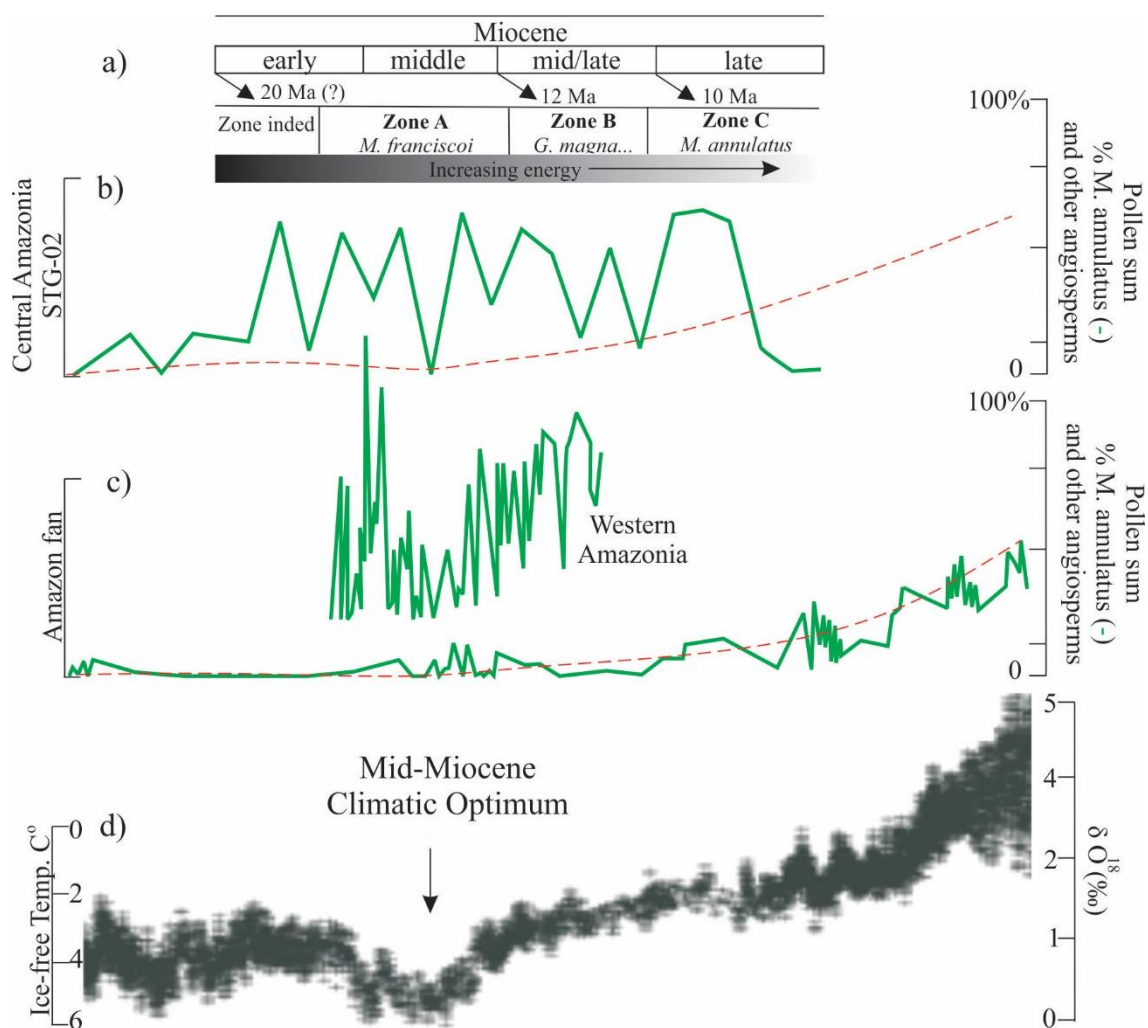


Figure 3- Integrated areas of an abundance of *Mauritidites franciscoi*, *Grimsdalea magnaclavata*, and *Monoporopollenites annulatus* for the Miocene of Amazonia according to the intensity of the energy flow paleoenvironments, based on palynological and geophysical data (Jorge *et al.* 2019). b) Diagram with % *Monoporopollenites annulatus* x other angiosperms for Central Amazonia (this work). c) Diagram with % *Monoporopollenites annulatus* x other angiosperms for the Amazon fan (Hoorn *et al.* 2017) and Western Amazonia (Jaramillo *et al.* 2017) as described by Kirschner & Hoorn (2020). d) Temperature curve for the Neogene (Zachos *et al.* 2008) emphasizing the climatic optimum that occurred in the Middle Miocene. The dotted line in red represents a trend of variation for *Monoporopollenites annulatus*, in green, the percentage variation of that pollen for the Miocene.

4.6 INDIGENOUS AND REWORKED POLLEN GRAINS

The Amazon displays a rate of organic decomposition that can exceed five times found in temperate environments, it is no wonder that in tropical zones, the preservation of pollen grains is hampered by the significant loss of soil organic matter (Tomescu 2000). However, according to its genetics and the conditions of the depositional environment, each species responds differently to the other, generating particular pollen assemblage for each site (Phumphumirat *et al.* 2009, Twiddle & Bunting 2010).

Pollen grains and spores are preserved according to inherent internal factors, for example, exine thickness and structure. In addition to externals, physical-chemical, where the preservation is directly proportional to the degree of compaction of the sedimentary material and the percentage of sporopollenin, composed of carbon, hydrogen, and oxygen (Mackenzie *et al.* 2015), that sporopollenins are a mixture of biopolymers or molecules rather than a single, homogeneous macromolecule (Guilford *et al.* 1988, Domínguez *et al.* 1999), as well as anaerobic chemical conditions since they are susceptible to oxidation, abrasion of pollen grains is usually minimal (Erdtman, 1960, Punt *et al.*, 2007, Bernard *et al.* 2009, Lowe *et al.* 2015).

So far, the best prognosis for understanding susceptibility to corrosion, one of the elements involved in pollen decomposition, is the sporopollenin content. When we analyze the range of sporopollenin in *Alnus* it is acceptable to agree with the fact that this grain can be considered semi-stable, meaning that it would have excellent resistance to chemical weathering and other decomposition processes. (Fig. 4).

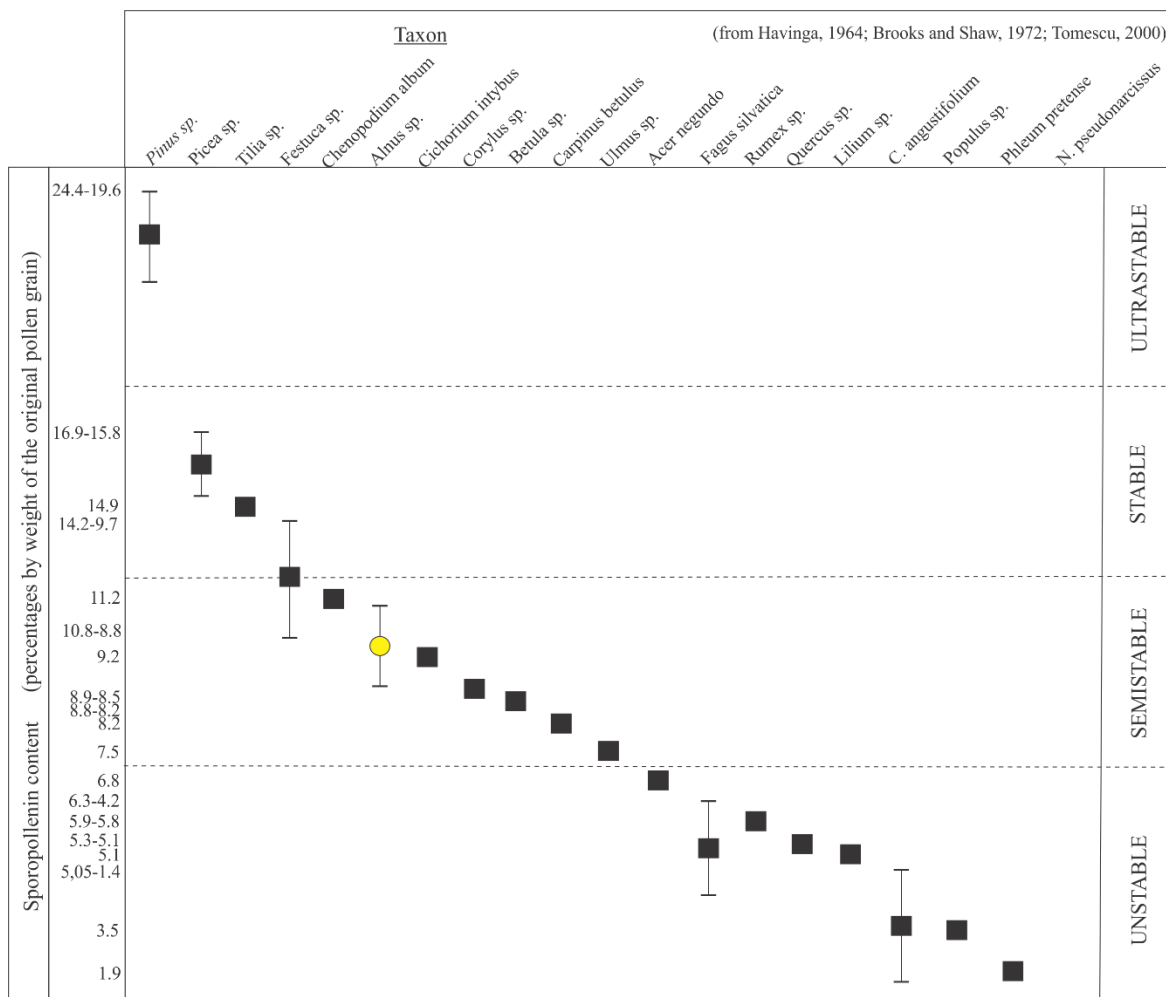


Figure 4- Degree of preservation of pollen grains versus the amount of sporopollenin, with emphasis on the *Alnus* area, considered as semi-stable because it contains a large amount of sporopollenin. (mod. Havinga 1964, 1967, Brooks & Shaw 1972, Tomescu 2000).

As previously mentioned, the Solimões Formation consists of large lakes generated from the stagnation of water from the reversal of the Amazon River's flow caused by the Andean uplift, thus forming swampy regions. Phuphumirat *et al.* (2009) show that in the swamp clay, pollen preservation was low. There was an evident loss of more than 75% of the pollen grains of *Wedelia trilobata*, *Acacia auriculiformis*, *Hibiscus rosasinensis*, and *Merremia umbellata* already in the first two months of burial, given that, in swamps, frequent wet-dry cycles influenced by water level fluctuations (Havinga 1967, 1984, Phuphumirat *et al.* 2009). Repeated cycles of soil hydration and dehydration can lead to the destruction of the grains since the walls tend to stretch and contract depending on the environment's humidity. This constant repetition weakens pollen grains over time and

destroys them. Many experiments have shown that after a few dry-drying cycles, significant damage to pollen grains occurs (Holloway 1989, Campbell 1991, Campbell & Campbell 1994, Bryant 2005, Phuphumirat *et al.* 2009).

The approach to the problem of reworked palynomorphs extends for decades (Iversen 1936, Erdtman 1954, Muller 1959, Ananova 1960, Davis 1961, Stanley 1965, 1966, Batten 1991, Tyson 1995, Smith & Higgs 2001). In this paper, we use the identification suggestions, permitted the establishment of objective criteria for the recognition of reworked grains, of authors as Stanley (1965, 1966), which exemplified that the variation in the grain tonality, often generating small spots on its surface, Batten (1991) raised the possibility that reworked palynomorphs have, in general, darker tones than those found *in situ*, suggesting factors such as thermal alteration and erosion rate speed as crucial for this.

Conceptualize aspects such as deterioration in fossil pollen grains, crumpled, broken, corroded, and degraded, necessarily indicative of reworking. It's a misinterpretation. At first, it should be considered only as a possibility (Wilmshurst & McGlone 2005, Twiddle & Bunting 2010). However, many fossil grains exhibit some of these features (Tweddle & Edwards 2010). Some palynomorphs like the Acritarchs are easily preserved even in visibly reworked sedimentary layers, there is not sufficiently adequate information about their retransportation and redeposition, being difficult to relate their pristine preservation to the transport distance but can be used to identify the source area (Streel & Bless 1980, Tyson 1995 McLean 1995). Understanding reworked palynomorphs still require greater attention because of their potential as a tool in the identification of erosive processes and provenance (fig. 5).

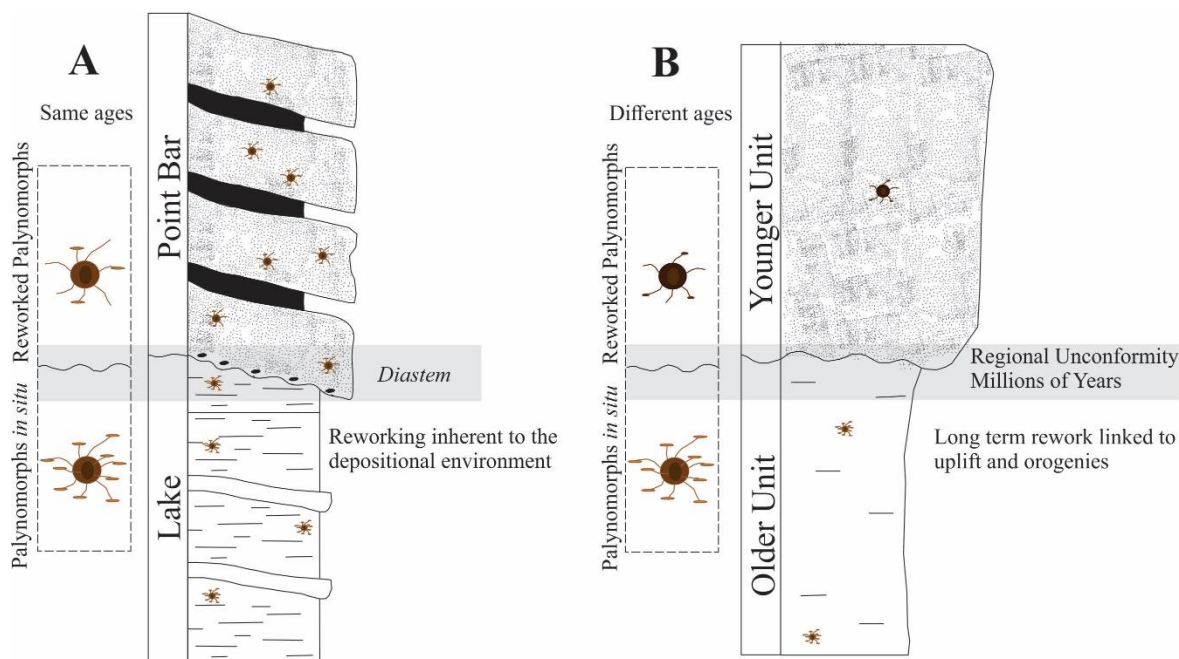


Figure 5- Difference between reworked pollen grains. a) in diastema and b) in regional unconformity.

When identifying pollen grains that have undergone some reworking degree, usually associate them with geological unconformity processes called a *regional unconformity*. This surface results from pronounced erosion of rocks before the deposition of the stratigraphic layers above. Often exceeds the order of millions of years. Consequently, the youngest unit includes elements that previously belonged to the temporally oldest unit (fig 5a). However, what is little discussed are the unconformity caused by processes inherent to the unit's depositional system called *diastem*, for example, in a fluvial environment, it's common to find deposits linked to channel migration, the so-called point bar, structure generated from a high energetic flow, reworking old preexisting deposits, such as the river floodplain, that is, processes that do not present significant temporal variation and that are linked to the same unit. Thus, in addition to paying attention to the grain's visual elements, it is essential to understand the depositional environment in which it was found. (fig. 5b).

The occurrence of Miocene and Paleozoic palynomorphs reworked in the studied sequence corroborates an erosion event that marks the top of the Solimões Formation Urucu-Coari region. Miocene reworked palynomorphs such as *Cyatheacidites annulatus*,

Foveotriletes ornatus, and *Grimsdalea magnaclavata* occur in the association of point bar facies. Moreover, several forms of reworked acritarchs are found that reach up to 25% of the palynomorph content, especially *Maranhites brasiliensis* (Silveira 2005) and many indeterminate acanthomorphs. The reworked Miocene palynomorphs indicate the meandering fluvial system's action removing part of the Mesomiocene deposits from the Solimões Formation. The abundance of reworked palynomorphs from the Paleozoic is an index of the top of the Solimões Formation in the Urucu-Coari region not observed in the Içá Formation (fig. 6).

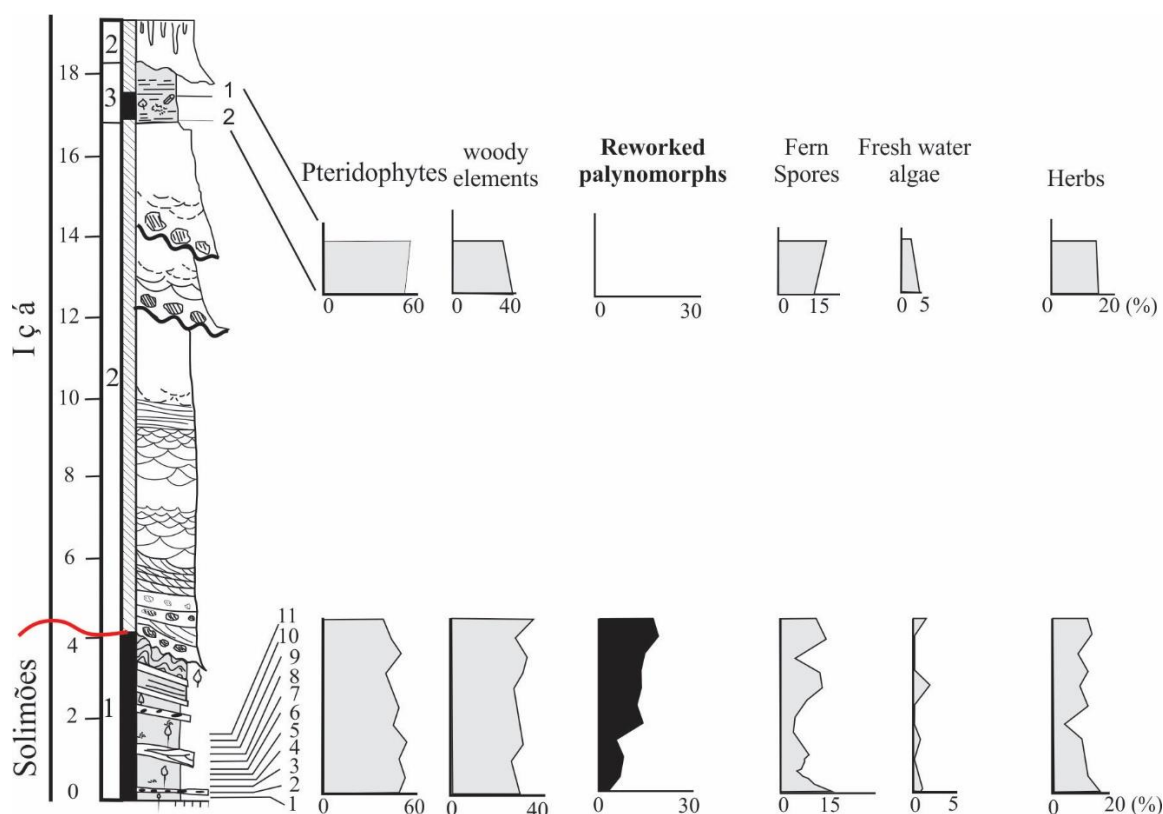


Figure 6- Quantitative graphical representation (percentage) of the main groups of palynomorphs found in the transition between Solimões and Içá Formation in Urucu-Coari region, Central Amazonia. Observe the frequency of reworked palynomorphs present mainly at the top of the Solimões Formation.

During the Late Miocene and Pleistocene, rocks of the Upper Paleozoic of the Amazon Basin's northwestern edge were eroded entirely, indicated by reworked palynomorphs of the Upper Devonian and spores of the Upper Carboniferous (fig. 8). Well-preserved acritarchs, such as *Maranhites brasiliensis*, *Gorgonisphaeridium* spp. suggest rapid deposition, probably related to the Paleozoic rocks of the region of Purus

Arch and the western margin of the Amazon Basin, raising doubts about an Andean origin (Campbell & Frailey 1984, Frailey *et al.* 1988, Latrubesse 1992, Hoorn 1993, Hoorn *et al.* 1995).

A probable source area is the northwest border of the Amazon Basin, which belongs to Purus Arch—indicating that an elevated Purus Arch drainage system was oriented westward towards the Solimões Basin during the Upper Miocene. The guide species for chronostratigraphy are not reworked, a fact indicated by the finer lacustrine facies, presence of flagella, abundance, and coloring, so it was possible to formulate a more accurate chronostratigraphy.

4.7 A PALYNOLOGICAL ZONATION FOR THE URUCU-COARI REGION

The assemblage containing *Magnastriatites grandiosus*, *Monoporopollenites annulatus*, *Perisyncolporites pokorny*, *Cicatricosisporites dorogenesis*, *Echiperiporites akanthos* present abundant quantities and wide temporal distribution. Other palynomorphs show large amplitudes but less frequently, such as *Corsinipollenites undulatus*. The palynoflora found in the prodelta, delta front, and point bar facies associations of the Solimões Formation belong to the *Echitriporites spinosus* Zone and indicate an Upper Miocene age, according to Muller *et al.* (1987), the top is marked by the appearance of *G. magnaclavata* and coexistence of *B. ciriloensis*. The forms that allowed the establishment of this age, besides those already cited, are *Crassoretitriletes vanraadshovenii*, *E. akanthos*, *Echiperiporites stela*, *Fenestrites spinosus*, *Psilastephanoporites tesseroporus* (Fig. 7).

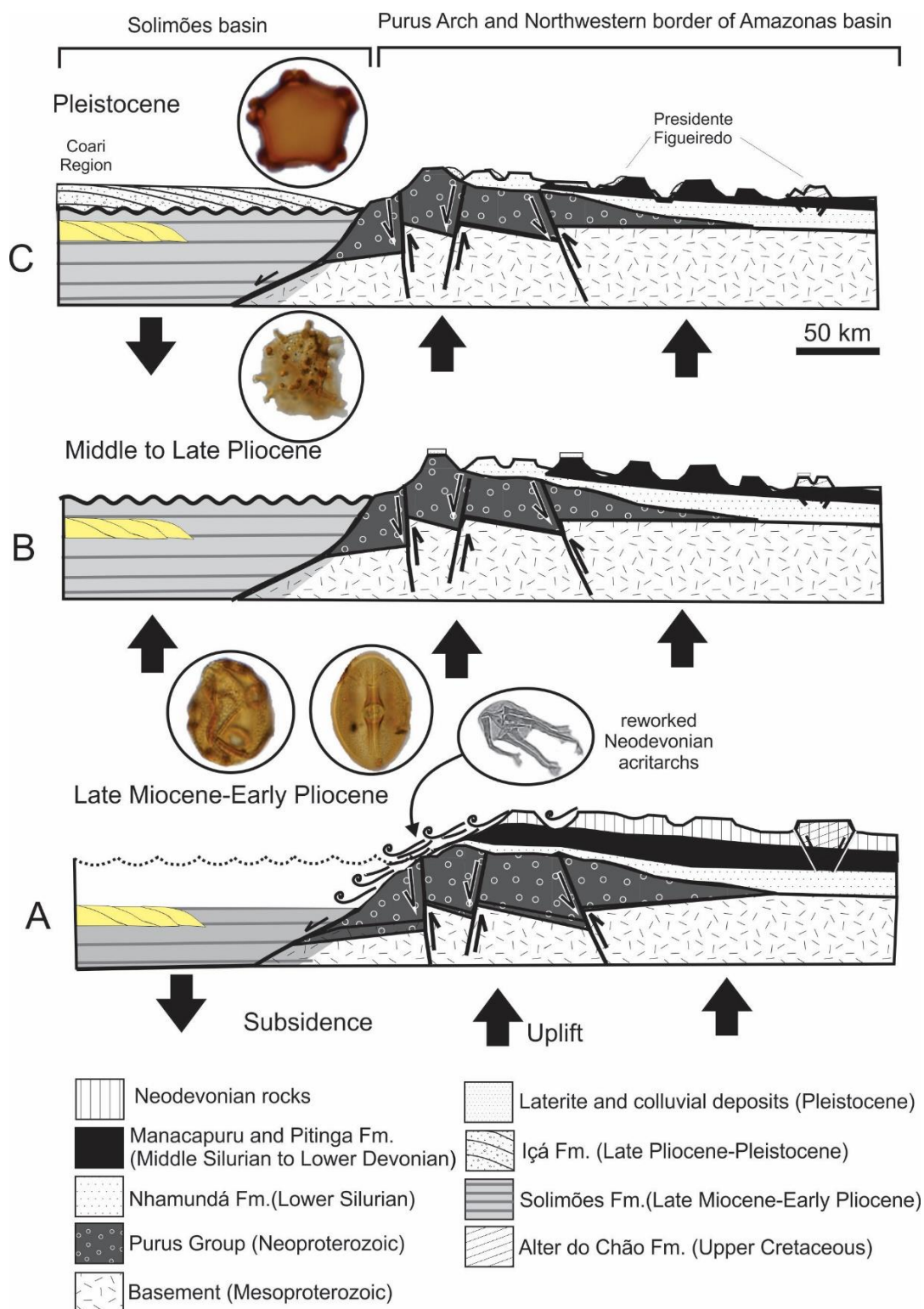


Figure 7- The Purus Arch may have acted as a barrier to the development of transcontinental drainage, capturing the influx of the Amazon River. A) The exposed Paleozoic rocks contain a diversified palinoflora, whose age is not higher than Lochkovian (Steeman *et al.* 2008). During the Upper Miocene, it appears to have played a geographical barrier between the Solimões and Amazonas Basins. The

divergence at the top of the Solimões Formation, observed over hundreds of kilometers, implies that the Solimões Basin in the central and eastern portions and the Arch were raised and eroded, an event that may have lasted from the Upper Miocene to the Pliocene. B) The Cenozoic barrier of Purus Arch was confirmed by genetic and paleogeographic data from the ancestral distribution of *Psophia*, a trumpeter bird, restricted to the Eastern Amazonia during the Pliocene (Ribas *et al.* 2011). C) During the Pleistocene, this arch subsidized and deposited sediments of the Içá Formation. Thus, this event may represent the first stage in the evolution of the Amazon River's transcontinental drainage.

The palynological ages obtained here can be compared with those of other regions. They can help establish the chronology of events and enable the correlation of stratigraphic units of the Amazon basins (Fig. 8). For example, *Grimsdalea magnaclavata* is found in the Novo Remanso Formation in the Amazon Basin (Dino *et al.* 2006) and indicates the Upper Miocene. This form has been described in the association with *Crassoretitriletes vanraandshoovenii*, typical of the Mesomiocene, in the Upper Barreiras Formation in the Bragantina Platform of northern Brazil (Arai *et al.* 1988, 1994). In the drill core STG-02, the presence of *Alnipollenites verus* is rare, and *Grimsdalea magnaclavata* is abundant, however when we compare with the outcrop data, the opposite occurs, an abundance of *Alnipollenites verus* and scarcity of *Grimsdalea magnaclavata*. An explanation is related to the outcrops be the last records of the Solimões Formation, that is, the end of the Miocene, which changes in the settings, influenced by the increase in the influx of siliciclastic material, did not favor the permanence of this fossil palm.

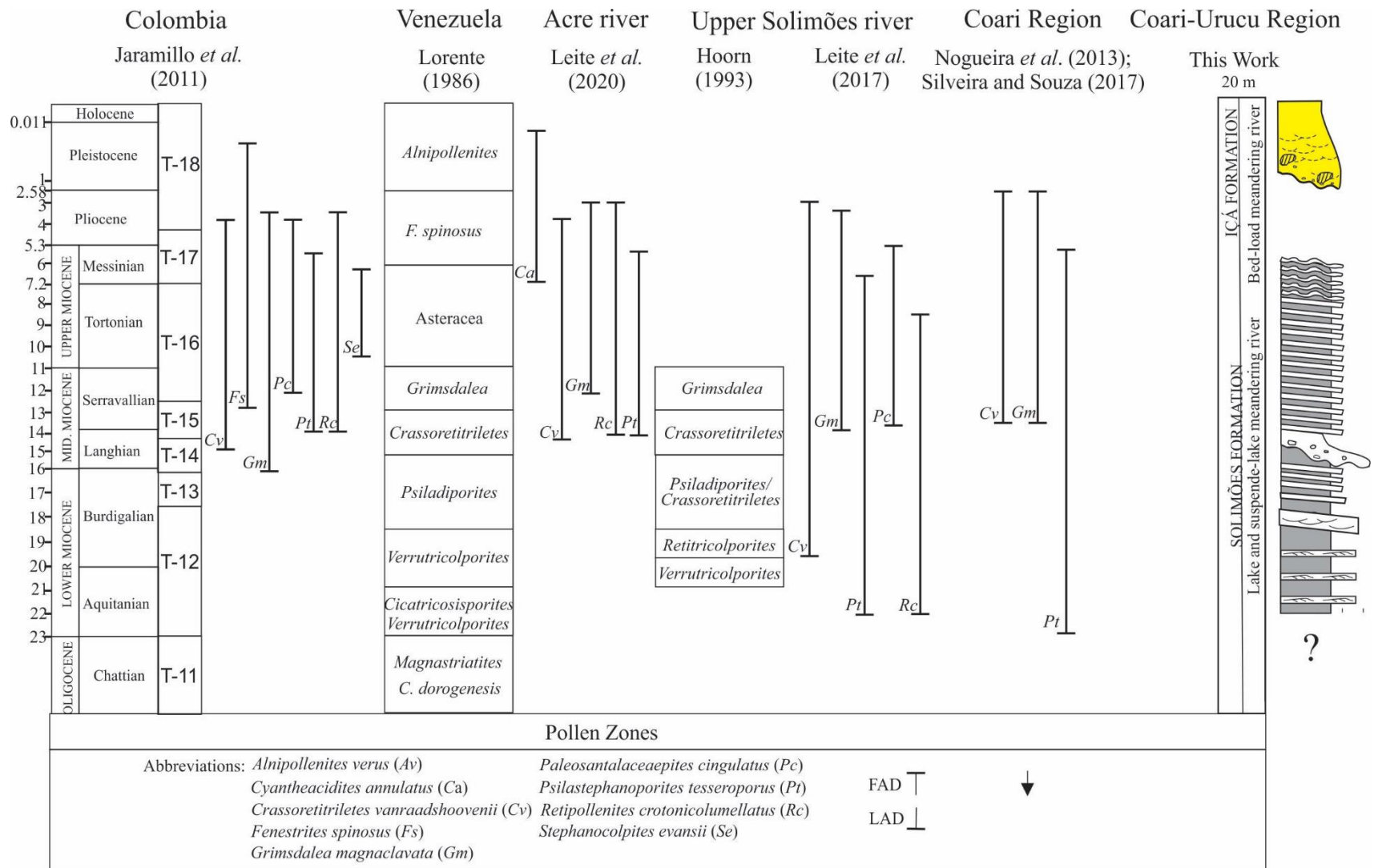


Figure 8- Stratigraphic range of guide species identified in this work according to the literature.

The palynomorphs that occur in a reworked form in the Solimões Formation in the Urucu-Coari region, supporting the post-Neomiocene age obtained. The Upper Miocene-Lower Pliocene Madre de Dios Formation of Western Amazônia (e.g., Campbel Jr. *et al.* 2001) is only correlated with the Solimões Formation of Central Amazonia and not with the Içá Formation, considered here of Pleistocene age. Based on Jaramillo *et al.* (2011) it was possible to correlate ages according to proposed zoning, the Zona T-12 *Horniella lunarensis* LAD of *Cicatricosisporites dorogensis*, and FAD *Echitricolporites maristellae*=*Malvacipolloides maristellae* (Muller *et al.* 1987, Silva-Caminha *et al.* 2010), *Clavainaperturites microclavatus*, *Foveotricolporites etayoi* (23-17.7), correspond to Superzone *Echitriletes muelleri* of Regali *et al.* (1974), Zona *psiladiporites* of Lorente (1986) and Zone *Psiladiporites-Crototricolpites* (Hoorn 1993), thus, age was defined between late Oligocene and Lower Miocene for the base of the Solimões Formation. Zona T-13 *Echitricolporites maristellae* (Jaramillo *et al.* 2011), FAD *Grimsdalea magnaclavata*, *Echitricolporites maristellae*, *Bombacacidites baculatus* and *Echitricolporites spinosus* (17.7-16.1), *Psiladiporites* Zone (Lorente 1986), *Echitricolporites maristellae*–*Psiladiporites minimus* Zone (Muller *et al.* 1987).

Zone T-14 *Grimsdalea magnaclavata* corresponds to the interval between (16.1-14.2 Ma) FAD *Crassoretitriletes vanraadshooveni*, *Grimsdalea magnaclavata*, LAD *Multimarginites vanderhammeni*, *Echitricolporites maristellae*–*Psiladiporites minimus* Zone (Muller *et al.* 1987). Zone T-15 *Crassoretitriletes vanraadshooveni* FAD *Fenestrites spinosus*, *Crassoretitriletes vanraadshooveni*, *Psilastephanoporites tesseroporus*, *Retipollenites crotonicolumellatus* (14.2-12.7). Zone T-16 *Fenestrites spinosus*, FAD *Fenestrites spinosus*, *Stephanocolpites evansii* and *Palaeosantalaceaepites cingulatus* LAD *Psilatricolporites caribbiensis* (12.7-7.1). Zone T-17 *Cyatheacidites annulatus*, LAD *Psilastephanoporites tesseroporus*, *Stephanocolpites evansii* (7.1-4.8), corroborating the Upper Miocene - Lower Pliocene to the top of the Solimões Formation.

4.8 NEOGENE-PLEISTOCENE EVOLUTION OF CENTRAL AMAZONIA

4.8.1 The sediment bypass zone and origin of unconformity

The inference of an unconformity between the Solimões and Içá formations has been demonstrated based on lithostratigraphic, faciological, mineralogical and palynological data

(Maia *et al.* 1977, Rossetti *et al.* 2005, Nogueira 2008, Nogueira *et al.* 2013, Horbe *et al.* 2013, Rossetti *et al.* 2015). This surface has been mapped for hundreds of kilometers along the right bank of the Solimões River and following this assertive is more compatible with regional unconformity (Fig. 9). The possibility that this surface represents a simple physiological change linked to the migration of river bars, as highlighted by Pupim *et al.* (2019), serves only to justify the reduced time interval of 200 Ka BP obtained by these authors.

The unconformity at the top of the Solimões Formation was responsible for the unit's significant thickness reduction. This surface is considered a subaerial unconformity (cf. Sloss *et al.* 1949) formed under subaerial conditions resulting from fluvial erosion or bypass, with expressive soil development. Subaerial unconformities may develop in both downstream- and upstream-controlled settings, most commonly during periods of negative accommodation (Catuneanu *et al.* 2011). The landscape gradient was steeper in Central Amazonia during Miocene due to the Andean Cordillera's proximity under continuous uplift phase (Fig. 9).

The uplift concomitant with the Lower Tortonian sea-level fall generated the expressive unconformity observed in the Solimões Formation (Fig. 9). This event is intimately related to the Andean Amazon River's onset in 9,5 Ma (Hoorn *et al.* 1993, Nogueira 2008, Figueiredo *et al.* 2009, Gorini *et al.* 2014, Nogueira *et al.* 2021). The high gradient promoted an eastern fast trajectory of the fluvial inflow to the lowlands or Atlantic shoreline. Subaerial unconformity may also form during periods of positive accommodation and transgression. This surface can be considered initially as a lowstand unconformity (cf. Schlager 1992), passing along the time to a "regressive surface of fluvial erosion" (cf. Plint & Nummedal 2000).

In this work, we adopt the term "subaerial unconformity" because it does not link, nor restrict, the formation of this surface to stages of lowstand or regression. Identifying a "subaerial unconformity" in the rock record requires the preservation of continental deposits (fluvial or aeolian) on top, once that, the overlaid Solimões Formation facies are not diagnostic to the identification of this surface. The time of sediment bypass or non-depositional hiatus is difficult to estimate precisely, mainly if it is subsequently reworked and replaced by younger unconformities. In this case, form a composite unconformity that includes the older and the younger erosive surfaces. In Central Amazonia, the Pleistocene Içá fluvial system was developed under the eroded top of Solimões Formation, obliterating any evidence of an older fluvial system

(Fig. 9).

Records indicate that the observed unconformity in the Central-Eastern Solimões Basin is younger than those found in Western Amazonia and named Ucayali (e.g., Campbell Jr. *et al.* 2001). Central Amazonia's uplifting partially eroded the Neomiocene-Pliocene Solimões deposits before the new subsidence event marked by the deposition of Pleistocene Içá deposits. Consequently, the development of this unconformity between Solimões and Içá can be estimated to have occurred in the Pliocene to Lower Pleistocene. This interpretation suggests that the Purus Arch region was a structural high or geographic barrier hindering the drainage connection between Solimões and Amazon basins during the Late Miocene.

4.8.2 The Andean Amazon River evolution influencing the palynomorphs amplitude zones

Neogene palynological assemblages previously registered for the succession of the Solimões Basin revealed ages that go back from the Lower Miocene to the Pleistocene (Nogueira *et al.* 2013, Silva-Caminha *et al.* 2010, Silveira & Souza 2015, 2016, Soares *et al.* 2017, D'Apolito *et al.* 2018, Gomes *et al.* 2019, Leite *et al.* 2020). This age interval agrees with those obtained in this work, taking into account the identified species' amplitude zones (Fig. 8). Adding all the amplitudes of these species, an interval of ~ 22 Ma would represent the 250m of the Solimões and Içá formations. Except for the 15 m of the Içá Formation dated in ~ 400 Ka, 235 m of Solimões Formation would have deposited during ~ 21.5 Ma. These confer a sedimentation rate around ~ 11 m / Ma, which would be too slow for an active fluvial-lacustrine system supplied by mountainous source-area. This region was also frankly subsided linked to the intracratonic basin during a back bulge foreland system (Roddaz *et al.* 2005). Thus, the eroded interval of the Upper Solimões Formation was underestimated by the previous biostratigraphic proposals.

The palynomorphs' amplitude zones were readjusted based on the existence of a significant sub-aerial unconformity (Fig. 8). This procedure was fundamental to restrict the age range of the exposed deposits of the Solimões Formation and correlate them with the episode linked to the beginning of the Andean Amazon River at 9.5 Ma (Fig. 9). This event is mainly identified in the Amapá platform wells associated with the Amazon fan's implementation (Figueiredo *et al.* 2009, Gorini *et al.* 2014, Cruz *et al.* 2019, Nogueira *et al.* 2021).

Thus, all palynomorph amplitude zones were truncated in the ~10 Ma, admitting that the Atlantic Ocean's fluvial inflow led to the initial erosion removed all Upper Solimões deposits. This siliciclastic input was concomitant with the denudation during the progressive Andes uplift (Fig. 9). The sediments removed from Central Amazonia were transferred entirely by the river mouth and submarine fan. It is difficult to estimate the sediment bypass time and when the Middle Pleistocene age of Içá Formation overlaid the Solimões deposits. Therefore, we suggest a hiatus of ~9,5 Ma considering the maximum age reached by the range of truncated palynomorphs amplitude zones (Fig. 9). That way, the maximum age found for the Solimões Formation is Upper Miocene, particularly the Lower Tortonian (~10Ma) (Fig. 9). This new understanding of the deposition period to the exposed Solimões Formation is adequate because it considers the consecrate geologic events. The Andean Amazon River implantation versus the Andes uplift constrains the relative ages conferred by the palynomorphs assemblage.

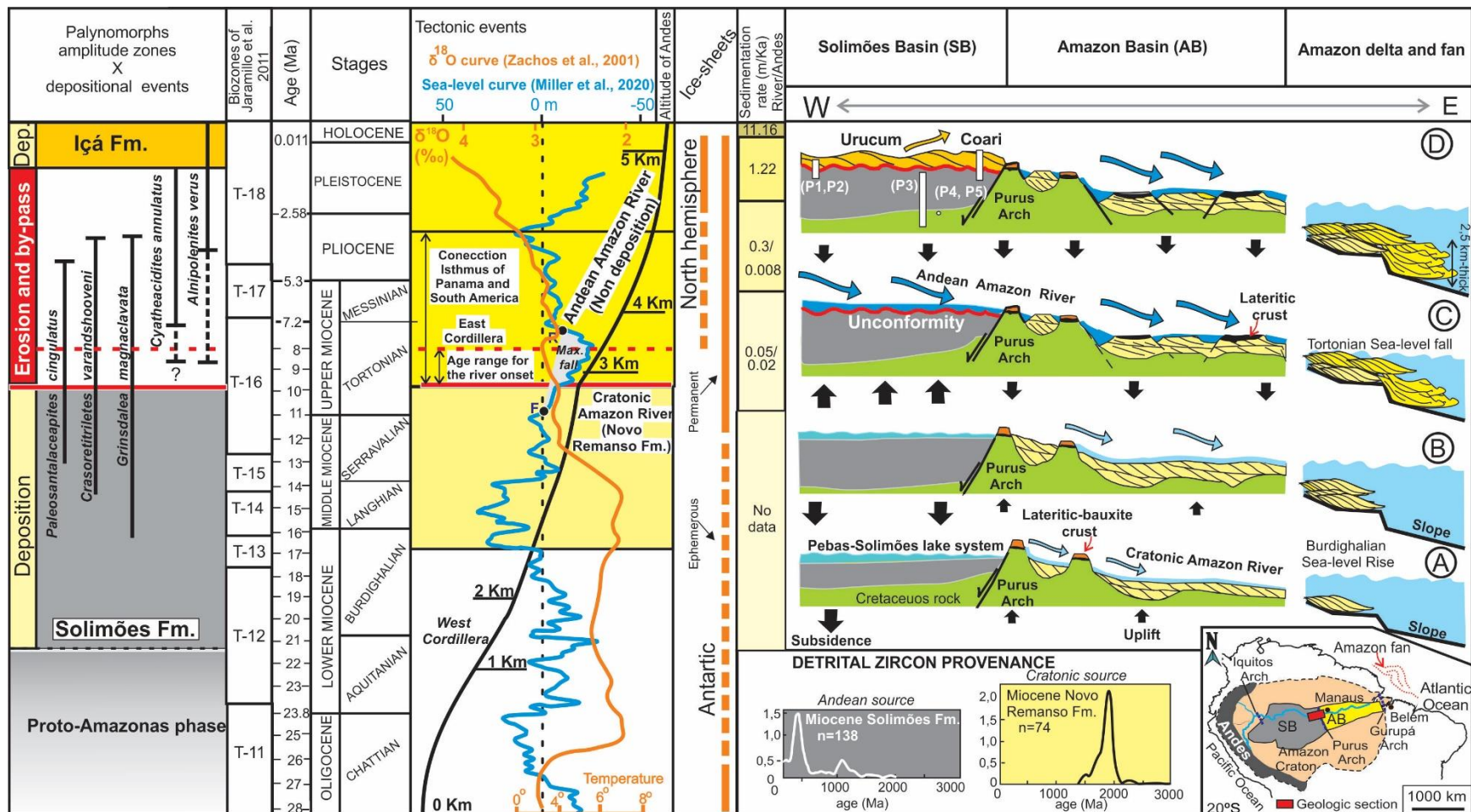


Figure 9- Neogene-Pleistocene evolution of Central Amazônia and their relation with the palynomorphs amplitudes zones from Solimões Formation. A) During late Burdighalian, the progressive subsidence of the Solimões Basin (SB), Western Amazonia cause the installation of Pebas-Solimões lake system (PSLS) confined by the uplift Purus Arch and Amazon Basin (AB) with the onset of the Cratonic Amazon River (CAR) record in the Novo Remanso Formation. Detrital zircon ages confirm the uplift of Andean west cordillera supplying the PSLs and cratonic inflow to CAR (cf. Mappes 2005). B) The increase of subsidence of SB in the Langhian-Serravalian was concomitant with the maximum eastward progradation of CAR with the developing a delta in the Atlantic Ocean (cf. Nogueira *et al.* 2021). C) The conjunction between the Lower-Middle Tortonian sea-level fall and the uplift of East Cordillera promoted a significant uplift and erosion of SB by the Ancean Amazon River's onset

(AAR) in 9,5 Ma, generating a sediment by-pass zone and an unconformity. The uplift AB during the Pliocene-Pleistocene has reduced accommodation space, and the sediments are preserved locally. Lateritic crust forms during this period. The transcontinental drainage sedimentation is transferred to the delta and submarine fan in the Atlantic Ocean. D) During Pleistocene (400 Ka BP), secondary drainage accumulates the Içá deposits covering the unconformity in the top of Solimões Formation. The gap estimate for the unconformity is ~9,5 Ma. The palynomorph amplitude zones of the Solimões Formation were truncated by the unconformity and recorded only as maximum age based on Upper Miocene (Tortonian).

4.9 SUGGESTION FOR NEW RANGE OF *ALNIPOLLENITES VERUS*

For the establishing of *Alnipollenites verus* into Amazonia lowlands before the Pleistocene, is considered the pioneering and adaptive character that responds favorably to forest disturbances, as well as its modern representative *Alnus* (Furlow 1979). In addition to research that records the presence of this fossil grain for the Upper Miocene (9.6 Ma) in the Gatun Formation, Panama (Jaramillo *et al.* 2014), Upper Miocene (11.6-5.3 Ma) Chiquimil Formation, approximately 5000 km from Central America, Argentina (Mautino & Anzótegui 2002), where radiometric data corroborated this age (Kleinert & Strecker 2001).

For to certify the Pleistocene age of the *Alnipollenites verus*, some hypothesis suggest a connection between the Americas through the isthmus of Panama a few million years ago Plio-Pleistocene (O'Dea *et al.* 2016), make it impossible the migration of the *Alnus*, placed on North America at Paleocene-Eocene (MacGinitie 1941, Johnson 1968, Leffingwell 1971, Wolfe 1977, Crane 1989, Lavrenko & Fot'janova 1993) and Paleocene ages for its fossil (Wing *et al.* 2003, Zetter *et al.* 2011). Although other research shows evidence of an older connection, it suggested collision initiated in Upper Miocene when South America first impinged upon the Panama Arch crust (Farris *et al.* 2011, Montes *et al.* 2015). It is important to note that other responses were obtained, such as Humiriaceae, Annonaceae, Euphorbiaceae was able to cross the Central American channel at least 10 Ma before other groups, mainly mammals (Jaramillo *et al.* 2014).

Even if favorable conditions of temperature have been established, for example, Optimal Climate at around 15 Ma (fig. 3), consider that the migratory process of a species occurs gradually. Hence, it is expected that the arrival of *A. verus* in South America took place only after the Middle Miocene, by the isthmus of Panama or other means, taking into account that the record of the Chiquimil Formation dates from events that precede the real connection between the Americas. Emphasizing that this vegetation's pre-existence does not imply the disappearance of the other lowland species characteristic of this tropical forest, not even that whole-plant communities have descended concurrently because two species haven't the same ecological tolerance (Bush *et al.* 1990). For example, the existence of *Alnus* that grew in banks of the forest stream into Pleistocene in Amazonia (Colinvaux *et al.* 2000) may be one of the keys to understanding the migratory dynamics that involved the arrival of *A. verus*. Thus, if this pollen's indigenous nature in Central Amazonia is proven, it will be a strong indication that *A. verus* was part of the Miocene vegetation.

The high-density of trees in the Amazon rainforest block and absorb part of the sun's rays may have generated, regional climate favorable for Andean species from the Middle Miocene since currently, the temperature inside tropical forests are lower than outside them (Davies -Colley *et al.* 2000), so we can infer that in the past the ability to amortize the external temperature by the forest has also been the same.

4.10 CONCLUSIONS

Solimões and Içá formations represent, respectively, deposits of the mega wetlands depositional system and meandering river. Mudrocks rich in organic matter are abundant in the Solimões Formation and represent the most favorable facies for preserving fossils, in contrast to the Içá Formation, where organic matter is rare and coarse-grained siliciclastics predominate. The occurrence of exclusively continental fossils pollen and spores confirm the wetland setting restricted to Western Amazonia compatible with lush vegetation and high diversity specimens, corroborating the continental settings.

Monoporopollenites annuulatus and other grasses indicate an oscillation between shrub and tree phases linked to dry and humid interval fluctuations. The upper Miocene-Pliocene ages for the Solimões Formation obtained are based on amplitudes zones identified mainly *Crassoretitriletes vanraadshovenii*, *Echiperiporites akanthos*, *Echiperiporites stelae*, *Fenestrites spinosus*, *Psilastephanoporites tesseroporus*, *Grimsdalea magnaclavata*, and *Alnipollenites verus*. The first appearance of *Alnipollenites verus* is modified for the Miocene.

The *Grimsdalea magnaclavata* zone associated with the *Crassoretitriletes vanraadshovenii* zone suggests an age between the Mesomiocene-Pliocene to the top Solimões Formation. Besides, an extensive terrestrial influx of reworked and well-preserved Neodevonian acritarchs probably originated from a drainage system derived from the Amazon Basin's northeast edge, topographically higher than the Solimões Basin, exposing Paleozoic rocks that supplied the prodelta lake of the Solimões Formation. The high abundance of *Mauritidites franciscoi*, *Grimsdalea magnaclavata*, and *Monoporopollenites anullatus*, respectively, suggests an energetic increase for the described paleoenvironments, from the Lower to the Upper Miocene, which coincides with the phases of the Cratonic and Andean Amazon River.

The unconformity between the Solimões and Içá formations in the Solimões Basin is more recent than the Ucayali event found in Western Amazonia. It represents an

extensive uplift event in Central Amazonia during the Pliocene, preceding the new subsidence event marked by Pleistocene's deposition of the Içá Formation. Thus, we understand that the Purus Arch region probably acted as a geographic barrier up to the upper Miocene but emphasizing that the Amazon Basin was at higher topographic levels. The installation of the transcontinental drainage was directed by the Andean tectonics and did not occur abruptly but took place in stages from the end of the Lower Oligocene-Miocene to the Quaternary. Reworked palynomorphs found in this succession indicate autocyclic processes related to the environmental dynamic, while acritarchs indicate erosion of Paleozoic source areas.

In this work, was not used the full range of amplitude of the observed fossils due to disagreement surfaces in the stratigraphic succession. The age adjustment took into account the elapsed time of erosion non-deposition. Thus, our data plotted with the significant regional geological events suggest that the maximum age of the palynomorphs found in the ~ 5m exposed of the Solimões Formation is from the Upper Miocene, particularly the base of the Tortonian at 10 Ma. We admit that part of the Miocene higher than 9.5 Ma up to the Middle Pleistocene (500 K) given by the deposits of the Içá Formation have been eroded or have not been deposited.

ACKNOWLEDGMENTS

This work is part of the Ph.D. dissertation of the first author with technical support from the Programa de Pós-Graduação em Geologia e Geoquímica (PPGG) of the University Federal of Pará (UFPA). This research program was supported by the Fundação de Amparo à Pesquisa do Estado do Pará (FAPESPA ICAAF 007/2014, Grant to A.C.R.N) and the Fundação de Amparo à Pesquisa do Estado de São Paulo (FAPESP, Grant 2012/50260-6 to Lucia Lohmann and NSF/NASA Grant 1241066 to Joel Cracraft). We thank CNPq (The Brazilian Scientific and Technology Developing Council) for financial support (proc. 141791/2018-7) during the Ph.D. program of W.J.S.L.J. and to the Coordination for the Improvement of Higher Education Personnel for the research grant received during this study's development (CAPES/PDSE, Proc. nº 88881.190548/2018-01, financial code 001). Thanks, are also extended to Petrobras, which provided well log data from the Urucu region, indispensable for this study. The paper **greatly benefited** from critical reviews of two Journal anonymous referees, and we thank them for their helpful suggestions and comments.

CAPÍTULO 5 CONSIDERAÇÕES FINAIS

As formações Solimões e Içá representam, respectivamente, depósitos flúvio/lacustre e meandrante. Os lamitos escuros ricos em matéria orgânica são abundantes na Formação Solimões e representam a fácies mais favorável à preservação dos palinórfos, em contraste com a Formação Içá, onde a matéria orgânica é rara e predominam os siliciclásticos de granulação grossa. Palinórfos continentais incluindo pólen e esporos, associados a abundantes fitoclastos lenhosos, como troncos de plantas terrestres, além de clastos não lenhosos, por exemplo fragmentos de cutícula, ocorrem em ambas unidades e são indicativos de uma fonte próxima, compatível com vegetação exuberante e alta diversidade de espécimes, reafirmando o paleoambiente continental.

A Zona *Grimsdalea magnaclavata* associada a Zona *Crassoretitriletes vanraadshovenii* indica uma idade entre o Mesomioceno-Plioceno para o topo da Formação Solimões. Além disso, um extenso influxo terrígeno com acritarcas do Neodevoniano em diferentes graus de retrabalhamento, provavelmente se originou de um sistema de drenagem derivado da borda nordeste da Bacia do Amazonas, que se encontrava topograficamente mais elevada que a Bacia do Solimões, expondo rochas paleozoicas que foram erodidas e abasteceram os depósitos de lago/rompimento de dique marginal da Formação Solimões. A elevada abundância de *Mauritidites franciscoi*, *Grimsdalea magnaclavata* e *Monoporopollenites anullatus*, respectivamente, sugerem um aumento energético para os paleoambientes descritos, desde o Mioceno Inferior até o Superior, que coincidem com as fases do Rio Amazonas Cratônico e Andino, respectivamente.

A discordância entre as formações Solimões e Içá na Bacia do Solimões é mais recente que o evento Ucayali encontrado na Amazônia Ocidental e representa um extenso evento de soerguimento na Amazônia Central durante o Plioceno, precedendo o novo evento de subsidência marcado pela deposição dos sedimentos pleistocenos da Formação Içá. Dessa forma, inferimos que a região do Arco de Purus provavelmente atuou como barreira geográfica até o Mioceno superior, no entanto, ressaltando que a Bacia do Amazonas se encontrava em níveis topográficos mais altos. A instalação da drenagem transcontinental foi dirigida pela tectônica andina e não ocorreu de forma abrupta, mas se deu em etapas desde o final do Oligoceno-Mioceno Inferior até o Quaternário.

Dessa forma, concluímos que os dados de palinologia, integralizados aos

principais eventos geológicos regionais, sugerem que a idade máxima dos palinomorfos encontrados nos ~ 5m expostos da Formação Solimões é do Mioceno Superior, particularmente da base do Tortoniano a 10 Ma. Com essa confirmação, admitimos que parte do Mioceno superior a 9,5 Ma até o Pleistoceno Médio (500 K) dada pelos depósitos da Formação Içá, tenha sofrido erosão ou não tenha sido depositada.

REFERÊNCIAS

- Abinader H.D. 2008. *Depósitos Cenozóicos da Porção Oeste da Bacia do Amazonas*. MS Dissertatio, em Geociências, Universidade Federal do Amazonas, Manaus, 98p.
- Absy M.L. 1979. *A palynological study of Holocene sediments in the Amazon basin*. PhD Thesis, University of Amsterdam, 86p.
- Albert J.S. & Reis R.E. (ed.). 2011. *Historical biogeography of neotropical freshwater fishes*. Berkeley, University of California Press, 388p.
- Albert J.S., Val P., Hoorn C. 2018. The changing course of the Amazon river in the neogene: center stage for neotropical diversification. *Neotropical Ichthyology*, **16**(3): e180033, Oct. doi: [10.1590/1982-0224-20180033](https://doi.org/10.1590/1982-0224-20180033).
- Allen J.R.L. 1983. Studies in fluvial sedimentation: bars, bar complexes and sandstones sheets (low-sinuosity braided streams) in the Brownstones (L. Denonian), Welsh Borders. *Sedimentary Geology*, **33**(2): 237-293.
- Ananova, Y. N. 1960. On the redeposited complex of pollen. Moscow Assoc. Naturalists Bull. **65**(3):p. 132-135
- Andrews G.W. 1976. Miocene marine diatoms from the Choptank formation, calvert county, Maryland. *U. S. Geol. Surv. Prof. Pap.* 910, p.1-26.
- Antoine P. O., Abello M. A., Adnet S., Sierra A. J. A., Baby P., Billet G., Boivin M., Calderón Y., Candela A., Chabain J., Corfu F., Croft D.A., Ganerød M., Jaramillo C., Klaus S., Marivaux L., Navarrete R.E., Orliac M.J., Parra F., e.n., María Encarnación Pérez M.E., Pujos F., Rage J.C., Ravel A., Robinet C., Roddaz M., Tejada-Lara J.V., Vélez-Juarbe J., Wesselingh F.P., Salas-Gismondi R. 2016. A 60-million-year Cenozoic history of Western Amazonian ecosystems in Contamana, eastern Peru. *Gondwana Research.*, **31**: p. 30-59, Mar.
- Antoine P.O., Franceschi D. de, Flynn J.J., Nel A., Baby P., Benammi M., Calderón Y., Espurt N., Goswami A., Salas-Gismondi R. 2006. Amber from Western Amazonia reveals Neotropical diversity during the Middle Miocene. *Proceedings of the National Academy of Sciences of the United States of America*, **103**: p. 13595–13600.
- Antonelli A., Nylander J.A.A., Persson C., Sanmartín I. 2009. Tracing the impact of the Andean uplift on Neotropical plant evolution. *Proceedings of the National Academy of Sciences*, **106**(24): p. 9749-9754.
- Arai M., Truckenbrodt W, Nogueira A.C.R., Góes A.M., Rossetti D.F. 1994. Novos dados sobre a Estratigrafia e ambiente deposicional dos sedimentos Barreiras,NE do Pará. 4º. In: SBG, 4º, Simpósio de Geologia da Amazônia, *Resumos Expandidos*. SBG, **1**: p.185-187.
- Arai M., Truckenbrodt W., Nogueira A.C.R., Góes A.M., Rossetti D.F. 1994. Novos dados sobre a Estratigrafia e ambiente deposicional dos sedimentos Barreiras,NE do Pará. In: SBG, 4º, Simpósio de Geologia da Amazônia, Manaus-AM. *Boletim de Resumos Expandidos*. **1**: p. 185-187.
- Ashburner K. 1986. *Alnus*: a survey. *Plantsman*, **8**: p. 170-188.
- Batten D.J. 1991. *Reworking of plant microfossils and sedimentary provenance*. Geological Society, London. **1**: p. 79-90. (Special Publications. **57**).
- Bernard S., Benzerara K., Beyssac O., Brown Jr. G. E., Stamm L. G., Düringer P. 2009.

Ultrastructural and chemical study of modern and fossil sporoderms by Scanning Transmission X-ray Microscopy (STXM). *Review of Palaeobotany and Palynology*, **156**(1-2): p. 248-261.

Bezerra P.E.L. & Ribeiro D.T. 2015. Evolução tectônica Cenozoica da Amazônia Ocidental. In: Gorayeb P.S.S. & Lima A.M.M. (eds.). *Contribuições à geologia da Amazônia*. Belém-Pa, Sociedade Brasileira de Geologia (SBG)- Núcleo Norte, **9**: p. 139-155.

Blackmore S., Steinmann J.A.J., Hoen P.P., Punt W. 2003. The northwest European pollen flora, Betulaceae and Corylaceae. *Review of Paleobotany and Palynology*, **123**: p. 71-98.

Boonstra M., Troelstra S.R., Lammertsma E.I., Ramos M.I.F., Antoine P.O., Hoorn C., 2015. Marine connections of Amazonia: evidence from foraminifera and dinoflagellate cysts (early to middle Miocene, Colombia/Peru). *Palaeogeogr. Palaeoclimatol. Palaeoecol.*, **417**: p. 176-194.

Bormann B.T. & Sidle R.C. 1990. Changes in productivity and distribution of nutrients in a chronosequence at Glacier Bay National Park, Alaska. *Journal of Ecology*, **78**: p. 561-578.

Bousquet J., Strauss S.H., Li P. 1992. Complete congruence between morphological and rbcL-based molecular phylogenies in birches and related species (Betulaceae). *Mol Biol Evol.*, **9**:p. 1076-1088.

Brooks J. & Shaw G. 1972. Geochemistry of sporopollenin. *Chemical Geology*, **10**: p. 69-87

Brown S.M. 1993. Migrations and evolution: computerized maps from computerized data. In: Boulter M.C. & Fisher H.C. (ed.). *Cenozoic plants and climates of the Arctic*. Berlin, Springer Verlag, p. 327-333.

Bryant V.M. 2005. *Pollen analysis of archaeological sediments from CA-SD1-13978 and CA-SD1-4420*: MCB camp Joseph H. Pendleton, California. Final report prepared for RECON in San Diego, California, Palynology Laboratory, Texas A&M University: Texas.

Bush M.B., Colinvaux P.A., Wiemann M.C., Piperno D.R., Liu K. 1990. Late Pleistocene temperature depression and vegetation change in Ecuadorian Amazonia. *Quat. Res.*, **34**: p. 330-345.

Bush M.B., Stute M., Ledru M.-P., Behling H., Colinvaux P.A., Oliveira P.E.de, Grimm E.C., Hooghiemstra H., Haberle S., Leyden B.W., Salgado-Labouriau M.-L., Webb R. 2000. Paleotemperature estimates for the lowland Americas between 303S and 303N at the last glacial maximum. New York, Academic Press, p. 293-306.

Buso Jr. A.A., Pessenda L.C.R., Oliveira P.E. de, Giannini P.C.F., Cohen M.C.L., Volkmer-Ribeiro C., Oliveira S.M.B. de, Rossetti D.F., Lorente F.L., Borotti Filho M.A., Schiavo J.A., Bendassolli J.A., França M.C., Guimarães J.T.F., Siqueira G.S. 2013. Late Pleistocene and Holocene vegetation, climate dynamics, and Amazonian taxa in the Atlantic Forest, Linhares, SE Brazil. *Radiocarbon*, **55**(2-3): p. 1747-1762.

Campbell Jr. K.E. & Frailey C.D. 1984. Holocene flooding and species diversity in Southwestern Amazonia. *Quaternary Research*, **21**: p. 369-375.

Campbell Jr. K.E., Heizler M., Frailey C.D., Romero P.L., Prothero D.R. 2001. Upper Cenozoic chronostratigraphy of the southwestern Amazon Basin. *Geology*, **29** (7): p.

595-598.

Campbell Jr. K.E., Heizler M., Frailey C.D., Romero P.L., Prothero D.R. 2001. Upper Cenozoic chronostratigraphy of the southwestern Amazon Basin. *Geology*, **29** (7): p. 595-598.

Campbell I.D. 1991. Experimental mechanical destruction of pollen grains. *Palynology*, **15**: p. 29-33.

Campbell I.D. & Campbell C. 1994. Pollen preservation: Experimental wet-dry cycles in saline and desalinated sediments. *Palynology*, **18**: 5-10.

Caputo M.V., Rodrigues R., Vasconcelos D.N.N. 1971. Litoestratigrafia da Bacia do Rio Amazonas. *Relatório Técnico Interno Petrobrás*, Belém, **641-A**: p. 35-46.

Caputo M.V. & Silva, O.B. 1991. Sedimentação e tectônica da Bacia do Solimões. In: G.P. Raja Gabaglia & E.J. Milani. Origem e Evolução das Bacias Sedimentares. Rio de Janeiro: *PETROBRAS*, p. 169-193.

Caputo M.V. & Soares E.A.A. 2016. Eustatic and tectonic change effects in the reversion of the transcontinental Amazon River drainage system. *Brazilian Journal of Geology*. **46**(2): p. 301-328.

Caputo M.V. 2012. Age of the Juruá Orogeny – Brazil and Peru. In: 16° Congreso Peruano de Geología y SEG Conference. SGP. Sesión Geología Regional y Tectónica Andina. *Expanded Abstract*, SGPSEG009.pdf. Lima, Peru. 5p

Caputo M.V. 2014. Juruá Orogeny: Brazil and Andean Countries. *Brazilian Journal of Geology*, **44**: p. 181-190.

Caputo M.V., Rodrigues R., Vasconcelos D.N.N. 1971. Litoestratigrafia da bacia do rio Amazonas. *Relatório Técnico Interno Petrobrás*, Belém, **641-A**: p. 35-46.

Carrapa B., Clementz M., Feng R. 2019. Ecological and hydroclimate responses to strengthening of the Hadley circulation in South America during the Late Miocene cooling. *Proceedings of the National Academy of Sciences*, **116**: p. 9747-9752.

Catuneanu O., Abreu V., Bhattacharya J.P., Blum M.D., Dalrymple R.W., Eriksson P.G., Fielding C.R., Fisher W.L., Galloway W.E., Gibling M.R., Giles K.A., Holbrook J.M., Jordan R., Kendall C.G.S.C., Macurda B., Martinsen O.J., Miall A.D., Neal J.E., Nummedal D., Pomar L., Posamentier H.W., Pratt B.R., Sar J.F., Shanley K.W., Steel R.J., Strasser A., Tucker M.E., Winker C., 2009. Towards the standardization of sequence stratigraphy. *Earth-Science Rev.*, **92**: p. 1-33.

Catuneanu O., Galloway W.E., Kendall C.G.St.C., Miall A.D., Posamentier H.W. Strasser A. and Tucker M.E., 2011. Sequence stratigraphy: methodology and nomenclature. *Newsl. Stratigr.*, **44**(3): p. 173-245.

Chapin F.S., Walker L.R., Fastie C.L., Sharman L.C. 1994. Mechanisms of primary succession following deglaciation at Glacier Bay, Alaska. *Ecological Monographs*, **64**: p. 149-175.

Chen Z. & Li J. 2004. Phylogenetics and biogeography of *Alnus* (Betulaceae) inferred from sequences of nuclear ribosomal DNA ITS region. *International Journal of Plant Sciences*, **165**: p. 325–335.

Chen Z.D. 1994. Phylogeny and phytogeography of the Betulaceae. *Acta Phytotaxonomica Sinic.*, **32**(1): p. 1-31 (in Chinese with English summary).

Clapperton C.W. 1993. *Quaternary geology and geomorphology of South America*.

Elsevier, Amsterdam.

Cleef, A.M., Hooghiemstra, H. 1984. Present vegetation of the area of the high plain of BogotaH. In: Hooghiemstra, H. (Ed.), *Vegetational and Climatic History of the High Plain of BogotaH, Colombia: A Continuous Record of the Last 3.5 million Years*. *Dissertaciones Botanicae*, Vol. 79. J. Cramer, Vaduz, p. 42-66. (Also in: *The Quaternary of Colombia*, 10).

Coelho L.G. 1994. *Relatório final de estágio na área de Palinologia*. [S.l.], Petrobrás, CENPES/DIVEX/SEPIBE (internal report). (Projeto Palinoestratigrafia do Devoniano Médio-Carbonifero Inferior das Bacias Paleozóicas Brasileiras).

Colin J.P., Tambareau Y., Krasheninnikov V.A., 1997. An early record of the genus *Cytheridella* daday, 1905 (ostracoda, limnocytheridae, timiriaseviinae) from the Upper Cretaceous of Mali, West Africa: palaeobiogeographical and palaeoecological considerations. *Journal of Micropalaeontology*, **16**: p. 91-95.

Colinvaux P.A., Bush M.B., Steinitz-Kannan M., Miller M.C. 1997. Glacial and Postglacial Pollen Records from the Ecuadorian Andes and Amazon. *Quat. Res.*, **48**: p. 69-78.

Colinvaux P.A., Oliveira P.E. de., Bush M.B. 2000. Amazonian and neotropical plant communities on glacial time-scales: The failure of the aridity and refuge hypotheses. *Quat. Sci. Rev.*, **19**: p. 141-169.

Colinvaux P.A., Oliveira P.E. de., Moreno J.E., Miller M.C., Bush M.B. 1996. A long pollen record from lowland Amazonia: forest and cooling in glacial times. *Science*, **274**: 85-88.

Connell J.H. & Slatyer R.O. 1977. Mechanisms of succession in natural communities and their role in community stability and organization. *The American Naturalist*, **111**: p. 1119-1144.

Conrad T.A., 1874. Remarks on the Tertiary clay of the Upper Amazon, with descriptions of new shells. *Proc. Acad. Nat. Sci. Phila*, **26**: p. 25-32.

Costa M. L., Albuquerque C. A., Barriga V. M. F., D'Antona R. de J.G., Siqueira N.V. M. 1999. Evidências de Lateritos Metamorfizados na Amazônia. In: SBG, 6º Simpósio de Geologia da Amazônia, Manaus, AM. *Expanded Abstracts*, p. 383-386.

Crane P.R. 1989. Early fossil history and evolution of the Betulaceae. In: Crane P.R. & Blackmore S. (eds.). *Evolution, systematics, and fossil history of the hamamelidae*. "Higher" Hamamelidae. Oxford, Clarendon, **2**: p. 87-116.

Cremon E.H., Rossetti D.F., Sawakuchi A.O., Cohen M.C.L. 2016. The role of tectonics and climate in the late Quaternary evolution of a northern Amazonian River. *Geomorphology*, **272**: p. 22-39.

Cross T.A. & Homewood P.W. 1997. Amanz Gressly's role in founding modern stratigraphy. *Geological Society of America Bulletin*, **109**: p. 1617-1630.

Cruz A.M., Reis A.T., Suc J.P., Silva C.G., Praeg D., Granjeon D., Rabineau M., Popescu S.M., Gorini C., 2019. Neogene evolution and demise of the Amapá carbonate platform, Amazon continental margin, Brazil. *Mar. Pet. Geol.*, **105**: p. 185-203. <https://doi.org/10.1016/j.marpetgeo.2019.04.009>.

Cruz N.M.C. 1984. *Palinologia do Linhito do Solimões no Estado do Amazonas*. SBG, 2º Simpósio de Geologia da Amazônia, Manaus, *Anais[...]* **2**: p. 473-480.

- Cozzuol M.A., 2006. The Acre vertebrate fauna: age, diversity, and geography. *Journal of South American Earth Science*, **21**: 185-203.
- D'Apolito C. 2016. *Landscape evolution in Western Amazonia: palynostratigraphy, palaeoenvironments and diversity of the Miocene Solimões Formation, Brazil*. PhD Thesis. University of Birmingham. 365p.
- D'Apolito C., Silva-Caminha S.A.F., Jaramillo C., Dino R. & Soares E.A. 2018. The Pliocene-Pleistocene palynology of the Negro River, Brazil. *Palynology*, **43**(2): p. 223-243.
- Daemon R.F. & Contreiras C.J.A., 1971. Zoneamento palinológico da bacia do Amazonas. *In: SBG, 25º Congr. Bras. Geol., São Paulo, Anais[...]*, **3**, p. 79-91.
- Dašková J. 2008. In situ pollen of *Alnus kefersteinii* (Goepfert) Unger (Betulales: Betulaceae) from the Oligocene of Bechlejovice, Czech Republic. *Jour. Nat. Mus. (Prague)*, Nat. Hist. Ser., **177**(2): p. 27-31.
- Davis M.B. 1961. The problem of rebedded pollen in the Late-Glacial sediments at Taunton, Massachusetts. *American Journal of Science*, **259**: p. 211-222.
- Davis M.B., Brubaker L., Webb L. 1973. Calibration of absolute pollen influx. *In: Birks, H.J.B., West, R.G. (Eds.), Quaternary Plant Ecology*. Blackwell Science, Oxford. p. 9-25.
- Davis M.B., Deevey E.S. 1964. Pollen Accumulation Rates: Estimates from Late Glacial Sediment of Rogers Lake. *Science*, **145**: p. 1293-5.
- Dino R., Soare E.A.A. Riccomini C., Antonioli L., Nogueira A.C.R. 2006. Caracterização Palinestratigráfica de Depósitos Miocênicos na Bacia do Amazonas, região de Manacapuru, AM. *In: 7º Simpósio do Cretáceo do Brasil, 1º Simpósio do Terciário do Brasil, Serra Negra, Rio Claro. Anais[...]*, Serra Negra, Rio Claro, UNESP, **1**: p. 43-43.
- Domínguez E., Mercado J.A., Quesada M.A., Heredia A. 1999. Pollen sporopollenin: degradation and structural elucidation, *Sex. Plant Reprod.*, **12**(3): p. 171-178.
- Dueñas H. 1980. Palynology of Oligocene-Miocene strata of borehole Q-E22, Planeta Rica, Northern Colombia. *Review of Palaeobotany and Palynology*, **10**: p. 318-328.
- Eiras J.F., Becker C.R., Souza E.M., Gonzaga F.G., Silva J.G.F. da., Daniel L.M.F., Matsuda N.S. & Feijó F.J. 1994. Bacia do Solimões. *Boletim de Geociências da Petrobrás*, **8**: p. 17-45.
- Erdtman G. 1954. *An Introduction to Pollen Analysis*. Waltham, Mass, Chronica Botanica Co.239p.
- Espurt N., Bab P., Brusset S. Roddaz M., Hermoza W., Regard V., Antoine P.O., Salas-Gismondi R. 2007. How does the Nazca Ridge subduction influence the modern Amazonian foreland Basin? *Geology*, **35**: p. 515-518.
- Fægri K., Iversen J.K., Kaland P.E., Krzywinski K. 1989. *Textbook of pollen analysis*. 4th ed. London: Wiley.
- Farris D.W., Jaramillo C., Bayona G., Restrepo-Moreno S.A., Montes C., Cardona A., Mora A., Speakman R.J., Glascock M.D., Valencia V. 2011. Fracturing of the Panamanian Isthmus during initial collision with South America. *Geology*, **39**(11): p. 1007-1010.

- Feitosa A.A.S., Gobbo-Rodrigues S.R. Kellner A.W.A. 2003. Partes vegetativas de Carófitas fossilizadas no Membro Romualdo (Albiano, Formação Santana), Bacia do Araripe, Nordeste brasileiro. *Boletim do Museu Nacional*. Nova Série Geologia, Rio de Janeiro, **70**: p. 1-8.
- Feitosa Y.O., Absy M.L., Latrubesse E.M., Stevaux J.C. 2015. Late Quaternary vegetation dynamics from central parts of the Madeira River in Brazil. *Acta Bot. Bras.*, **29**(1): p. 120-128. <http://dx.doi.org/10.1590/0102-33062014abb3711>
- Figueiredo J., Hoorn C., Van der Vem P., Soares E. 2009. Late Miocene onset of the Amazon River and the Amazon deep-sea fan: Evidence from the Foz do Amazonas Basin. *Geology*, **37**(7): p, 619-622.
- Flynn J.J. & Swisher C. 1995. Cenozoic South American land mammal ages: correlation to global geochronologies. In: W.A. Berggren, D.V. Kent, M.P. Aubry & J. Hardenbol (eds.) *Geochronology, Time Scales, and Global Stratigraphic Correlation*, Society of Sedimentary Geology, p. 317-333.
- Fong Y.S. & Said U. 2002. Palynological study on a rock sequence at bandar Tenggara, Johor. In: Geological Society of Malaysia Annual Geological, *Conference*.
- Frailey C.D. 1986. Late Miocene and Holocene Mammals, exclusive of the Notoungulata, of the Rio Acre region, Western Amazonia. *Contributions in Science*, **374**:p. 1-46.
- Frailey C.D., Lavina E., Rancy A., Souza Filho J. de. 1988. A proposed Pleistocene/Holocene lake in the Amazon Basin and its significance to Amazonian geology and biogeography. *Acta Amazonica*, **18**(3-4): p. 119-143.
- Furlow J.J. 1979. The systematics of the American species of *Alnus* (Betulaceae). *Rhodora*, **81**: p.1-121, 151-248.
- Fürstenberg S., Frenzel P., Peng, P., Henkel K., Wrozyna C., 2015. Phenotypical variation in *Leucocytherella sinensis* Huang, 1982 (Ostracoda): a new proxy for palaeosalinity in Tibetan lakes. *Hydrobiologia*, **751**: p. 55-72.
- Gentry A.H. 1993. *A Field Guide to the Families and Genera of Woody Plants of Northwest South America (Colombia, Ecuador, Peru)*: with Supplementary Notes on Herbaceous Taxa. Conservation International: Washington, DC. 53
- Germeraad J.H. Hopping C.A. & Muller J. 1968. Palynology of Tertiary sediments from the tropical areas. *Review of Palaeobotany and Palynology*, **6**(3-4): p. 189-348.
- Gingras M.K., Räsänen M.E. & Ranzi A. 2002. The Significance of Bioturbated Inclined Heterolitic Stratification in the southern Part of the Miocene Solimoes Formation, Rio Acre, Amazonia Brazil. *Palaios*, **17**: p. 591-601.
- Goillot C., Antoine P.O., Tejada J., Pujos F., Salas Gismondi R. 2011. Middle Miocene Uruguaytheriinae (Mammalia, Astrapotheria) from Peruvian Amazonia and a review of the astrapotheriid fossil record in northern South America. *Geodiversitas*, **33**(2): p. 331-345.
- Gonçalves Jr. E.S., Soares E.A.A., Tatumi S.H., Yee M., Mittani J.C.R. 2016. Pleistocene-Holocene sedimentation of Solimões-Amazon fluvial system between the tributaries Negro and Madeira, Central Amazon. *Brazilian Journal of Geology*, **46**(2): p. 167-180.
- Gorini C., Haq B.U., Reis A.T., Silva C.G., Cruz A., Soares E., Grangeon D. 2014. Late Neogene sequence stratigraphic evolution of the Foz do Amazonas Basin, Brazil. *Terra*

Nova, **26**: p. 179-185. <https://doi.org/10.1111/ter.12083>.

Govaerts R.H.A. & Frodin D. 1998. *World checklist and bibliography of fagales (Betulaceae, Corylaceae, Fagaceae and Ticodendraceae)*. The Board of Trustees of the Royal Botanic Gardens, Kew. viii, 408 p. ISBN 1-900347-46-6.

Grabandt R.A.J. 1980. Pollen rain in relation to arboreal vegetation in the Colombian Cordillera Oriental. *Review of Palaeobotany and Palynology*, **29**: p. 65-147.

Grabandt R.A.J. 1985. *Pollen Rain in Relation to Vegetation in the Colombian Cordillera Oriental*. University of Amsterdam: Amsterdam.

Gros M., Piller W.E., Ramos M.I., Paz J.D.S. 2011. Late Miocene sedimentary environments in south-western Amazonia (Solimões Formation, Brazil). *Journal of South American Earth Science*, **32**: p. 169-181.

Gros M., Ramos M.I., Caporaletti M., Piller W.E., 2013. Ostracods (Crustacea) and their paleoenvironmental implication for the Solimões Formation (Late Miocene, Western Amazonia/Brazil). *Journal of South American Earth Science*, **42**: p. 216-241.

Gross M., Ramos M.I., Piller W.E., 2014. On the Miocene Cyprideis species flock (ostracoda, Crustacea) of Western Amazonia (Solimões Formation): refining taxonomy on species level. *Zootaxa*. **3899**(1):p. 1-69p.

Gross M., Ramos M.I.F., Piller W.E., 2015. A minute ostracod (Crustacea: cytheromatidae) from the Miocene Solimões Formation (Western Amazonia, Brazil): evidence for marine incursions? *Journal of Systematic Palaeontology*, **14**(7), p. 581-602.

Guilford W.J., Schneide D.M., Labowitz J., Opella S.J. 1988. High resolution solid state ¹³C NMR spectroscopy of sporopollenins from different plant taxa. *Plant Physiol.*, **86**: p. 134-136.

Guimarães J.T.F., Nogueira A.C.R., Silva Jr. J.B.C., J., Soares J.L., Alves R., Kern A.K. 2015. Palynology of the Middle Miocene-Pliocene Novo Remanso Formation, Central Amazonia, Brazil. *Ameghiniana*, **52**(1): p. 107-134.

Guimarães J.T.F., Nogueira A.C.R., Silva Jr. J.B.C., Soares J.L., Silveira R. 2013. Fossil fungi from Miocene sedimentary rocks of the central and coastal Amazon region, North Brazil. *Journal of Paleontology*, **87**(3): p. 484-492.

Gulliford Alice R., Flint Stephen S., Hodgson David M. 2017. Crevasse splay processes and deposits in an ancient distributive fluvial system: The lower Beaufort Group, South Africa. *Sedimentary Geology*, **58**(1): p. 1-18.

Haberle S. 1997. Upper Quaternary vegetation and climate history of the Amazon Basin: correlating marine and terrestrial pollen records. In: Flood, R.D., Piper, D.J.W., Klaus, A., Peterson, L.C. (Eds.). *Proceedings of the Ocean Drilling Program, Scientific Results*. College Station, p. 381-396.

Haeussler P. J., Saltus R. W., Stanley R. G., Ruppert N., Lewis K., Karl S. M., Bender A. 2017. The Peters Hills basin, a Neogene wedge-top basin on the Broad Pass thrust fault, south-central Alaska. *Geosphere*, **13**(5): p.1464-1488.

Hansen B.C.S. & Rodbell D.T. 1995. A late-glacial/Holocene pollen record from the eastern Andes of Northern Peru. *Quaternary Research*, **44**: p. 216-227.

Havinga A.J. 1964. Investigation into the differential corrosion susceptibility of pollen and spores. *Pollen Spores*. **6**: p. 621-635.

Havinga A.J. 1967. Palynology and pollen preservation. *Review of Palaeobotany and*

Palynology, **2**: p. 81-98.

Havinga A.J. 1984. A 20-year experimental investigation into the differential corrosion susceptibility of pollen and spores in various soil types. *Pollen Spores*, **26**: p. 541-558.

Hesse M., Halbritter H., Zetter R., Weber M., Buchner R., Frosch-Radivo A., Ulrich S. 2008. *Pollen Terminology: an Illustrated Handbook*. Springer, New York, 264p.

Heywood V.H. 1993. *Flowering plants of the world*. New York, Updated ed. Oxford University Press.

Holloway R.G. 1989. Experimental mechanical pollen degradation and its application to Quaternary age deposits. *Tex. J. Sci.*, **41**: p. 131-145.

Hooghiemstra H. 1984. *Vegetational and climatic history of the high plain of Bogotá, Colombia: a continuous record of the last 3.5 million years*. (Cramer), Berlin, Stuttgart. 368p. (Dissertationes Botanicae, Band, v. 79).

Hooghiemstra H. 1989. Quaternary and upper pliocene glaciations and forest development in the tropical Andes: evidence from a long high resolution pollen record from the sedimentary basin of Bogota, Colombia. *Paleogeogr. Palaeoclimatol. Palaeoecol.*, **72**: 11-26. doi:10.1016/0031-0182(89)90129-6.

Hooghiemstra H., Cleef A.M. 1995. Pleistocene climatic change and environmental and generic dynamics in the north Andean montane forest and paramo. In: Churchill S.P., Balslev H., Forero E., Luyeyn J.L. (eds.). *Biodiversity and conservation of neotropical montane forests*. New York, Botanical Garden. p. 35-49.

Horn C. 1993. Marine incursions and the influence of Andean tectonics on the Miocene depositional history of northwestern Amazonia: results of a palynostratigraphic study. *Palaeogeography, Palaeoclimatology, Palaeoecology*, **105**: 267-309.

Horn C. 1994a. An environmental reconstruction of the Paleo-Amazon river system (Middle late Miocene, NW Amazonian). *Palaeogeography, Palaeoclimatology, Palaeoecology*, **112**: p. 187-238.

Horn C., Guerrero J., Sarmiento G. 1995. Andean tectonics as a cause for changing drainage patterns in Miocene Northern South America. *Geology*, **23**: p. 237-240.

Horn C. 2006a. Mangrove forests and marine incursions in Neogene Amazonia (Lower Apaporis River, Colombia). *Palaios*, **21**: p. 197-209p.

Horn C. 2006b. The birth of the mighty Amazon. *Scientific American*, **294**(5): p. 52-59.

Horn C., Wesselingh F. P., ter Steege H., Bermudez M. A., Mora A., Sevink J., Sanmartín I., Sanchez-Meseguer A., Anderson C.L., Figueiredo J.P., Jaramillo C., Riff D., Negri F.R., Hooghiemstra H., Lundberg J., Stadler T., Särkinen T., Antonelli A. 2010a. Amazonia through time: Andean uplift, climate change, landscape evolution, and biodiversity. *Science*, **330**(6006): p. 927-931.

Horn C., Wesselingh F.P., Hovikoski J., Guerrero J. 2010b. The development of the Amazonian mega-wetland (Miocene, Brazil, Colombia, Peru, Bolivia). In: Horn C. & Wesselingh F.P. (eds.). *Amazonia: landscape and species evolution, a look into the past*. London, Wiley-Blackwell, p. 123-142.

Horn C., Bogotá-A G.R., Romero-Baez M., Lammertsma E.I., Flantua S.G.A., Dantas E.L., Dino R., Carmo D.A., Chemale Jr. F. 2010c. The Amazon at sea: onset and stages of the Amazon River from a marine record, with special reference to Neogene plant turnover in the drainage basin. *Global and Planetary Change*, **153**: 51-65.

- Hoorn C., Bogotá-A. G.R., Romero-Baez M., Lammertsma E.I., Flantua S.G.A., Dantas E.L., Dino R., Carmo D.A.do, Chemale Jr. F. 2017. The Amazon at sea: onset and stages of the Amazon River from a marine record, with special reference to Neogene plant turnover in the drainage basin. *Global and Planetary Change*, **153**: p. 51-65.
- Horbe A.M.C., Motta M.B., Almeida C.M.de, Dantas E.L., Vieira L.C. 2013. Provenance of Pliocene and recent sedimentary deposits in western Amazônia, Brazil: consequences for the paleodrainage of the Solimões-Amazonas River. *Sediment. Geol.*, **296**:9–20. <http://dx.doi.org/10.1016/j.sedgeo.2013.07.007>.
- Horbe A.M.C., Nogueira A.C.R., Souza V., Soares E.A.A. 1999. A laterização na Evolução morfológica da Região de Presidente Figueiredo, Estado do Amazonas. In: SBG-NO, 6º Simpósio de Geologia da Amazônia, Manaus, AM. *Boletim de resumos expandidos*, p. 399-402.
- Hovikoski J., Wesselingh F.P., Räsänen M.E., Gingras M.K., Vonhof H.B. 2010. Marine influence in Amazonia: evidence from the geological record. In: Hoorn C. & Wesselingh F.P. (eds.). *Amazonia: landscape and species evolution, a look into the past*. London, Wiley-Blackwell, p. 143-161.
- Hovikoski J., Räsänen M.E., Gingras M., Lopéz S., Romero L., Ranzi A., Melo J. 2007. Palaeogeographical implications of the Miocene Quendeque Formation (Bolivia) and tidally-influenced strata in southwestern Amazonian. *Palaeogeography, Palaeoclimatology, Palaeoecology*, **243**: p. 23-41.
- Hu F.S., Finney B.P., Brubaker L.B. 2001. Effects of Holocene *Alnus* expansion on aquatic productivity, nitrogen cycling, and soil development in southwestern Alaska. *Ecosystems*, **4**: p. 358–368.
- Hulten E. 1968. *Flora of Alaska and neighboring territories*. Stanford (CA), Stanford University Press.
- Iversen J. 1936. *Sedundäres pollen als fehlerquelle*. Danmarks Geol. Undersogelse. **2**. p. 3-25.
- Jaramillo, C. & Rueda M. 2017. A morphological electronic database of cretaceous-tertiary and extant pollen and spores from Northern South America, v. 2017. [Panama]: Smithsonian Institution, *Carlos Jaramillo's Databases*. <http://biogeodb.stri.si.edu/jaramillosdb/web/morphological/>. Registration required. Acesso em 22/01/2021
- Jaramillo, C. & Rueda, M.J. 2013. A Morphological Electronic Database of Cretaceous-Tertiary and Extant pollen and spores from Northern South America, v. 2012/2013. *Carlos Jaramillo's Databases*. Accessible at <http://biogeodb.stri.si.edu/jaramillo/palynomorph/>. Acesso em 22/01/2021
- Jaramillo C. & Dilcher D.L. 2001. Middle paleogene palynology of central Colombia, South America: a study of pollen and spores from tropical latitudes. *Palaeontographica Abteilung B*, **258**: p. 87-213.
- Jaramillo C., Moreno E., Ramírez V., Silva S.A.F., Barrera A., Barrera A., Sánchez C., Morón S., Herrera F., Escobar J., Koll R., Manchester S.R., Hoyos N. 2014. "Palynological record of the last 20 million years in Panama" In: Stevens W.D., Montiel O.M., Raven P. *Paleobotany and biogeography: a festschrift for Alan Graham in his 80th year*, St. Louis, Missouri Botanical Garden Press.
- Jaramillo C., Hoorn C., Silva S.A., Leite F., Herrera F., Quiroz L., Dino R., Antonioli L. 2010. The origin of the modern Amazon rainforest: implications of the palynological and

- palaeobotanical record. *In*: Hoorn C. & Wesselingh F. (ed.). *Amazonia, landscape and species evolution: a look into the past*. [S.l.], Wiley-Blackwell, p.317- 334.
- Jaramillo C., Romero I., D’Apolito C., Bayona G., Duarte E., Louwye S., Duarte E., Luque J., Carrillo-Briceño J.D., Zapata V., Mora A., Schouten S., Zavada M., Harrington G., Ortiz, J., Wesselingh F.P. 2017. Miocene flooding events of western Amazonia. *Science Advances*, **3**(5): p.1601693. doi: 10.1126/sciadv.1601693.
- Jaramillo, C.A, Rueda, M., Torres, V. 2011. A palynological zonation for the Cenozoic of the Llanos and Llanos Foothills of Colombia. *Palynology*. v. 35. p. 46-84.
- Johnson F.D. 1968. Taxonomy and distribution of Northwestern Alders. *In*: Trappe J.M., Franklin J.F., Tarrant R.F., Hansen G.M. (ed.). *Biology of Alder. Pacific NW forest and range experiment station*. Portland (OR), US Forest Service. p. 1-8.
- Jolley D.W. & Whitham A.G. 2004. A stratigraphical and palaeoenvironmental analysis of the sub-basaltic Palaeogene sediments of East Greenland. *Petroleum Geoscience*, **10**(1): p. 53-60.
- Jorge V., D’Apolito C., Silva-Caminha S.A.F. 2019. Exploring geophysical and palynological proxies for paleoenvironmental reconstructions in the Miocene of western Amazonia (Solimões Formation, Brazil). *Journal of South American Earth Sciences*, **94**, 102223. Oct. <https://doi.org/10.1016/j.jsames.2019.102223>
- Jorissen F.J. 1988. Benthic foraminifera from the Adriatic sea, principles of phenotypic variation. *Utrecht Micropaleontol. Bull*, **37**: p. 1-176.
- Kachniasz K.E. & Silva-Caminha S.A.F. 2016. Palinoestratigrafia da Formação Solimões: comparação entre bioestratigrafia tradicional e o método de associações unitárias. *Revista Brasileira de Paleontologia*, **19**(3): p. 481-490.
- Kender S., Stephenson M.H., Riding J.B., Leng M.J., Knox R.W.O’B., Vane C.H., Peck V.L., Kendrick C.P., Ellis M.A., Jamieson R. 2011. Oceanographic, vegetation and climatic change at the Palaeocene–Eocene boundary in the North Sea region. *Berichtete der Geologischen Bundesanstalt*, 85, S: 99. (ISSN 1017-8880).
- Kleinert K. & Strecker M. R. 2001. Climate change in response to orographic barrier uplift: Paleosol and stable isotope evidence from the late Neogene Santa Maria Basin, northwestern Argentina. *Geological Society of America Bulletin*, **113**(6): p. 728-742.
- Lacourse T. 2009. Environmental change controls postglacial forest dynamics through interspecific differences in life-history traits. *Ecology*, **90**: p. 2149–2160.
- Latrubesse E. 1992. *El Cuaternario fluvial de la cuenca del Purús en el estado de Acre, Brasil*. PhD Thesis (unpublished), Universidad Nacional de San Luis, Argentina. 214p.
- Latrubesse E.M., Rancy A., Ramonell C.G., Souza Filho J.P.de. 1994. A Formação Solimões: uma Formação do Mio-Plioceno da Amazônia Sul-Occidental. *In*: 4º Simpósio Nacional de Estudos Tectônicos, Belém, Pa. *Resumos Expandidos*, p.20.
- Latrubesse E.M., Bocquentin J., Santos J.C.R., Ramonell C.G. 1997. Paleoenvironmental model for the Late Cenozoic of southwestern Amazonia: paleontology and geology. *Acta Amazonia*, **27**(2): p. 103-118.
- Latrubesse E.M., Silva S.A.F.da, Cozzuol M., Absy M.L. 2007. Late Miocene continental sedimentation in southwestern Amazônia and its regional significance: biotic and geological evidence. *Journal of South American Earth Science*, **23**: p. 62-80.
- Latrubesse E.M., Cozzuol M., Silva-Caminha S.A.F., Rigsby C.A., Absy M.L., Jaramillo

- C. 2010. The Late Miocene paleogeography of the Amazon Basin and the evolution of the Amazon River system. *Earth-Science Reviews*, **99**: p. 99-124.
- Lavrenko O.D. & Fot'Janova L.I. 1993. Some Early Paleogene species from western Kamchatka. In: Boulter M.C., Fisher H.C. (ed.). *Cenozoic plants and climates of the arctic*. Berlin, Springer Verlag, p. 315-321.
- Leandro L.M., Vieira C.E.L., Santos A., Fauth G. 2019. Palynostratigraphy of two Neogene boreholes from the northwestern portion of the Solimões Basin, Brazil. *Journal of South American Earth Sciences*, **89**: p. 211-218.
- Leffingwell H.A. 1970. Palynology of the Lance (Late Cretaceous) and Fort Union (Paleocene) Formations of the type Lance Area, Wyoming. In: Symposium on Palynology of the Late Cretaceous Early Tertiary San Francisco, California, GSA, p. 1-64. (Geological Society of America Special Paper, 127).
- Leite F.P.R. 2006. *Palinologia da Formação Solimões, Neógeno da Bacia do Solimões, Estado do Amazonas: implicações paleoambientais e bioestratigráficas*. Ph.D Thesis, Universidade de Brasília, Instituto de Geociências, Brasília,DF, 128p.
- Leite F.P.R. 2004. Palinologia. In: Rossetti D.F., Góes A.M. (eds.), *O Mioceno na Amazônia Oriental*: Belém-Pa, Ed. Museu Paraense Emílio Goeldi, p. 55-90.
- Leite F.P.R., Paz J., Carmo D.A. do, Silva-Caminha S.A. 2017. The effects of the inception of Amazonian transcontinental drainage during the Neogene on the landscape and vegetation of the Solimões Basin, Brazil. *Palynology*, **41**(3): p. 412-422. [doi: http://dx.doi.org/10.1080/01916122.2016.1236043](http://dx.doi.org/10.1080/01916122.2016.1236043).
- Leite F.P.R., Silva-Caminha S.A.F.D., D'Apolito C. 2020. New Neogene index pollen and spore taxa from the Solimões Basin (western Amazonia), Brazil. *Palynology*, **45**(1): <https://doi.org/10.1080/01916122.2020.1758971>.
- Lenz O.K., Riegel W., Wilde V. 2020. Greenhouse conditions in lower Eocene coastal wetlands? Lessons from Schöningen, Northern Germany. *PloS one*, **16**(1), e0232861. <https://doi.org/10.1371/journal.pone.0232861>.
- Leopold, E.B., Liu, G.W. 1994. A long pollen sequence of Neogene age, Alaska Range. *Quaternary International*. v. 22/23. p. 103-140.
- Leopold E.B. & Liu G.W. 1994. A long pollen sequence of Neogene age, Alaska Range. *Quaternary International*, **22-23**: p. 103-140.
- Lima Jr. W.J.S., Cohen M.C.L., Rossetti D.F., França M.C. 2018. Late Pleistocene glacial forest elements of Brazilian Amazonia. *Palaeogeography, Palaeoclimatology, Palaeoecology*, **490**: p. 617-628.
- Linhares A.P., Ramos M.I.F., Gaia V.C.S., Friaes Y.S. 2019. Integrated biozonation based on palynology and ostracods from the Neogene of Solimões Basin, Brazil. *Journal of South American Earth Sciences*. <https://doi.org/10.1016/j.jsames.2019.01.015>.
- Linhares A.P., Gaia V.C.S., Ramos M.I. 2017. The significance of marine microfossils for paleoenvironmental reconstruction of the Solimões Formation (Miocene), western Amazonia, Brazil. *Journal of South American Earth Sciences*, **79**: p. 57-66.
- Linhares A.P., Ramos M.I.F., Gross M., Piller W.E. 2011. Evidence for marine influx during the Miocene in southwestern Amazonia, Brazil. *Geología Colombiana*, **36**(1), p. 91-104.
- Lisboa L.G.S., Wanderley Filho J.R., Travassos W.A.S. 2013. Bacia do Solimões-arco

ou rampa de Carauari? In: SBG, 13º Simpósio de Geologia da Amazônia, Belém-Pa. *Anais*[...], p. 89-91.

Liu G.W., Leopold E.B. 1994. Climatic comparison of Miocene floras from northern E-China and south-central Alaska, USA. *Palaeogeography, Palaeoclimatology, Palaeoecology*, **108**: p. 217–228.

Lorente M.A. 1986. *Palynology and palynofacies of the upper tertiary in Venezuela*. Iss. Bot. Berlin, Stuttgart. 222p.

Lovejoy N.R., Albert J.S., Crampton W.G.R. 2006. Miocene marine incursions and marine/freshwater transitions: evidence from Neotropical fishes. *Journal of South American Earth Science*, **21**: p. 5-13.

Lowe A.J., Cavers S., Boshier D.M., Breed F., Hollingsworth P.M. 2015. The resilience of forest fragmentation genetics – No longer a paradox – We were just looking in the wrong place. *Heredity*, **115**: p. 97–99.

Lund J. 1988. A late Paleocene non-marine microflora from the interbasaltic coals of the Faeroe Islands, North Atlantic. *Bulletin of the Geological Society of Denmark*, **37**: p. 181-203.

Lundberg, J.G., Marshall L.G., Guerrero J., Horton B., Malabarba M.C.S.L., Wesselingh F.P. 1998. The stage for Neotropical fish diversification: a history of tropical South American rivers. In: Malabarba L.R., Reis R.E., Vari R.P., Lucena Z.M., Lucena C.A.S. (eds.). *Phylogeny and classification of neotropical fishes*, Porto Alegre, Editora PUC-RS, p. 13-48.

MacGinitie H.D. 1941. *A middle eocene flora from the central Sierra Nevada*. Carnegie, Institution of Washington (Publication, 534).

Mackenzie G., Boa A. N., Diego-Taboada A., Atkin S. L., Sathyapalan T. 2015. Sporopollenin, the least known yet toughest natural biopolymer. *Frontiers in Materials*, **2**: 66. Oct. <https://doi.org/10.3389/fmats.2015.00066>.

Maia M.A.M., Marmos J. L. (org.). 2010. *Geodiversidade do estado do Amazonas*. Manaus, AM, CPRM, 275p.

Maia R.G., Godoy H.K., Yamaguti H.S, Moura P.A. de, Costa F.S. da, Holanda A.M. de, Costa J. 1977. *Projeto de Carvão no Alto Solimões*. Relatório Final, Rio de Janeiro, CPRM-DNPM, 137p.

Malabarba M.C. & Dutra M.F.A. 2002. Fossil fish remains from the Solimões Formation (Miocene) of the state of Amazonas, Brazil. *Acta Geol. Leopoldensia*, **54**: 11-19.

Mandaokar B. D. 2003. Age and depositional environment of the Upper Bhuban Formation of Champhai area (Eastern Mizo hills) India-A palynological approach. *Palaeobotanist.*, **53**(1-3): p. 143-153

Mautino L. R. & Anzótegui L. M. 1998. Palinología de la Formación Chiquimil (Mioceno Superior) en Vallecito, provincia de Catamarca, Argentina. Parte I. Esporas: especies nuevas. *Ameghiniana*, **35**(2): p. 227-233.

May L. & Lacourse T. 2012. Morphological differentiation of *Alnus* (alder) pollen from western North America. *Review of Palaeobotany and Palynology*, **180**: p. 15-24.

Mayle F.E. & Beerling D.J. 2004. Late Quaternary changes in Amazonian ecosystems and their implications for global carbon cycling. *Palaeogeogr. Palaeoclimatol. Palaeoecol.*, **214**: p. 11-25.

- McDonald J. 1992. Palynology of the triporate pollen and paleoecology of the tertiary fossil forests of eastern Axel Heiberg Island, NWT, Canada. PhD Thesis, Carleton University, xi, [192p.].
- McLean D. 1995. Provenance of reworked palynomorphs from the Greenmoor Rock (Langsettian, Late Carboniferous) near Sheffield, England. *Review of Palaeobotany and Palynology.*, **89**: p. 305-317.
- Mendes A.C., Truckenbrodt W., Nogueira A.C.R. 2012. Análise faciológica da Formação Alter do Chão (Cretáceo, Bacia do Amazonas), próximo a cidade de Óbidos, Pará, Brasil. *Revista Brasileira de Geociências*, **42** (1): p. 39-57p.
- Miall A.D. 1996. *The geology of fluvial deposits: sedimentary facies, basin analysis, and petroleum geology*. Berlin, Springer, 582p.
- Miall A.D. 1992. Alluvial deposits *In*: Walker R.G. & James N.P. (eds) *Facies models: response to sea level change*. St. John's, Geological Association of Canada, p. 119-142.
- Miall A.D. 1985. Architectural-element analysis: a new method of facies analysis applied to fluvial deposits. *Earth Science Reviews*, **22**: p. 261-300.
- Miki A. 1977 Late cretaceous pollen and spore floras of northern Japan: composition and interpretation. *J Fac Sci Hokkaido Univ Ser IV Geol Mineral.* **17**: p. 399-436.
- Milani E.J. & Zalán P.V. 1999. An outline of the geology and petroleum systems of the Paleozoic interior basins of South America. *Episodes*, **22**: p. 199-205.
- Monsch K.A. 1998. Miocene fish faunas from the northwestern Amazonia Basin (Colombia, Peru, Brazil) with evidence of marine incursions. *Palaeogeography, Palaeoclimatology, Palaeoecology*, **143**: p. 31-50.
- Montes C., Cardona A., Jaramillo C., Pardo A., Silva J.C., Valencia V., Ayala C., Pérez Angel L.C., Rodríguez-Parra L.A., Ramirez V., Niño H. 2015. Middle Miocene closure of the Central American Seaway. *Science*, **248** (6231):226–229. <http://dx.doi.org/10.1126/science.aaa2815>.
- Mora A., Baby P., Roddaz M., Parra M., Brusset S., Hermoza W., Espurt N. 2010. Tectonic history of the Andes and sub-Andean zones: implications for the development of the Amazon drainage basin. *In*: Hoorn C. & Wesselingh E.P. (eds.). *Amazonia: landscape and species evolution, a look into the past*. [S.l.], Wiley-Blackwell, p. 38-60.
- Muller J. 1959. Palynology of Recent Orinoco delta and shelf sediments. *Micropaleontology*, **5**: p. 1-32.
- Muller J., Giacomo E., Van Erve A.W. 1987. A palynological zonation for the cretaceous, tertiary and Quaternary of Northern South America. *Am. Ass. Stra. Palyn, Contribution Series*, **19**: p. 7-76.
- Muñoz-Torres F., Whatley R., Van Harten D. 1998. The endemic non-marine Miocene ostracod fauna of the upper Amazon Basin. *Revista Española de Micropaleontología*, **30** (3): p. 89-105.
- Muñoz-Torres F., Whatley R., Van Harten D. 2006. Miocene ostracod (Crustacea) biostratigraphy of the upper Amazon Basin and evolution of the genus *Cyprideis*. *Journal of South American Earth Science*, **21**: p. 75-86.
- Murai S. & Morioka S. 1968. Relationships of allied species between northwestern U.S.A. and Japan on the genus *Alnus*. *In*: Trappe J.M., Franklin J.F., Tarraut R.F., Hansen G.M. *Biology of alder*. Washington (DC), Pullman. p. 23–35. (Proceedings of a

Symposium held at Northwest Scientific Association, 40th Annual Meeting).

Murai S. 1964. Phytotaxonomical and geobotanical studies on gen. *Alnus* in Japan. III. Taxonomy of whole world species and distribution of each sect. *Bull Gov For Exp Stn Jpn* **171**: p. 1-107.

Murray J.W. 1991a. *Ecology and paleoecology of Benthic Foraminifera*. New York, Longman Scientific & Technical, 397p.

Murray J.W. 1991b. Ecology and distribution of benthic foraminifera. In: Lee J.L., Anderson R. (eds.). *Biology of Foraminifera*. New York, Academic Press, p. 221-253.

Nogueira A. C. R., Amorim K. B., Góes A. M., Truckenbrodt W., Petri S., Nogueira A. A. E., Bandeira J., Soares J.L., Baía L.B., Imbiriba Jr. M., Bezerra I.S., Ribasf C.C., Cracraft J. 2021. Upper Oligocene-Miocene deposits of Eastern Amazonia: Implications for the collapse of Neogene carbonate platforms along the coast of northern Brazil. *Palaeogeography, Palaeoclimatology, Palaeoecology*, **563**: 110178. Feb. <https://doi.org/10.1016/j.palaeo.2020.110178>.

Nogueira A.A.E., Neita J.S.G., Nogueira A.C.R. 2018. Foraminíferos planctônicos do Oligo-Mioceno da Formação Pirabas (município de Primavera, Pará). *Boletim do Museu de Geociências da Amazônia* **5**: p. 1-9.

Nogueira A.C.R., Silveira R., Guimarães J.T.F. 2013. Neogene-Quaternary sedimentary and paleovegetation history of the eastern Solimões Basin, central Amazon region. *Journal of South American Earth Sciences*, **46**: p. 89-99.

Nogueira A.C.R. 2008. Guinada para o Atlântico, Scientific American Brasil, agosto, 22-27.

Nogueira A.C.R., Souza V., Soares E.A.A. 1997. Contribuição a tectônica cenozóica da região de Presidente Figueiredo, norte de Manaus – AM. In: SBG- Núcleo Brasília, DF, 6º Simpósio Nacional de Estudos Tectônicos. *Boletim de resumos expandidos*. Pirenópolis, GO, p. 123-125.

Nowosad J. 2018. *Forecasting of Corylus, Alnus, and Betula pollen concentration in the air in Poland*. MD Dissertation, Poznań, Adam Mickiewica University in Poznań, 101p.

O'Dea A. et al. 2016. Formation of the Isthmus of Panama. *Sci. Adv.*, **2**(8): e1600883. <http://dx.doi.org/10.1126/sciadv.1600883> (35 authors).

Paz J.D.S., Ramos M.I.F., Moraes-Santos H.M., Silva-Caminha S.A. 2015. Depósitos fluviais e deltaicos da Formação Solimões, Bacia do Solimões, Eirunepé (AM), Brasil. In: Gorayeb P.S.S. & Lima A.M.M. (eds.). *Contribuições à geologia da Amazônia*. Belém-Pa, Sociedade Brasileira de Geologia, Núcleo Norte, **9**: p. 81-92.

Phumphumirat W., Mildenhall D.C., Purintavaragul C. 2009. Pollen deterioration in a tropical surface soil and its impact on forensic palynology. *The Open Forensic Science Journal*, **2**: p. 34-40.

Plint A.G. & Nummedal D. 2000. The falling stage systems tract: recognition and importance in sequence stratigraphic analysis. In: Hunt D., Gawthorpe R.L. (ed.). *Sedimentary response to forced regression*. London, Geological Society. p. 1-17. (Geol. Soc. London Speci. Publ, v. 172).

Potonié R. 1956. *Synopsis der Gattungen der Sporae dispersae. I. Teil*: Sporites. Hannover, 103p. (Beihefte zum Geologischen Jahrbuch, 23).

Potonié R. 1958. *Synopsis der Gattungen der Sporae dispersae. II. Teil*: Sporites

(Nachträge), Saccites, Aletes, Praecolpates, Polyplicates, Monocolpates. (Beihefte zum Geologischen Jahrbuch, 31).

Potonié R. 1960. *Synopsis der Gattungen der Sporae dispersae. III. Teil: Nachträge Sporites, Fortsetzung Pollenites, Mit Generalregister zur Teil I-III.* p. 1-189. (Beihefte zum Geologischen Jahrbuch. v. 39).

Potonié R. 1966. *Synopsis der Gattungen der Sporae dispersae. IV. Teil: Nachträge zu allen Gruppen (Turmae).* p. 244. (Beihefte zum Geologischen Jahrbuch, 72).

Potonié R. 1975. *Synopsis der Gattungen der Sporae dispersae. VII. Teil: Nachträge zu allen Gruppen (Turmae).* p. 23-151. (Fortschritte in der Geologie von Rheinland und Westfalen, 25).

Potter P.E. 1997. The Mesozoic and Cenozoic paleodrainage of South America: a natural history. *Journal of South American Earth Science*, **10**: p. 331-344.

Prinzhofer A., Rostirolla S., Magnier C., Takaki T. 2014. Oil versus gas charge in the Solimões basin. In: 14th Latin-American Congress on Organic Geochemistry- Alago, Búzios, Rio de Janeiro, 2014. *Extended Abstract[...]* Disponível em: http://alago.org/alago/docs/ALAGO_2014/GS03.pdf. Acesso em: 22/01/2021.

Punt W., Hoen P., Blackmore S., Nilsson S., Le Thomas. 2007. A. Glossary of pollen and spore terminology. *Rev. Palaeobot Palynol.*, **143**: p. 1-81.

Punyasena S.W., Dalling J.W., Jaramillo C., Turner B.L. 2011. Comment on "The response of vegetation on the Andean flank in western Amazonia to Pleistocene climate change". *Science*, **333** (6051): p. 1825. doi: [10.1126/science.1207525](https://doi.org/10.1126/science.1207525).

Pupim F.N., Sawakuchi A.O., Almeida R.P., Ribas C.C., Kern A.K., Hartmann G.A., Chiessi C.M., Tamura L.N., Mineli T.D., Savian J.F., Grohmann C.H., Bertassoli Jr. D.J., Stern A.G., Cruz F.W., Cracraft J. 2019. Chronology of Terra Firme formation in Amazonian lowlands reveals a dynamic Quaternary landscape. *Quaternary Science Reviews*, **210**: p. 154-163.

Pupim F.N., Sawakuchi A.O., Mineli T.D., Nogueira L. 2016. Evaluating isothermal thermoluminescence and thermally transferred optically stimulated luminescence for dating of Pleistocene sediments in Amazonia. *Quaternary Geochronology*, **36**: p. 28-37.

Purper I. 1977a. Some ostracods from the upper Amazon basin, Brazil. Environment and age. In: Löffler H. & Danielopol D. (eds.). *Aspects of ecology and zoogeography of recent and fossil ostracoda*. Saalfelden, Sixth International Ostracods Symposium, p. 353-367.

Purper I. 1977b. *Ostracodes Cenozóicos da Amazônia Ocidental*. PhD Thesis. Universidade Federal do Rio Grande do Sul, Instituto de Geociências, Porto Alegre, 131p.

Purper I. 1979. Cenozoic ostracods of the Upper Amazon Basin, Brazil. *Pesquisas*, **12**: p. 209-281.

Quan C., Liu Y.S., Utescher T. 2011. Paleogene evolution of precipitation in northeastern China supporting the iddle Eocene intensification of the East Asian monsoon. *Palaios.*, **26**(11): p. 743-753.

Rêasfanen M.E., Linna A.M., Santos J.C.R., Negri F.R. 1995. Late Miocene tidal deposits in the Amazonian foreland basin. *Science*, **269**: p. 386-390.

Radambrasil 1977. *Folha SB.19 Juruá: geologia, geomorfologia, pedologia, vegetação e*

uso potencial da terra. Rio de Janeiro, DNPM, Brasil, 436p.

Ramos M.I.F. 2006. Ostracods from the Neogene Solimões Formation (Amazonas, Brazil). *Journal of South American Earth Science*, **21**: p. 87-95p.

Reading H.G. (eds.). 1980. *Sedimentary environments and facies*. Oxford, Blackwell Scientific Publications, 615p.

Rebata L.A. 2012. The sedimentology, ichnology and hydrogeochemistry of the Late Miocene, Marginal Marine, Upper Pebas and Nauta Formations, Amazonian Foreland Basin, Peru. PhD Thesis, University of Turku, *Annales Universitatis Turkuensis*, **27**: p.1-45.

Regali M.S.P., Uesugui N., Santos A.S. 1974a. Palinologia dos sedimentos Mesocenozóicos do Brasil (I). *Boletim Técnico da Petrobrás*, **17**: p. 177-190.

Regali M.S.P., Uesugui N., Santos A.S. 1974b. Palinologia dos sedimentos Mesocenozóicos do Brasil (II). *Boletim Técnico da Petrobrás*, **17**: p. 263-301.

Reinink-Smith L. M. 2010. Variations in alder pollen pore numbers: a possible new correlation tool for the Neogene Kenai lowland, Alaska. *Palynology*, **34**(2): p. 180-194.

Reis A.T., Araújo E., Silva C.G., Cruz A.M., Gorini C., Droz L., Migeon S., Perovano R., King I., Bache F. 2016. Effects of a regional d'ecollement level for gravity tectonics on late Neogene to recent large-scale slope instabilities in the Foz do Amazonas Basin, Brazil. *Mar. Pet. Geol.* **75**: p. 29–52. <https://doi.org/10.1016/j.marpetgeo.2016.04.011>.

Ribas C.C., Aleixo A., Nogueira A.C.R., Miyaki C.Y., Cracraft J. 2012. A palaeobiogeographic model for biotic diversification within Amazonia over the past three million years. *Proc. R. Soc. B* **279**: p. 681–689. <http://dx.doi.org/10.1098/rspb.2011.1120>.

Roddaz M., Hermoza W., Mora A., Baby P., Parra M., Christophoul F., Brusset S., Espurt N. 2010. Cenozoic sedimentary evolution of the Amazonian foreland basin system. In: Hoorn C. & Wesselingh F.P. (eds.). *Amazonia: landscape and species evolution, a look into the past*. [S.l.], Wiley-Blackwell, p. 61-88.

Roddaz M., Viers J., Brusset S., Baby P., Hérial G. 2005. Sediment provenances and drainage evolution of the Neogene Amazonian foreland basin. *Earth and Planetary Science Letters*, **239**: p. 57-78.

Roddaz M., Baby P., Brusset S., Hermoza W., Darrozes J.M., 2005. Forebulge dynamics and environmental control in Western Amazonia: the case study of the Arch of Iquitos (Peru). *Tectonophysics*, **399**: p. 87-108

Roddaz M., Baby P., Brusset S., Hermoza W. 2002. Foreland basin dynamics in western Amazonia inferred from forebulge evolution: the case study of the arch of Iquitos (Peru). In: 5th International Symposium on Andean Geodynamics, Paris, IRD- Institut de Recherche Pour Le Developpement, *Resumes etendus*, p. 529-532.

Roddaz M., Viers J., Brusset S., Baby P., Hérial G. 2005. Sediment provenances and drainage evolution of the Neogene Amazonian foreland basin. *Earth and Planetary Science Letters*, **239**: p. 57-78.

Rossetti D. F., Toledo P.M., Góes A.M. 2005. New Geological framework for Western Amazonia Implications for Biogeography and Evolution. *Quaternary Research*. **63**: p. 78-79.

Rossetti D.F., Cohen M.C.L., Tatumi S.H., Sawakuchi A.O., Cremon E.H., Mittani

- J.C.R., Bertani T.C., Munita C.J.A.S., Tudela D.R.G., Yee M., Moya G. 2015. Mid-Late Pleistocene OSL chronology in western Amazonia and implications for the transcontinental Amazon pathway. *Sedimentary Geology*, **330**: p. 1-15.
- Rossetti D.F., Souza L.S.B., Elis V.R. 2012. Neotectonics in the Northern Equatorial Brazilian margin. *J. S. Am. Earth Sci.*, **37**: p. 175-190.
- Rossetti G. & Martens K. 1998. Taxonomic revision of the Recent and Holocene representatives of the family Darwinulidae (Crustacea, Ostracoda), with a description of three new genera. *Bull. l'Institut R. Sci. Nat. Belg.*, **68**: p. 55-110.
- Rouse G.E., Hopkins Jr, W. S., Piel K. M. 1970. Palynology of some late cretaceous and early tertiary deposits in British Columbia and adjacent Alberta. *In: Symposium on Palynology of the Late Cretaceous Early Tertiary San Francisco, California, GSA*, p. 123–246. (Geological Society of America Special Paper, 127).
- Roxo M.G.O. 1924. Breve notícia sobre os fósseis Terciários do Alto Amazonas. *Bol. do Serviço Geol. Miner. do Bras.* **11**: p. 41-52.
- Ruiz F., Abad M., Bodergat A.M., Carbonel P., Rodríguez-Lázaro J., González-Regalado M.L., Toscano A., García E.X., Prenda J., 2013. Freshwater ostracods as environmental tracers. *Int. J. Environ. Sci. Technol.* **10**: p. 1115-1128.
- Sá N.D.P., Absy M.L., Soares E.A.A. 2016. Late Holocene paleoenvironments of the floodplain of the Solimões River, Central Amazonia, based on the palynological record of Lake Cabaliana. *Acta Botanica Brasilica*, **30**(3): p. 473-485.
- Sakallı A. 2017. Simulation of potential distribution and migration of *Alnus* spp. under climate change. *Applied Ecology and Environmental Research*, **15**(4): p. 1039-1070.
- Salamanca S., van Soelen E.E., Teunissen-van Manen M.L., Flantua S.G.A., Santos R.V., Roddaz M., Dantas E.L., van Loon E., Sinninghe-Damste J.S., Kim J.H., Hoorn C. 2016. Amazon forest dynamics under changing abiotic conditions in the Early Miocene (Colombian Amazonia). *Journal of Biogeography*, **43**: p. 2424-2437.
- Salas-Gismondi R., Flynn J.J., Baby P., Tejada-Lara J.V., Claude J., Antoine P.O. 2016. A new 13 million year old gavialoid crocodylian from proto-amazonian megawetlands reveals parallel evolutionary trends in skull shape linked to longirostry. *Plos One*, **11**(4): e0152453.
- Salas-Gismondi R., Flynn J.J., Baby P., Tejada-Lara J.V., Wesselingh F.P., Antoine P.O. 2015. A Miocene hyperdiverse crocodylian community reveals peculiar trophic dynamics in proto-Amazonian mega-wetlands. *Proceedings of the Royal Society B: Biological Sciences*, **282**(1804): 20142490.
- Sánchez F.A.W. & Herrera T. I. 1998. Geología de los cuadrángulos de Moyobamba, Saposoa y Juanjui. Hojas 13-j, 14-j y 15-j. *Boletín del Instituto Geológico, Minero y Metalúrgico del Perú*, A-**122**: p. 1-269.
- Schlager W. 1992. *Sedimentology and sequence stratigraphy of reefs and carbonate platforms: a short course*. Tulsa, The American Association of Petroleum Geologists, 71 p.
- Schobbenhaus C., Campos D.A., Derze G.R., Asmus H.E. 1984. *Geologia do Brasil: texto explicativo do mapa geológico do Brasil e da Área Oceânica adjacente incluindo depósitos minerais*, Escala 1:2.500.000. Brasília,DF, DNPM, p. 93-127.
- Schröder T. 1992. A palynological zonation for the Paleocene of the North Sea Basin.

Journal of Micropalaeontology, **11**(2): p. 113-126.

Shepard L. & Bate R. 1980. Plio-pleistocene ostracods from the upper Amazon of Colombia and Peru. *Palaeontology*, **23**(1): p. 97-124.

Shephard G.E., Müller R.D., Liu L., Gurnis M. 2010. Miocene drainage reversal of the Amazon River driven by plate-mantle interaction. *Nature Geoscience Letters*, **3**: p. 870-875.

Silva-Caminha S.A.F., Jaramillo C.A., Absy M.L. 2010. Neogene palynology of the Solimões Basin, Brazilian Amazonia. *Palaeontographica*, **283**(1-3): p. 1-67.

Silveira R.R. & Souza P.A. 2015. Palinologia (grãos de pólen de angiospermas) das formações Solimões e Içá (Bacia do Solimões), nas regiões de Coari e Alto Solimões, Amazonas. 2015. *Revista Brasileira de Paleontologia*, **18**(3): p. 455-474.

Silveira R.R. & Souza P.A. 2016. Palinologia (esporos de fungos e pteridófitas, grãos de pólen de gimnospermas, cistos de algas e escolecodonte) das formações Solimões e Içá (Neogeno e Pleistoceno, Bacia do Solimões), Amazonas, Brasil. *Pesquisas em Geociências*, **43**(1): p. 17-39.

Silveira R.R. & Souza P.A. 2017. Palinoestratigrafia da Formação Solimões na Região do Alto Solimões (Atalaia do Norte e Tabatinga), Amazonas, Brasil. *Geociências*, v. **36**(1): p. 100-117.

Silveira R.R. 2005. *Cronoestratigrafia e interpretação paleoambiental dos depósitos Miocenos da Formação Solimões, região de Coari, AM*. PhD Theses, UFAM, Manaus, 111p.

Ślōdkowska B. 2009. Palynology of the Palaeogene and Neogene from the Warmia and Mazury areas (NE Poland). *Geologos*, **15**(3-4): p. 219-234.

Smith J. & Higgs K. T. 2001. Provenance implications of reworked palynomorphs in Mesozoic successions of the Porcupine and North Porcupine basins, offshore Ireland. London, *Geological Society*, **1**: p. 291-300. (Special Publications, 188).

Soares E.A.A., Tatumi S.H., Riccomini C. 2010. OSL age determinations of pleistocene fluvial deposits in central Amazonia. *Academia Brasileira de Ciências*, **82**(3): p. 14-9.

Soares E.A.A., D'Apolito, C., Jaramillo C., Harrington G., Caputo M.V., Barbosa R.O., Santos E.B., Dino R., Goncalves A.D. 2017. Sedimentology and palynostratigraphy of a Pliocene-Pleistocene (Piacenzian to Gelasian) deposit in the lower Negro River: Implications for the establishment of large rivers in Central Amazonia. *Journal of South American Earth Sciences*, **79**: p. 215-229.

Souza R. G., Cidade G. M., Campos D. D. A., Riff D. 2016. New crocodylian remains from the Solimões Formation (Lower Eocene–Pliocene), State of Acre, southwestern Brazilian Amazonia. *Revista Brasileira de Paleontologia*, **19**(2): p. 217-232.

Srivastava S. K. 1966. Upper cretaceous microflora (Maestrichtian) from Scollard, Alberta, Canada. *Pollen et Spores*, **8**: p. 497-552.

Stanley E.A. 1965. The use of reworked pollen and spores for determining the Pleistocene-Recent and the intra-Pleistocene boundaries. *Nature*, **206**: p. 289-291.

Stanley E.A. 1966. The problem of reworked pollen and spores in marine sediments. *Marine Geology*, **4**(6): p. 397-408.

Steehan P., Rubinstein C., Melo J.H. de. 2008. Siluro-Devonian miospore

biostratigraphy of the Urubu River area, western Amazon Basin, northern Brazil. *Geobios*, **41**(2): p. 263-282.

Streel M. & Bless M.J.M. 1980. Occurrence and significance of reworked palynomorphs. *Mededelingen Rijks Geologische Dienst.*, **32**: p. 69-80.

Takahashi K. 1970. Some palynomorphs from the upper cretaceous sediments of Hokkaido. *Trans. Proc. Palaeont. Soc.* Ikepan, N.S., **78**: p. 265-275.

Titus J.H. 2009. Nitrogen-fixers *Alnus* and *Lupinus* influence soil characteristics but not colonization by later successional species in primary succession on Mount St. Helens. *Plant Ecology.*, **203**: p. 289-301.

Tomescu A.M.F. 2000. Evaluation of Holocene pollen records from the Romanian Plain. *Review of Palaeobotany and Palynology*, **109**: p. 219-233.

Traverse A. 2007. *Paleopalynology*. 2. ed. Dordrecht, The Netherlands, Springer Science & Business Media. (Topics in Geobiology, v.28).

Tucker M. 2011. *Sedimentary rocks in the field: a practical guide*. Fourth ed. Chichester, Wiley-Blackwell, 288p.

Tweddle J.C. & Edwards K. J. 2010. Pollen preservation zones as an interpretative tool in Holocene palynology. *Review of Palaeobotany and Palynology*, **161**(1-2): p. 59-76.

Twiddle C.L. & Bunting M.J. 2010. Experimental investigations into the preservation of pollen grains: A pilot study of four pollen types. *Review of Palaeobotany and Palynology*, **162**: p. 621-630.

Tyson R. V. 1995. *Sedimentary organic matter*. London, Chapman & Hall.

Tyszka, J., 1997. *Miliammina gerochi* n.sp.- a Middle Jurassic Rzehakinid (Foraminiferida) from quasi-anaerobic biofacies. *Ann. Soc. Geol. Pol.*, **67**: p. 355-364.

Uesugui N. 1979. Palinologia: técnicas de tratamento de amostras. *Bol. Técnico da Petrobrás*, **22**(4): p. 229-240.

Van der Hammen, T. 1956a. Description of some genera and species of fossil pollen and spores. *Boletín Geológico*, Bogotá, **4**: p. 103-109.

Van der Hammen, T. 1956b. A palynological systematic nomenclature. *Boletín Geológico* (Bogotá), **4**: p. 63-101.

Van der Hammen T. 1974. The Pleistocene changes of vegetation and climate in tropical South America. *Journal of Biogeography*, **1**: p. 3-26.

Van der Hammen T. & Gonzalez E. 1960. Upper Pleistocene and Holocene climate and vegetation of the 'Sabana de Bogota' (Colombia, South America). *Leidse Geologische Medelingen*, **25**: p. 261-315.

Van der Hammen T. & Wymstra T.A. 1964. A palynological study on the Tertiary and Upper Cretaceous of British Guayana. *Leidse Geologische Medelingen*, **30**: p. 183-241.

Van Harten D. 2000. Variable nodding in *Cyprideis torosa* (Ostracoda, Crustacea): an overview, experimental results and a model from Catastrophe Theory. In: Horne D.J. & Martens K. (eds.). *Evolutionary biology and ecology of ostracoda*. Dordrecht, Springer, p. 131-139.

Van Soelen E.E., Kim J.H., Santos R.V., Dantas E.L., Almeida F.V., Pires J.P., Roddaz

- M., Damsté J.S.S. 2017. A 30 Ma history of the Amazon River inferred from terrigenous sediments and organic matter on the Ceará rise. *Earth Planet Sci Lett.*, **474**: p. 40-48.
- Vega A.M.L. 2006. Reconstituição paleoambiental dos depósitos miocenos na região centro Oriental da Bacia do Solimões. PhD Thesis, Manaus, UFAM. 92p.
- Vonhof H.B., Wesselingh F.P., Gringas G.K., 1998. Reconstruction of the Miocene western Amazonian aquatic system using molluscan isotopic signatures. *Palaeogeogr. Palaeoclimatol. Palaeoecol.*, **141**: p. 85-93.
- Vonhof H.B., Wesselingh F.P., Kaandorp R.J.G., Davies G.R., Van Hinte J.E., Guerrero, J., Räsänen M., Romero-Pittman L., Ranzi A. 2003. Paleogeography of Miocene Western Amazonia: isotopic composition of molluscan shells constrains the influence of marine incursions. *Geological Society of America Bulletin*, **115**: p. 983-993
- Walker R.G. 1992. Facies, facies models and modern stratigraphic concepts. In: Walker R.G. & James N.P. (eds.). *Facies models – response to sea-level change*. Ontario, Geological Association of Canada. p. 1-14.
- Wanderley Filho J.R. 1991. *Evolução crustal da bacia do Amazonas e sua relação com o embasamento*. PhD Thesis. Belém,UFPA, 109p.
- Wanderley Filho J.R., Eiras J.F., Cunha P.R.C., van der Ven P.H. 2010. The Paleozoic Solimões and Amazonas basins and the Acre foreland basin of Brazil. In: Hoorn C. & Wesselingh F.P. (eds.). *Amazonia: landscape and species evolution, a look into the past*. [S.l.], Wiley-Blackwell, p. 29-37.
- Wanderley Filho J.R., Eiras J.F., Vaz P.T. 2007. Bacia do Solimões. *Boletim de Geociências Petrobrás*, **15**: p. 217-225.
- Wanderley M.D. 2010. Técnicas de preparação de microfósseis. In: Carvalho I.S. (ed.). *Paleontologia: microfósseis, paleoinvertebrados*. Rio de Janeiro, Editora Interciência, p. 65-80.
- Watanasak M. 1990. Mid tertiary palynostratigraphy of Thailand. *Journal of Southeast Asian Earth Sciences*, **4**(3): p. 203-218.
- Weng C., Bush M.B., Chepstow-Lusty A.J. 2004. Holocene changes of Andean alder (*Alnus acuminata*) in highland Ecuador and Peru. *J. Quat. Sci.***19**: p. 685-691.
- Wesselingh F.P., Räsänen M.E., Irion G., Vonhof H.B., Kaandorp R.J.G., Renema W., Romero-Pittman L., Gringas M.K. 2002. Lake Pebas: a palaeoecological reconstruction of a Miocene, long-lived lake complex in western Amazonia. *Cainozoic Res.* **1**: p. 35-81.
- Wesselingh F.P. 2006. Molluscs from the Miocene Pebas Formation of Peruvian and Colombian Amazonia. *Scripta Geologica*, **133**: 19-290.
- Wesselingh F.P., Guerrero J., Räsänen M.E., Romero Pittmann L., Vonhof H.B., 2006a. Landscape evolution and depositional processes in the Miocene Amazonian Pebas lake/wetland system: evidence from exploratory boreholes in northeastern Peru. *Scr. Geol.* **133**: p. 323-381.
- Wesselingh F.P., Hoorn M.C, Guerrero J., Räsänen M.E., Pittmann L.R., Salo J.A. 2006b. The stratigraphy and regional structure of Miocene deposits in western Amazonia (Peru, Colombia and Brazil), with implications for late Neogene landscape evolution. *Scripta Geologica*, **133**. P. 291-322.
- Wesselingh F. P., & Salo J. A. 2006c. A Miocene perspective on the evolution of the Amazonian biota. *Scripta Geologica*, **133**: p. 439-458.

- Wesselingh F.P. & Ramos M.I.F. 2010. Amazonian aquatic invertebrate faunas (Mollusca, Ostracoda) and their development over the past 30 million years. *In*: Hoorn C. & Wesselingh F.P. (eds.). *Amazonia: landscape and species evolution, a look into the past*. Wiley-Blackwell, p. 302-316.
- Westaway, R., 2006. Late Cenozoic sedimentary sequences in Acre state, south-western Amazonia: fluvial or tidal? Deductions from the IGCP 449 field trip. *Journal of South American Earth Sciences*, **21**: p. 120-134.
- Whatley R.C., Muñoz-Torres F., Harten D. Van 2000. Skopaeocythere: a minute new limnocytherid (Crustacea, ostracoda) from the Neogene of the Amazon basin. *Ameghiniana*, **37** (2): p. 163-167.
- Whatley R.C., Muñoz-Torres F., Van Harten D. 1998. The Ostracoda of isolated Neogene saline lake in the western Amazon Basin. *In*: Crasquin-Soleau S., Braccini E., Lethiers F. (eds.). *What about ostracoda!* Actes du 3^e Congress European des Ostracodologistes, p. 231-245. (Bulletin du Centre de Recherches Elf Exploration Production, memoir, v.20).
- Wilmschurst J. M. & McGlone M. S. 2005. Origin of pollen and spores in surface lake sediments: comparison of modern palynomorph assemblages in moss cushions, surface soils and surface lake sediments. *Review of Palaeobotany and Palynology*, **136**(1-2): p. 1-15.
- Wing S.L., Harrington G.J., Bowen G.J., Koch P.L. 2003. *Floral change during the initial Eocene thermal maximum in the Powder river basin*, Wyoming, Geological Society of America.
- Wizevic M.C. 1991. Photomosaics of outcrops: useful photographic techniques. *In*: Miall A.D. & Tyler N. (eds.). *The three-dimensional facies architecture of terrigenous clastic sediments and its implications for hydrocarbon discovery and recovery*. Tulsa, Society for Sedimentary Geology/SEPM. p. 22-24.
- Wolfe J. 1973. Fossil forms of amentiferae. *Brittonia*, **25**: 334–355.
- Wolfe J.A. 1977. *Paleogene floras from the gulf of Alaska region*. [S.l.], U.S. Geological Survey. 7p. 107. (Professional Paper, 99).
- Worobiec E. & Worobiec G. 2016. Miocene palynoflora from the KRAM-P 218 leaf assemblage from the Belchatów Lignite Mine (Central Poland). *Acta Palaeobotanica*, **56**(2): p. 499-517.
- Zetter R., Farabee M.J., Pigg K.B., Manchester S.R., Vore M.L.de, Nowak M.D. 2011. Palynoflora of the late Paleocene silicified shale at Almont, North Dakota, USA. *Palynology*, **35**(2): p. 179-211.

SUPPLEMENTARY MATERIAL

Table 3- Pollen raw counts of samples from the Solimões Formation, Central Amazonia, Brazil. RW = reworked. Sample 5-01, 5-07 e 5-21 (profile 5), sample 1-02 (profile 1), samples 4-01, 4-02 e 4-07 (profile 4). (see figure 2. Cap. 3)

(continua)

Category	Family	Genus	Taxa	5-01	5-07	5-21	1-05	4-01	4-02	4-07
Pollen	Betulaceae	Alnus	<i>Alnipollenites verus</i>	32	17	02	07	07	18	27
Pollen	Malvaceae		<i>Bombacacidites ciriloensis</i>	07	01	16	01	07	06	09
Pollen	Malvaceae	Bombax	<i>Bombacacidites nacimientoensis</i>	-	-	-	-	-	01	-
Pollen	Cabombaceae		<i>Cabomba</i>	-	-	-	-	-	01	-
Pollen	Pteridaceae	Ceratopteres	<i>Cicatricosisporites pseudograndiosus</i>	-	-	02	-	-	01	-
Pollen	Asteraceae		<i>Cichoreacidites longispinosus</i>	-	-	-	01	-	05	-
Pollen	Chloranthaceae	Hedyosmum	<i>Clavainaperturites microclavatus</i>	-	-	-	-	-	03	-
Pollen	Onagraceae	Ludwigia	<i>Corsinipollenites oculusnoctis</i>	01	-	-	-	-	02	-
Pollen	Onagraceae		<i>Corsinipollenites undulatus</i>	-	01	-	-	-	-	01
Pollen			<i>Cricotriporites macroporus</i>	-	-	-	-	-	01	-
Pollen	Euphorbiaceae		<i>Crototricolpites euphorbienses</i>	-	-	-	-	-	02	-

(continuação)

4-02	4-07		<i>Echidiporites barbeitoi</i>	-	-	-	-	-	03	10
Pollen	Alismataceae	Sagittaria/Echinodorus	<i>Echiperiporites akanthos</i>	02	-	-	-	01	-	01
Pollen	Asteraceae		<i>Echitricolporites spinosus</i>	-	-	-	-	-	09	12
Pollen	Cucurbitaceae	Cayaponia	<i>Echitriporites jolyi</i>	-	03	-	-	-	-	-
RW Pollen	Ephedraceae		<i>Ephedripites aff. fusiformis</i>	-	-	-	-	01	-	03
Pollen	Asteraceae		<i>Fenestrites spinosus</i>	-	01	-	-	02	07	04
RW Pollen			<i>Foveotriporites hammenii</i>	-	-	-	01	-	02	-
Pollen	Arecaceae	Extinct	<i>Grimsdalea magnaclavata</i>	01	10	-	-	-	-	02
Pollen	Aquifoliaceae	Ilex	<i>Ilexpollenites tropicalis</i>	-	-	-	-	-	06	-
Pollen	Malvaceae		<i>Jandufouria seamrogiformis</i>	-	-	-	01	-	05	-
RW Pollen			<i>Longapertites vaneendenburgi</i>	-	-	-	-	-	-	01
Pollen	Malvaceae		<i>Malvacipolloides maristellae</i>	-	-	-	-	-	02	-
Pollen			<i>Margocolporites carinae</i>	-	-	-	-	-	-	01
Pollen	Arecaceae	Mauritia	<i>Mauritiidites franciscoi</i>	01	-	-	-	-	-	-
Pollen	Arecaceae	Mauritia	<i>Mauritiidites franciscoi var.</i>	-	01	-	-	-	-	-

			<i>pachyexinatus</i>							
Pollen	Achantaceae		<i>Multiareolites formosus</i>	-	-	-	-	-	01	-
Pollen			<i>Multiporopollenites crassinexinatus</i>	-	-	-	-	-	01	01
Pollen			<i>Paleosantalaceapites cingulatus</i>							
Pollen	Convolvulaceae	Merremia	<i>Perfoetricolpites digitatus</i>	01	-	-	-	-	-	01
Pollen	Malpighiaceae		<i>Perisyncolporites pokorny</i>	-	-	-	-	-	06	11
Pollen	Podocarpaceae	Podocarpus	<i>Podocarpites spp.</i>	07	07	02	01	01	01	07
Pollen	Celastraceae	Hippocratea	<i>Polyadopollenites macroreticulatus</i>	-	-	-	-	-	01	01
Pollen	leguminosae	Acacia	<i>Polyadopollenites mariae</i>	03	-	06	-	-	02	02
Pollen	Sapindaceae/Protea ceae	Allophylus?	<i>Proteacidites triangulatus</i>	-	-	-	-	01	-	06
Pollen	Sapindaceae		<i>Psilabrevitricolporites triangulares</i>	02	-	-	-	-	03	06
Pollen	Moraceae		<i>Psiladiporitis minimus</i>	-	-	-	01	-	-	04
Pollen			<i>Psilaperiporites multiporatus</i>	02	-	-	-	-	01	-
Pollen	Polygalaceae		<i>Psilastephanocolporites fissilis</i>	-	-	-	-	-	-	01
Pollen			<i>Psilastephanoporites microcaribienses</i>	-	-	-	03	01	-	-

(continuação)

Pollen	Loranthaceae	Struthanthus	<i>Psilasyncolporites reticolpatus</i>	-	-	-	-	-	01	-
Pollen	Salicaceae	Casearia	<i>Psilatricolporites costatus</i>	-	-	-	-	-	01	-
Pollen	Euphorbiaceae	Alchornea/Aparisthium	<i>Psilatricolporites operculatus minutus</i>	-	04	01	-	01	02	01
Pollen	Labiatae		<i>Retistephanocolpites hexalabiatus</i>	-	-	-	-	-	-	01
Pollen	Malvaceae	Quararibea	<i>Retistephanocolporites crassiannulatus</i>	-	-	-	-	-	01	04
Pollen	Phyllanthaceae	Amanoa	<i>Retitrescolpites? irregularis</i>	01	-	-	-	-	-	-
Pollen			<i>Retitriporites simplex</i>	-	-	-	-	-	01	-
Pollen	Rubiaceae	Chomelia	<i>Retitriporites crotonicolumellatus</i>	-	-	-	-	-	01	01
Pollen	Passifloraceae/Bignoniaceae/Fabaceae		<i>Rhoipites oblatus</i>	-	-	-	-	-	01	-
Pollen			<i>Spirosyncolpites spiralis</i>	-	-	-	01	-	08	08
Pollen	Rubiaceae	Spermacece	<i>Stephanocolpites evansii</i>	-	-	-	02	02	01	02
Pollen			<i>Striatricolporites digitatus</i>	-	-	-	-	-	03	-
Pollen	Leguminosae		<i>Striatopollis catatumbus</i>	02	-	-	-	-	-	-

(conclusão)

Pollen	Myrtaceae		<i>Syncolporites poricostatus</i>	-	-	-	01	-	04	-
RW Spore			<i>Camarozonosporites ambigens</i>	-	-	-	-	4	-	3
Spore			<i>Cingulatisporites rugulatus</i>	02	-	03	-	-	-	01
Spore	Schizaceae	Lygodium	<i>Crassoretitriletes vanraadshoovenii</i>	-	-	-	-	-	03	-
Spore	Selaginellaceae		<i>Echinatisporis circulares</i>	01	-	-	-	-	-	-
RW Spore			<i>Echinatisporis minutus</i>	-	-	-	-	-	-	04
Spore	Selaginellaceae	Selaginella	<i>Echinatisporis muelleri</i>	-	-	-	-	-	-	01
Spore	Lycopodiaceae	Huperzia	<i>Foveotriletes ornatus</i>							
Spore	Pteridaceae	Ceratopteris	<i>Magnastriatites grandiosus</i>							
Spore			<i>Polypodiaceoisporites? amazonensis</i>	-	-	-	-	-	03	-
Spore			<i>Psilatritetes lobatus</i>							
Spore			<i>Verrucatotriletes etayoi</i>	02	-	-	-	-	-	01
Spore	Pteridaceae	Ceratopteris	<i>Magnastriatites howardi</i>							

(continuação)

Category	Family	Genus	Taxa	46123	46124	46125	46126	46127	46128	46129	46130	46131	46132	46133	46134	46135
Pollen	Asteraceae		<i>Cichoreacidites longispinosus</i>	02	-	-	-	-	-	-	-	-	-	-	-	-
Pollen	Onagraceae	Ludwigia	<i>Corsinipollenites oculusnoctis</i>	-	-	01	-	-	-	-	-	-	-	-	-	-
Pollen	Onagraceae	Ludwigia	<i>Corsinipollenites psilatus</i>	-	-	-	01	-	01	-	-	-	-	-	-	-
Pollen	Onagraceae		<i>Corsinipollenites undulatus</i>	02	04	-	01	-	-	02	02	02	02	01	01	-
Pollen	Leguminosae	Dioclea	<i>Crassiectoapertites columbianus</i>	01	03	06	-	01	-	02	-	02	-	-	-	-
Pollen	Alismataceae	Sagittaria/Echinodorus	<i>Echiperiporites akanthos</i>	04	21	20	10	12	16	15	26	29	03	15	06	07
Pollen	Malvaceae	Hibiscus	<i>Echiperiporites stelae</i>	-	-	-	-	-	-	-	-	-	-	-	-	-
Pollen	Asteraceae		<i>Echitricolporites spinosus</i>	-	-	-	-	-	-	-	-	-	-	-	01	-
Pollen			<i>Echitriporites sp.</i>	-	-	-	01	-	-	-	-	-	-	-	-	-
Pollen	Asteraceae		<i>Fenestrites spinosus</i>	-	-	-	01	-	-	-	03	-	03	01	-	-

(continuação)

Category	Family	Genus	Taxa	46123	46124	46125	46126	46127	46128	46129	46130	46131	46132	46133	46134	46135
Pollen	Achantaceae	Bravaisia	<i>Multimarginites vanderhammeni</i>	-	-	01	-	-	-	-	-	-	-	01	-	-
Pollen	Malpighiaceae		<i>Perisyncolporites pokorny</i>	01	01	04	04	01	10	02	08	07	-	07	02	02
Pollen	Podocarpaceae	Podocarpus	<i>Podocarpidites sp.</i>	-	04	02	01	04	01	-	-	1	-	1	-	03
Pollen	leguminosae	Acacia	<i>Polyadopollenites mariae</i>	-	-	05	-	04	01	-	-	-	02	02	-	-
Pollen	Phyllanthaceae	Amanoa	<i>Retitrescolpites? irregularis</i>	-	-	-	-	-	-	-	-	04	-	-	-	-
Pollen			<i>Spirosyncolpites spiralis</i>	03	05	07	07	02	02	-	03	04	-	05	03	1
Pollen			<i>Syncolporites sp.</i>	01	-	-	-	-	-	-	-	-	-	-	-	-
Spore	Schizaceae	Lygodium	<i>Crassoretitriletes vanraadshoovenii</i>	-	-	-	-	-	02	02	-	01	-	-	-	-
Spore	Selaginellaceae	Selaginella	<i>Echinatisporis muelleri</i>	-	-	04	-	-	03	02	02	01	02	-	-	-

(continuação)

Category	Family	Genus	Taxa	46123	46124	46125	46126	46127	46128	46129	46130	46131	46132	46133	46134	46135
Pollen			<i>Echitriporites sp.</i>	-	-	-	-	-	-	-	-	-	-	-	-	-
Pollen	Asteraceae		<i>Fenestrites spinosus</i>	-	01	-	-	-	-	-	-	-	-	-	-	-
Pollen			<i>Foveotricolporites sp.</i>	-	-	04	-	-	-	-	-	-	-	-	-	-
Pollen	Arecaceae		<i>Grimsdalea magnaclavata</i>	09	15	12	02	19	13	19	119	106	22	23	03	15
Pollen	Euphorbiaceae	Sapium	<i>Ladakhipollenites? Caribbiensis</i>	01	-	-	-	-	-	-	-	-	-	-	-	-
Pollen			<i>Longapertites sp.</i>	10	07	-	08	01	-	01	15	16	01	06	-	-
Pollen			<i>Malvacipollis spinulosa</i>	02	-	-	-	-	-	-	-	-	-	-	-	-
Pollen	Arecaceae	Mauritia	<i>Mauritiidites franciscoi</i>	15	18	8	51	20	16	18	110	76	-	30	07	13
Pollen	Poaceae		<i>Monoporopollenites annulatos</i>	-	198	29	212	08	115	11	70	58	-	25	04	-

SYSTEMATIC DESCRIPTION

Genus *Ovoidites* Pontonié (1951)

Type species: *Ovoidites ligneolus* Pontonié (1951).

Ovoidites sp.

Description: Spore single, bilaterally symmetrical, elliptic, sporoderm 1 μm thick, psilate ornamentation. Total diameter 39 μm .

Occurrence: Australian Cretaceous to recent deposits (Cookson & Dettman 1958).

Botanical affinities: *Ovoidites* and *Schizosporis* represent spores of Zygnemataceae related with the current genus *Spirogyra* (Van Geel & Van der Hammen 1978).

Comparisons: *Ovoidites parvus* (Cookson & Dettman 1959) Nakoman 1966, is bigger (71-105 μm diameter).

Ecology: Green algae commonly found in freshwater lakes and open-water marsh (Rich *et al.* 1982).

4.1.3 Pteridophyte

Class Monoletes Ibrahim (1933)

Genus *Verrucatosporites* Thompson and Pflug (1953)

Type-species: *Verrucatosporites usmensis* (Van der Hammen 1956a) Germeraad *et al.* (1968)

Description: Spores single, bilaterally symmetrical, oblate, rounded ends, monolete, curvature absent, distinct laesura, verrucate ornamentation, verrucae 2 μm long and 2 μm wide, exine 2 μm thick, irregularly distributed over the entire grain. Equatorial diameter 50 μm , polar diameter 30 μm .

Occurrence: Upper Eocene-Lower Oligocene to Quaternary (Lorente 1986, Germerrad *et al.* 1968). Lower Eocene to Pliocene (Salard-Cheboldaeff 1990), Upper Eocene to Upper Miocene (Regalli *et al.* 1974a, b).

Botanical affinities: The species resembles with *Stenochlaena palustris* of Blechnaceae (Germeraad *et al.* 1968) and *Polypodim* - Polypodiaceae (Lorente, 1986).

Comparisons: *Laevigatosporites ovatus* Wilson & Webster (1946) has thinner exine (e.g. Santos 2006).

Ecology: Fern from semi-aquatic environment (Hoorn 1994a).

Class Triletes Reinsch emend. Dettmann (1963)

Genus *Crassoretitriletes* (Germeraad *et al.* 1968)

Type species: *Crassoretitriletes vanraadshoovenii* (Germeraad *et al.* 1968)

Description: Spores single, symmetry radial, triangular-obtuse-convex, rounded corners, trilete, curvature absent, margo absent, commissure straight, sporoderm 4 µm thick, sculpture reticulate and fossulate, lumina 2 µm wide, muri 3-4 µm wide and 4-5 µm long. Equatorial diameter length 60-70 µm, equatorial diameter width 50-70 µm.

Occurrence: Middle Miocene to Pliocene (Germeraad *et al.* 1968, Jaramillo *et al.* 2011).

Botanical affinities: *Lygodium microphyllum* (Germeraad *et al.* 1968).

Type species: *Foveotriletes ornatus* Regali *et al.* (1984)

Description: Spores single, symmetry radial, foveolated body, psilate sclerine, triangular and concave sides, curvature absent, margo absent. Isopolar. polar axis 35-40 µm, sclerine 0,5 µm. foveolae uniformly distributed over entire body, lumina 1 µm wide, 2 to 4 µm apart.

Occurrence: Early Miocene Jaramillo *et al.* (2014)

Botanic affinity: Lycopodiaceae, *Huperzia* D'Apolito (2020)

Genus *Magnastriatites* Germeraad *et al.* (1968) emend. Dettmann & Clifford (1992)

Type species: *Magnastriatites howardi* Germeraad *et al.* (1968).

Magnastriatites grandiosus Kedves & De Porta (1963)

Description: Spores single, radially symmetrical, triangular-obtuse-straight, trilete, curvature absent, laesura distinct, sporoderm two-layered, exine 3-4 µm thick, cicatricose ornamentation on distal face, striae 3-4 µm wide, 2-4 µm apart, psilate ornamentation on proximal face. Equatorial diameter 58 µm.

Occurrence: Lower Oligocene to Upper Miocene (Germeraad *et al.* 1968, Ampaiwan *et al.* 2003, Jaramillo *et al.* 2010).

Botanical affinities: *Ceratopteris* - Parkeriaceae (Dueñas 1980b).

Comparisons: *Striatriletes elegantis* Jaramillo *et al.* 2007 is smaller (28 µm).

Ecology: Aquatic fern of shallow water lakes and river banks on the alluvial plain and coastal swamps (e.g. Germeraad *et al.* 1968).

4.1.4 Angiosperms

Class Monocolpatae Iversen and Troels-Smith (1950)

Type species: *Mauritiidites crassibaculatus* Van Hoeken-Klinkenberg (1964).

Mauritiidites franciscoi var. *franciscoi* (Van der Hammen 1956a).

Description: Monad, bilaterally symmetrical, anisopolar, spheroidal, monosulcate, sulcus simple with around 28 μm long, intectate, nexine 1-2 μm thick, echinate ornamentation, spines 3-3.3 μm long, 1.5 μm wide at the base and 0.3 μm wide at the top, tips rounded. Equatorial diameter 40-48 μm .

Occurrence: Paleocene to Pleistocene (Muller *et al.* 1987)

Comparisons: It also has taxonomic affinity with *Mauritia*, Areaceae (Germeraad *et al.* 1968). *Mauritiidites franciscoi* var. *minutes* Van der Hammen and Garcia (1966) is smaller (25-33 μm) and it also has shorter spines (0.5-1.8 μm height).

Class Monoporatae Iversen and Troels-Smith 1950

Genus *Monoporopollenites* Meyer 1956

Type species: *Monoporopollenites gramineoides* Meyer 1956

Monoporopollenites annulatus (Van der Hammen 1954) Jaramillo and Dilcher 2001

Description: Monad, bilaterally symmetrical, isopolar, spheroidal, monoporate, similar shape of ectopore and endopore, annulate, annulus 3 μm wide, protruding, pore diameter 4 μm , exine 1 μm thick, collumelae indistinct, psilate ornamentation. Equatorial diameter 40-44.

Occurrence: Middle Eocene to Pleistocene (Germeraad *et al.* 1968), Paleocene to Pleistocene (Lorente 1986).

Comparisons: *Monoporopollenites parvus* Sarmiento (1992) has thicker exine (>1.5 μm).

Ecology: Wet forests (also aquatic) and grassland.

Class Fenestratae Iversen and Troels-Smith 1950

Genus *Fenestrites* Van der Hammen 1956b

Type species: *Fenestrites spinosus* Van der Hammen 1956b

Fenestrites spinosus Van der Hammen, 1956b

Description: Monad, radially symmetric, isopolar, circular, tricolporate, pores indistinct, tectate, nexine 0.5 μm , tectum 0.5 μm , fenestrate and echinate ornamentation, lacunae 6-7 μm wide, hexagonal, lophae 3 μm , spines 1-2 μm long. Equatorial diameter 26-28 μm , polar diameter 28-30 μm .

Occurrence: Last part of the Middle Miocene until Pleistocene (Jaramillo *et al.* 2011).

Botanical affinities: Asteraceae.

Ecology: Grassland.

Cichoreacidites longispinosus Silva-Caminha *et al.* (2010)

Description: Monad, radially symmetric, isopolar, circular, tricolporate, pore indistinct, tectate, nexine 0.3 μm thick, tectum 0.2 μm thick, fenestrate and echinate ornamentation, lacunae 3-5 μm wide, hexagonal, lophae 2 μm , spines 4 μm long with one perforation in the basal portion.

Dimensions: Polar diameter 22-23 μm , equatorial diameter 20-21 μm .

Occurrence: Upper Miocene until Pleistocene (Jaramillo *et al.* 2011)

Botanical affinities: Asteraceae.

Ecology: Grassland.

Class Tricolporatae Iversen and Troels-Smith 1950

Genus *Bombacacidites* Couper 1960

Type species: *Bombacacidites bombaxoides* Couper 1960

Bombacacidites baculatus Muller *et al.* 1987

Description: Monad, radially symmetric, isopolar, triangular-obtuse, tricolporate, colpi costate, nexine 0.6 μm thick, sexine 0.6 μm thick, baculate, baculae 1.5 μm long, 1 μm wide, lumina 1 μm wide at the mesocolpia, muri 0.4 μm wide, ornamentation changes to reticulate at the mesocolpia.

Stratigraphic range: Last part of the Lower Miocene to Upper Pleistocene (Jaramillo *et al.* 2011).

Dimensions: Equatorial length 45.2 μm , equatorial width 47.3 μm .

Taxonomic affinity: *Pachira*, Bombacaceae.

Comparisons: *Bombacacidites psilatus* Jaramillo and Dilcher (2001) changes to micropitted at the mesocolpia.

Ecology: Freshwater forests.

Genus *Retitrescolpites* Sah 1967

Type species: *Retitrescolpites typicus* Sah 1967.

Retitrescolpites? irregularis (Van Der Hammen and Wijmstra 1964) Jaramillo and Dilcher 2001

Description: Monad, radially symmetric, elliptical, tricolporate, distinct colpi, costate, costae 1-2 μm wide, tectate, exine 2-3 μm thick, reticulate ornamentation, heterobrochate, lumina with an irregular thickness from pole to the equator, 3-4 μm wide, muri 1 μm wide, curvurate. Equatorial length 25 μm , equatorial width 23 μm .

Occurrence: Lower Eocene to Pleistocene (Germeraad *et al.* 1968, Muller *et al.* 1987)

Botanical affinities: *Amanoa oblongifolia* - Euphorbiaceae.

Comparisons: *Ilexpollenites tropicalis* Silva-Caminha *et al.* 2010 is intectate, it has smaller equatorial diameter (18 μm) and clavate ornamentation. *Retitrescolpites? traversei* Silva-Caminha *et al.* (2010) has larger lumina (4-7 μm) and is semitectate.

Ecology: Common along creeks and rivers on peaty mud (Hoorn 1994b).

Class Pantoporatae Iversen and Troels-Smith 1950

Genus *Echiperiporites* Van Der Hammen and Wymstra (1964) Anzótegui 1990

Type species: *Echiperiporites akanthos* Van de Hammen and Wymstra 1964

Echiperiporites estelae Germeraad *et al.* 1968

Description: Monad, radially symmetric, isopolar, spheroidal, pantoporate (around 10-12 pores), pore diameter 4-4.5 μm , exine 2-2.8 μm thick, columellate, columellae 1 μm thick, echinate ornamentation, spines 5-9 μm height and 3.4-3.8 μm wide at the base and 0.5-1.2 μm wide at the top, area interspines presents micropitted or reticulate ornamentation, lumina 1 μm wide, muri 0.8 μm wide. Equatorial length 51-72 μm , equatorial width 41 μm .

Occurrence: Upper Eocene to Pliocene (Germeraad *et al.* 1968, Muller *et al.* 1987, Salard-Cheboldaeff 1990), Lower Eocene to Middle Pleistocene (Jaramillo *et al.* 2011).

Botanical affinities: *Thespesia* or *Hibiscus* - Malvaceae (Germeraad *et al.* 1968).

Comparisons: *Echiperiporites akanthos* Van der Hammen and Wymstra (1964) have smaller spines. *Echiperiporites jutaiensis* Silva-Caminha *et al.* (2010) has thicker exine (3.5 μm) and shorter dimensions (equatorial length 28-30 μm and equatorial width 28-29 μm).

Ecology: Freshwater forests.

Class Pantocolporatae Iversen and Troels-Smith 1950

Genus *Perisyncolporites* Germeraad *et al.* 1968

Type species: *Perisyncolporites pokorny* Germeraad *et al.* 1968

Perisyncolporites pokorny Germeraad *et al.* 1968

Description: Monad, radially symmetric, isopolar, spheroidal, syncolporate, straight or curved colpi, costate, costae 1 μm thick, circular or oval pores with 2.2-3 μm diameter, exine 3 μm thick, psilate ornamentation. Equatorial diameter 31 μm .

Occurrence: Middle Eocene to Pliocene (Muller *et al.* 1987, Lima and Amador 1985, Lorente 1986, Lima and Melo 1994). Eocene to Middle Pleistocene (Jaramillo *et al.*

2011).

Botanical affinities: *Banisteriopsis* - Malpighiaceae.

Comparisons: *Scabraperiporites asymmetricus* Regali *et al.* (1974a) is annulate.

Ecology: Freshwater forests.

Plate 1**Monolete**

1. *Echinosporis* sp.
2. *Perimonolotes* “*reticuloaciculares*”

Trilete

- 3-4. *Cicatricosisporites pseudograndiosus* D'Apolito *et al.* (2020) Informal
- 5-6. *Crassoretitriletes vanraadshoovenii* Germeraad *et al.* (1968)
- 7-8. *Echinatisporis muelleri* (Regali *et al.*, 1974) Silva-Caminha *et al.* 2010
9. *Echinatisporis* spp.
- 10-12. *Magnastriatites grandiosus* (Kedves and Sole de Porta 1963) Dueñas 1980

Plate 1

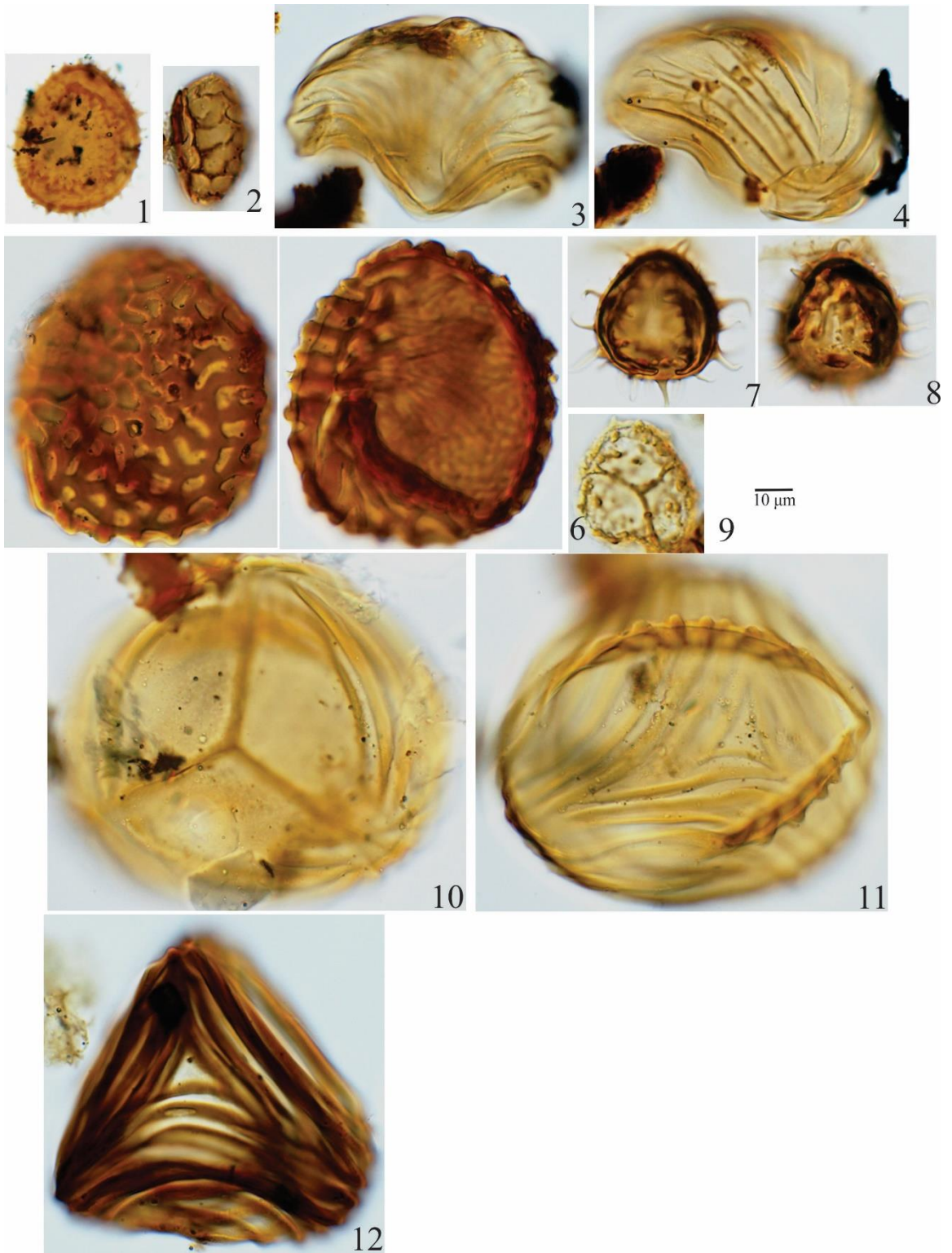


Plate 2

13. *Muerrigerisporis "socorrensis"*

14. *Psilatriteles lobatus* Hoorn (1994)

15-16. *Rugulatisporites* sp.

17-18. *Verrucatotriteles etayoi* Duenas (1980)

19-20. *Verrutriteles* spp

Inapertuate

21. *Clavainaperturites microclavatus* Hoorn (1994a)

22-23. *Crotonoidaepollenites reticulatus* Silva-Caminha *et al.* (2010)

24. *Crotonoidaepollenites* sp.

25-27. *Grimsdalea magnaclavata* Germeraad *et al.* (1968)

Plate 2

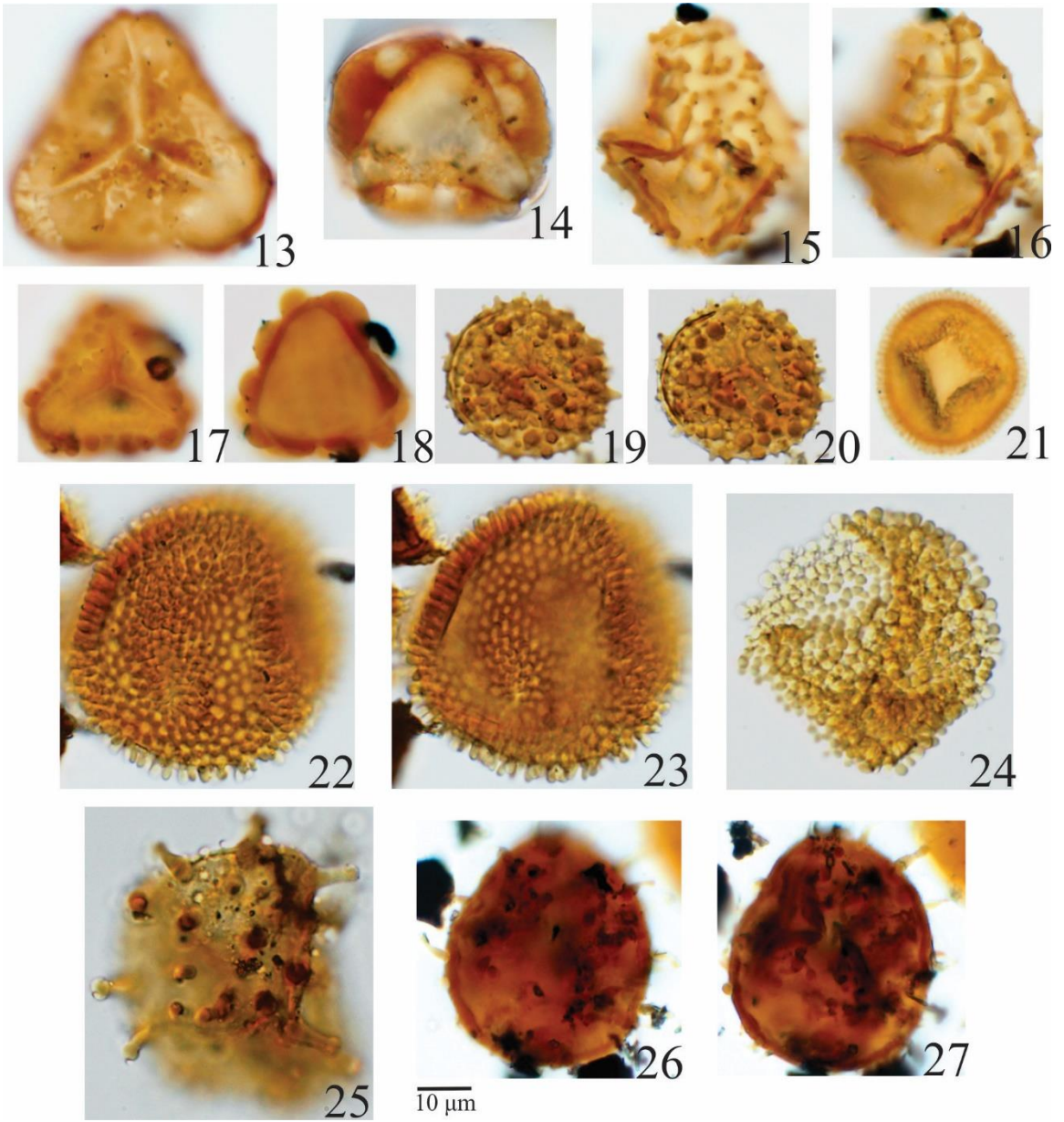


Plate 3

28. *Polyadopollenites mariae* Dueñas (1980)

Monosulcate

29-30. *Mauritiidites franciscoi* var. *franciscoi* Van der Hammen (1956) Van Hoeken Klinkenberg (1964)

Mauritiidites franciscoi pachyexinatus Van der Hammen and Garcia (1966)

Zonosulcate

31- *Proxapertites tertiaria* Van der Hammen and Garcia (1966)

Monoporate

32- *Monoporopollenites annulatus* Van der Hammen (1954) Jaramillo and Dilcher (2001)

Dicolporado

33-34 *Multiareolites formosus* Van der Hammen (1956), Germeraad *et al.* (1968)

35- *Multimarginites vanderhammeni* Germeraad *et al.* (1968)

Tricolpate

36. *Bombacacidites lorentae* Hoorn (1993), D'Apolito *et al.* (2020)

37- *Crassiectoapertites columbianus* Dueñas (1980), Lorente (1986)

38-39. *Retibrevitricolpites pseudoretibolus* D'Apolito *et al.* (2020)

40-41. *Retibrevitricolpites* sp.

Plate 3

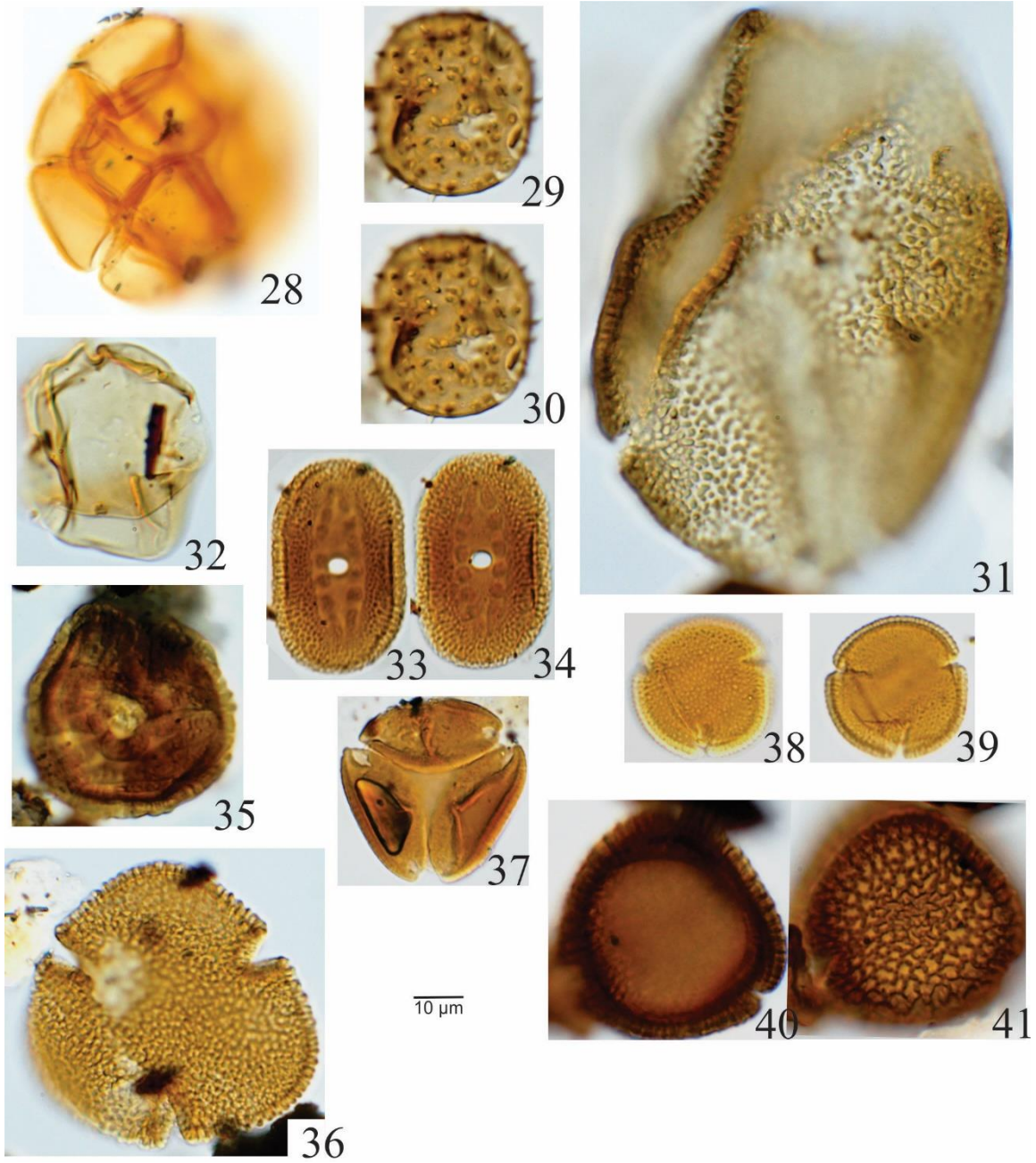


Plate 4

42-43. *Retitrescolpites? irregularis* Van der Hammen and Wymstra (1964), Jaramillo and Dilcher (2001)

44-45. *Spirosyncolpites spiralis* Gonzalez (1967)

Tricolporate

46. *Bombacacidites araracuarensis* Hoorn (1994)

47. *Bombacacidites baculatus* Muller *et al.* (1987)

48. *Bombacacidites nacimientoensis* Anderson (1960), Elsik (1968)

49. *Bombacacidites* spp

50. *Bombacacidites* spp.

51-54. *Cichoreacidites longispinosus* Lorente (1986), Silva-Caminha *et al.* 2010

55-57. *Echitricolporites spinosus* Van der Hammen (1956)

Plate 4

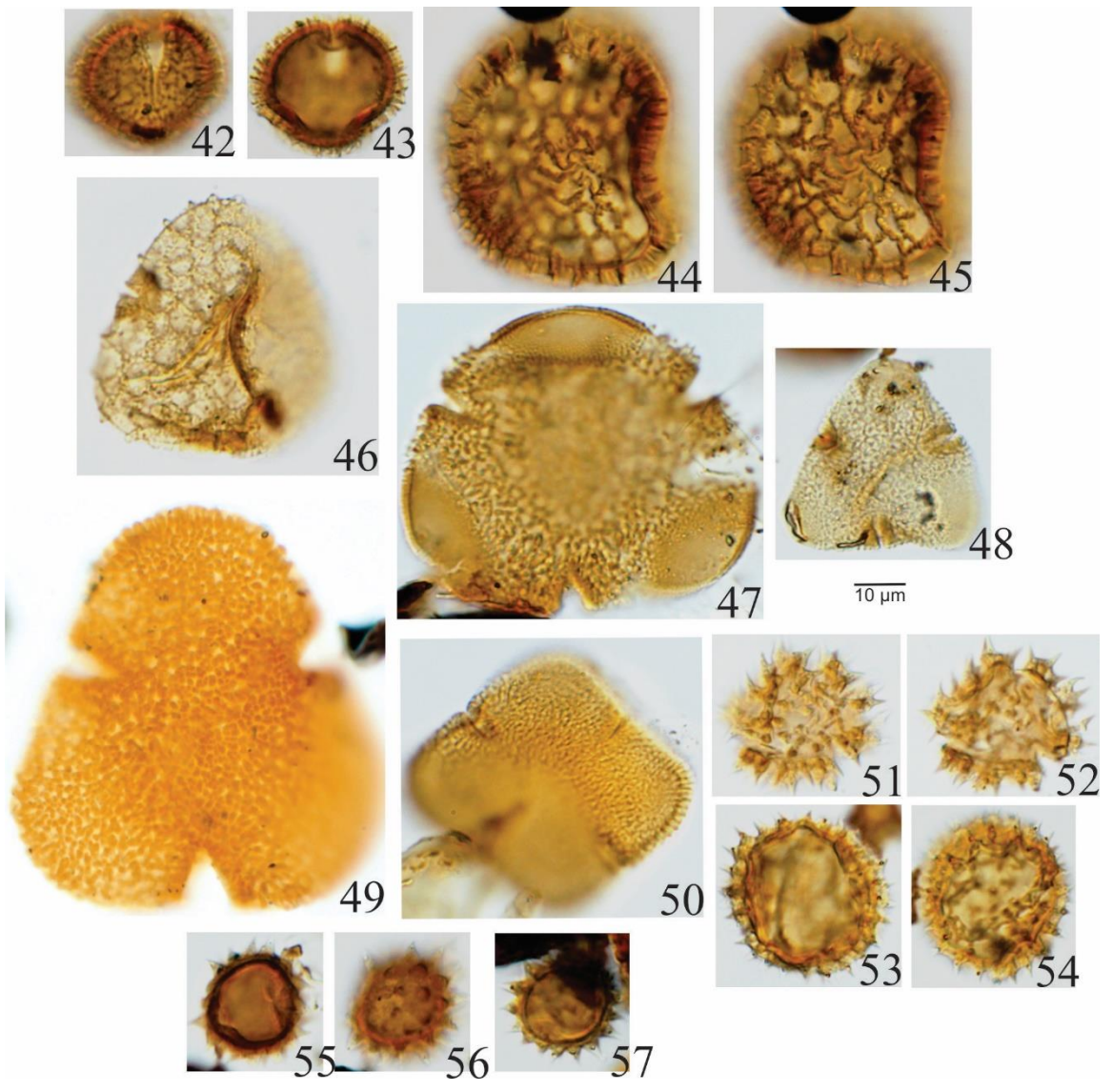


Plate 5

58-59. *Foveotricolporites* sp.

60. *Ilexpollenites tropicalis* Silva-Caminha *et al.* (2010)

61. *Tetracolporopollenites maculosus* Regali *et al.* (1974), Jaramillo and Dilcher (2001)

62-65. *Ladakhpollenites? Caribbiensis* (Muller *et al.* 1987), Silva-Caminha *et al.* (2010)

66-67. *Margocolporites carinae* Leite *et al.* (2020)

Triporate

68. *Corsinipollenites collaris* Silva-Caminha *et al.* (2010)

69. *Corsinipollenites oculusnoctis* Thiergart (1940), Nakoman (1965)

70. *Foveotriporites* sp.

71. *Proteacidites triangulates* Lorente (1986)

Pantocolpate

72-73. *Syncolporites foveolatus* D'Apolito *et al.* (2020)

Plate 5

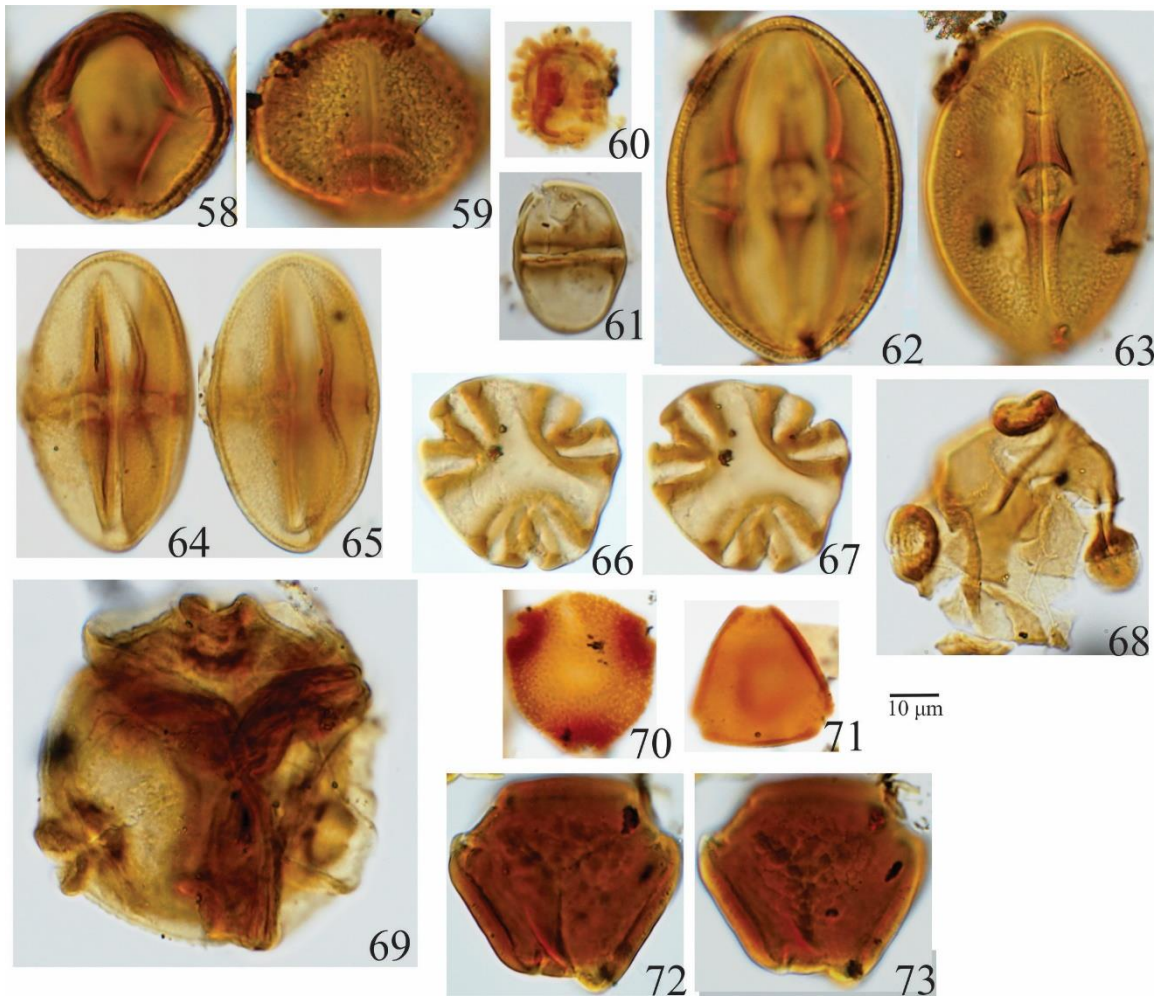


Plate 6**Stephanocolpate**

74-75. *Retistephanocolpites* “coariensi”

76-77. *Verrustephanocolpites* sp.

Stephanocolporate

78. *Retistephanocolporites elizabeteae* Leite *et al.* (2020)

79. *Stephanocolpites evansii* Muller *et al.* (1987)

80-81. *Psilastephanocolporites "ectoporatus"* D'Apolito *et al.* (2020)

Periporate

82-83. *Echiperiporites lophatus* Silva-Caminha *et al.* (2010), Leite *et al.* (2020)

84-85. *Echiperiporites germeraadii* Leite *et al.* (2020)

86. *Echiperiporites jutaiensis* Silva-Caminha *et al.* (2010)

87-88. *Echiperiporites* spp.

Plate 6

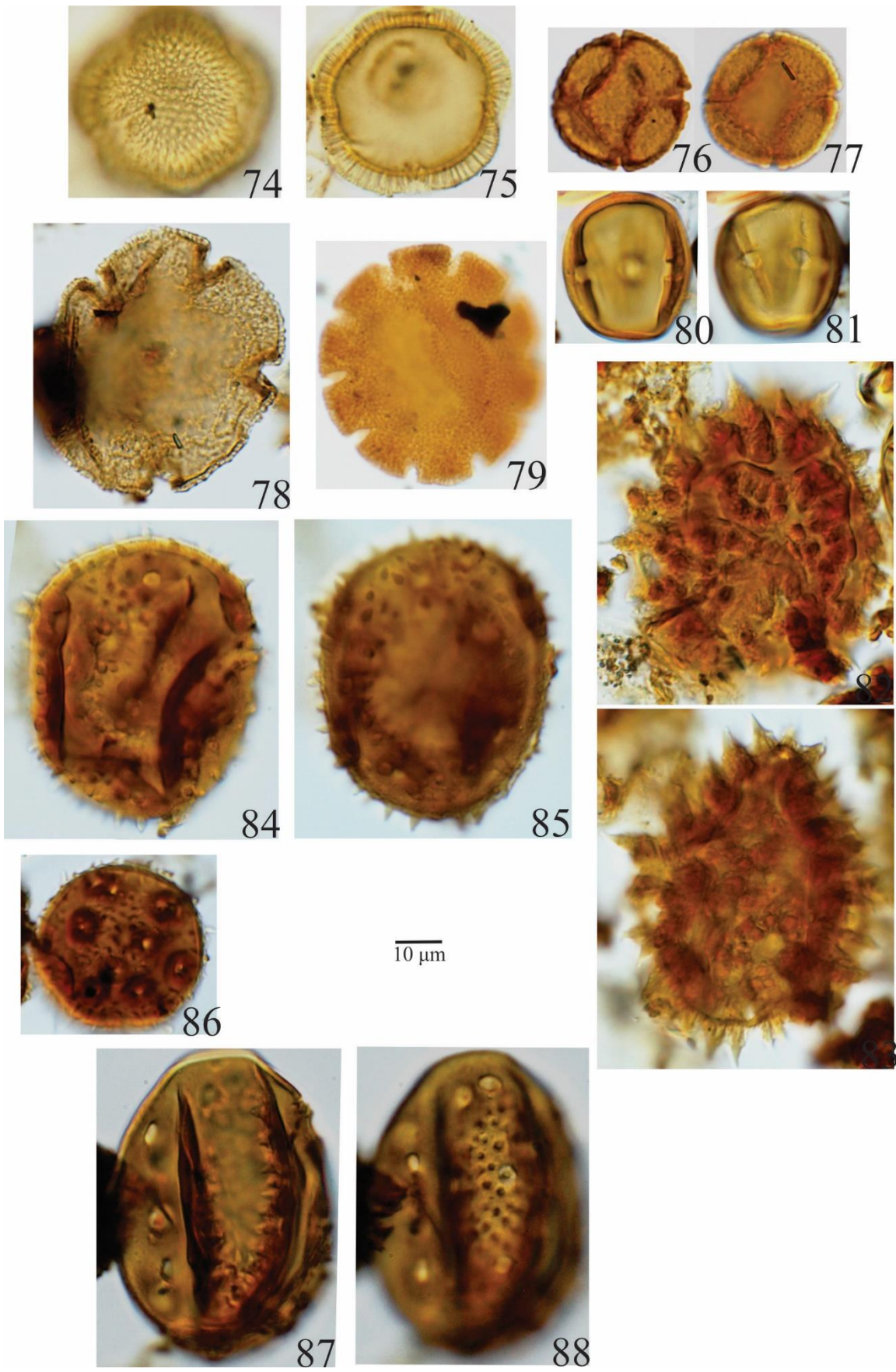


Plate 7

89. *Magnaperiporites* sp.

90-92. *Perisyncolporites pokornyi* Germeraad *et al.* (1968)

Stephanoporate

93-97. *Alnipollenites verus* Potonie (1931)

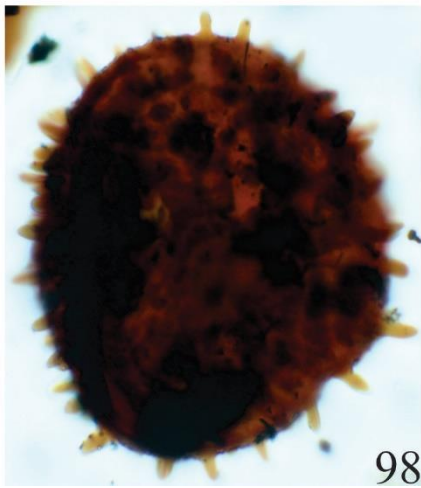
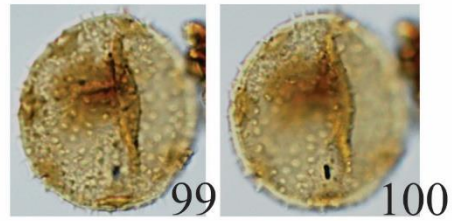
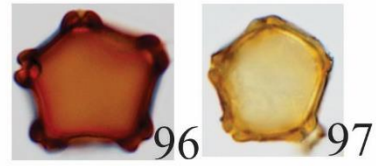
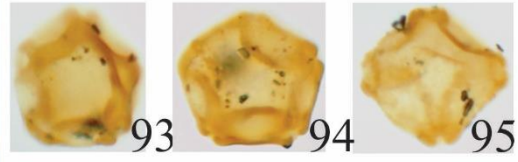
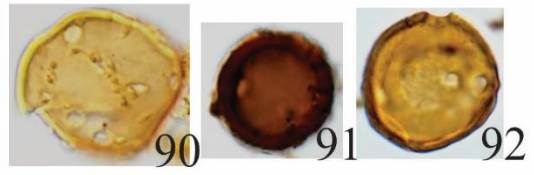
98. *Bacustephanoporites "grandiosus"* aff. (Urumaco) Informal

99-100. *Malvacipollis spinulosa* Frederiksen (1983)

101. *Psilastephanoporites tesseroporus* Regali *et al.* (1974)

102-103. *Retistephanoporites crassiannulatus* Lorente (1986)

Plate 7



10 μm

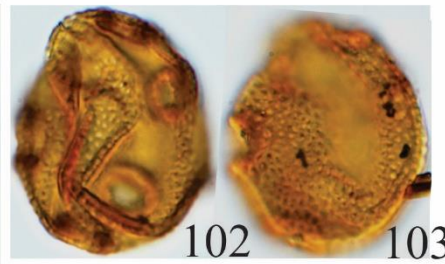


Plate 8**Other Palynomorphs**

104. *Botryococcus* sp.

105-106. *Micrhystridium* sp.

107. *Multiplicisphaeridium* sp.

108-109. *Heliosphaeridium* sp.

110-111. *Gorgonisphaeridium* sp.

Plate 8

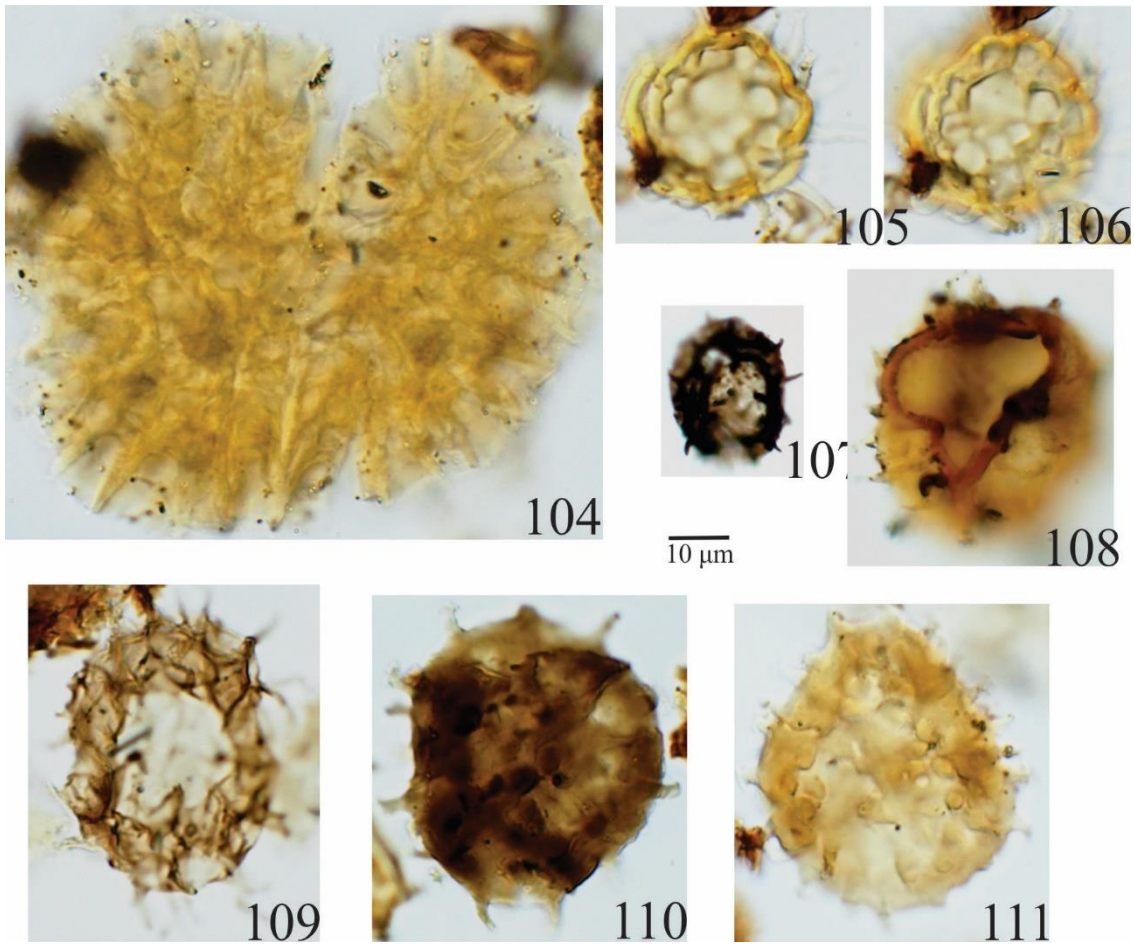


Figure 3- Percentage diagram of plant families and subfamilies for which botanical affinity is known drill core STG-02 (profile 3)

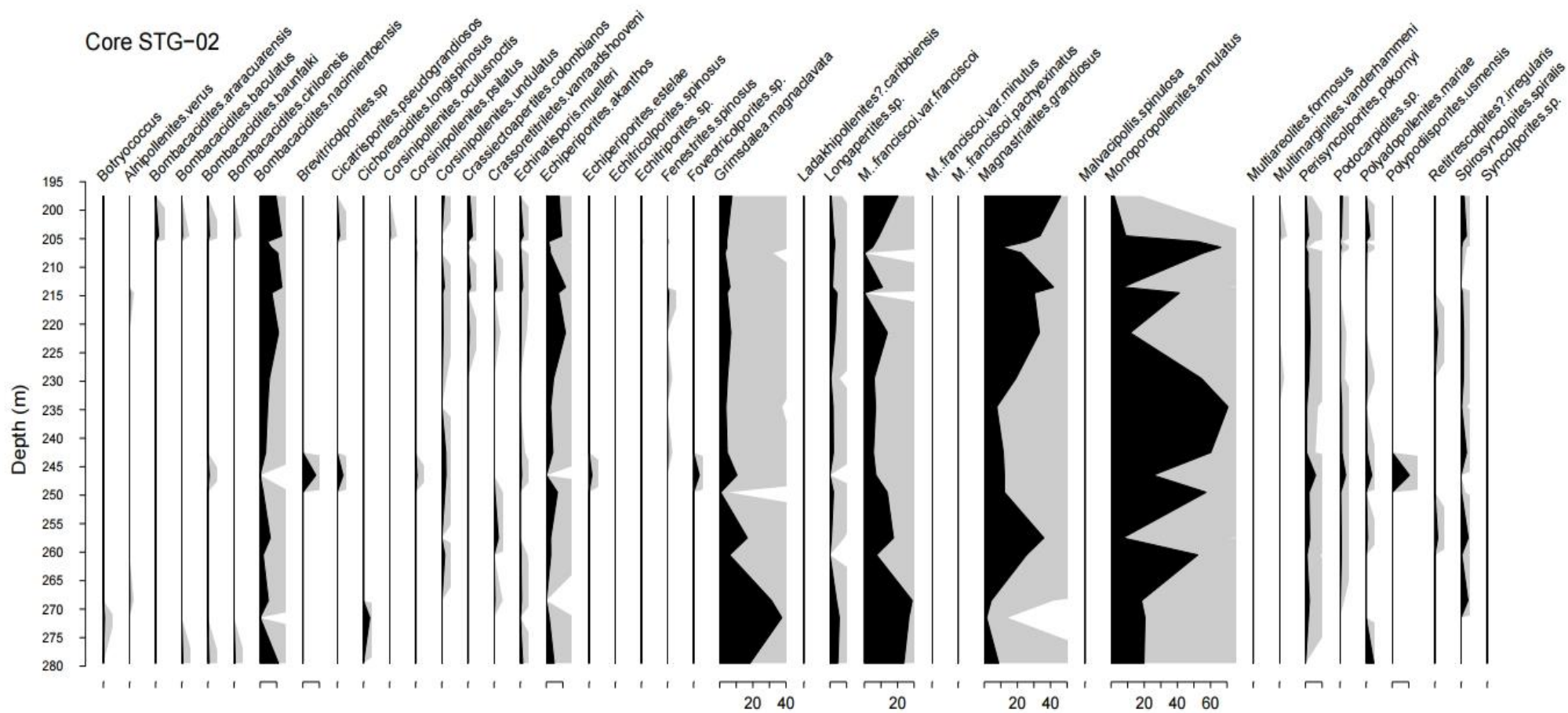
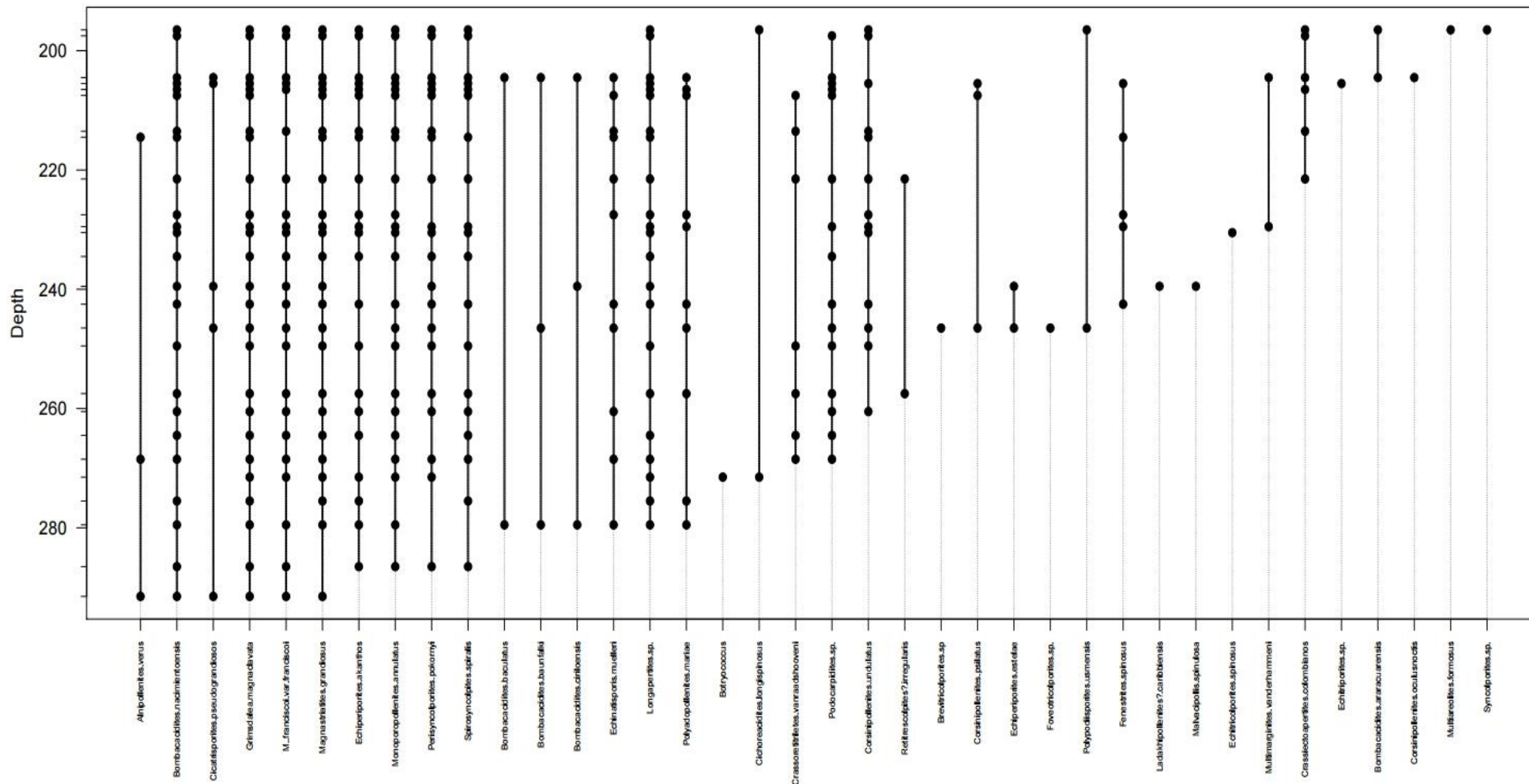


Figure 4- Range charts with pollen counts from drill core STG-02 (Profile 3)





UNIVERSIDADE FEDERAL DO PARÁ
INSTITUTO DE GEOCIÊNCIAS
PROGRAMA DE PÓS-GRADUAÇÃO EM GEOLOGIA E GEOQUÍMICA

PARECER

Sobre a Defesa Pública da Tese de Doutorado de WALMIR DE JESUS SOUSA LIMA JÚNIOR

A banca examinadora da Tese de Doutorado de **WALMIR DE JESUS SOUSA LIMA JÚNIOR** orientando do Prof. Dr. Afonso César Rodrigues Nogueira (UFPA), composta pelos professores doutores Ana Maria Góes - USP, Dermeval Aparecido do Carmo - UnB, Marlon Carlos França – IFPA/IFES e Joelson Lima Soares - UFPA, após apresentação da sua tese intitulada “**O NEÓGENO E PLEISTOCENO DA AMAZÔNIA CENTRAL: PALINOESTRATIGRAFIA, PALEOAMBIENTE E RELAÇÃO COM OS EVENTOS EVOLUTIVOS DO RIO AMAZONAS**”, emite o seguinte parecer:

O candidato realizou sua apresentação de forma clara, bem organizada e segura no tempo estipulado. Na arguição mostrou domínio da temática abordada e respondeu às perguntas formuladas pela banca. O trabalho escrito foi apresentado na forma de dois artigos submetidos a periódicos de impacto internacional. No entanto, os mesmos necessitam de correções de forma e questões pontuais de conteúdo.

Finalmente, a banca examinadora decidiu por unanimidade aprovar a tese de doutorado.

Belém, 19 de março de 2021.


Prof. Dr. Afonso César Rodrigues Nogueira
(Orientador – UFPA)

Prof^a. Dr^a. Ana Maria Góes
(Membro externo-USP)


Prof. Dr. Dermeval Aparecido do Carmo
(Membro externo-UnB)


Prof. Dr. Marlon Carlos França
(Membro interno-IFPA)


Prof. Dr. Joelson Lima Soares
(Membro interno-UFPA)